

**CONTRIBUTIONS TO PEPTIDOMIMETIC DESIGN:
PREDICTIVE COMPUTATIONAL STUDIES AND
SYNTHESES OF LINKER MOLECULES**

A Thesis

by

SANG Q. LAM

Submitted to the Office of Graduate Studies of
Texas A&M University
in partial fulfillment of the requirements for the degree of

MASTER OF SCIENCE

December 2005

Major Subject: Chemistry

**CONTRIBUTIONS TO PEPTIDOMIMETIC DESIGN:
PREDICTIVE COMPUTATIONAL STUDIES AND
SYNTHESES OF LINKER MOLECULES**

A Thesis

by

SANG Q. LAM

Submitted to the Office of Graduate Studies of
Texas A&M University
in partial fulfillment of the requirements for the degree of

MASTER OF SCIENCE

Approved by:

Chair of Committee,	Kevin Burgess
Committee Members,	Stephen A. Miller
	Jerry Tsai
Head of Department,	Emile A. Schweikert

December 2005

Major Subject: Chemistry

ABSTRACT

Contributions to Peptidomimetic Design:
Predictive Computational Studies and
Syntheses of Linker Molecules.

(December 2005)

Sang Q. Lam, B.S., The University of Texas at Dallas

Chair of Advisory Committee: Dr. Kevin Burgess

In an effort to partially mimic the complex interaction between nerve growth factor (NGF) and its membrane-bound tyrosine kinase A receptor (TrkA), several small organic molecules with functionalities similar to the side-chains of the amino acid residues of NGF critical to binding were devised. These molecules were studied computationally using the program Affinity. Each molecule was individually docked onto one of the binding sites on TrkA as determined by mutagenesis studies and the x-ray crystal structure obtained from the Protein Data Bank.

One of the strategies to enhance binding of active peptidomimetics to their target proteins is to link them together to form either homodimers or heterodimers. However, these dimers have low solubility in water and mimic only residues that are close together on the protein. Triethylene oxide- and hexaethylene oxide-based linker molecules were designed to circumvent these limitations. The increased polarity will improve the water-solubility and the added lengths, which can be controlled and varied by simple chemical manipulations, will allow for mimicking critical residues that are farther apart on the protein.

DEDICATION

I dedicate this manuscript to whoever cares to read it.

ACKNOWLEDGMENTS

I thank Professor Kevin Burgess for his patience with me through the various projects and giving me the opportunity to work in his research lab.

I thank Professor Stephen A. Miller and Professor Jerry Tsai for serving as members on my graduate advisory committee.

Thanks to everyone in the Burgess group for their friendship. Thanks to Dr. Genliang Lu for his camaraderie, chemical insights, and, most importantly, his help on the linker project.

TABLE OF CONTENTS

	Page
ABSTRACT.....	iii
DEDICATION.....	iv
ACKNOWLEDGMENTS.....	v
TABLE OF CONTENTS.....	vi
LIST OF FIGURES.....	vii
LIST OF SCHEMES.....	ix
LIST OF ABBREVIATIONS.....	x
CHAPTER	
I INTRODUCTION TO PROTEIN-PROTEIN INTERACTIONS AND PEPTIDOMIMETICS.....	1
1.1 Protein-Protein Interactions.....	1
1.2 Peptidomimetics.....	3
1.3 Summary.....	8
II PREDICTIVE COMPUTATIONAL STUDIES OF DESIGNED MOLECULES MIMICKING THE INTERACTION OF THE <i>N</i> -TERMINUS OF NGF AND TRKA.....	9
2.1 Introduction to Structure-Based Drug/Ligand Design.....	9
2.2 Mimetics Designed to Mimic the <i>N</i> -Terminus of NGF.....	14
2.3 Results and Discussion.....	23
III DESIGN AND SYNTHESSES OF LINKING MOLECULES.....	24
3.1 Multivalency in Biological Systems.....	24
3.2 Triethylene and Hexaethylene Glycol-Based Linking Molecules..	29
3.3 Results and Discussion.....	47
IV CONCLUSION.....	48
REFERENCES.....	49
APPENDIX A CHAPTER II EXPERIMENTAL PROCEDURES.....	57
APPENDIX B CHAPTER III EXPERIMENTAL PROCEDURES.....	58
VITA.....	123

LIST OF FIGURES

		Page
Figure 1.1	(A) General structures of an α -helix. Each turn of the helix incorporates 3.6 residues. (B) General structure of a β -turn.....	2
Figure 1.2	Small molecules that mimic or disrupt protein-protein interactions.....	4
Figure 1.3	(A) Herpes virus ribonucleotide reductase inhibitor. (B) Adenovirus inhibitor.....	5
Figure 1.4	β -turn peptidomimetic designs from various research groups.....	6
Figure 1.5	β -turn peptidomimetics that bind tyrosine kinase A and C receptors.....	6
Figure 1.6	Terphenyl, biphenyl, and indane as α -helical mimetics.....	7
Figure 2.1	Schematic representation of DOCK operation.....	10
Figure 2.2	Schematic representation of CAVEAT operation.....	11
Figure 2.3	Schematic representation of Affinity operation.....	12
Figure 2.4	The potential energy equation for CVFF.....	12
Figure 2.5	Potentials used to establish a 3-D grid around movable atoms in CVFF.....	13
Figure 2.6	Neurotrophin monomers, excluding NT-6, with loops 1-4.....	14
Figure 2.7	Interactions of neurotrophins with their specific tyrosine kinase receptors.....	15
Figure 2.8	Structures of monomeric tyrosine kinase (Trk) receptors and monomeric p75 receptor.....	16
Figure 2.9	Small molecules that mimic or disrupt NGF-TrkA interaction.....	17
Figure 2.10	Structure of NGF dimer <i>partially</i> interacting with two Trk receptors.....	18
Figure 2.11	Crystallographic structure of the NGF-TrkA interaction at the <i>N</i> -terminus of NGF.....	19
Figure 2.12	Designed molecules superimposed over the helical part of NGF containing H4 and I6 residues and docked onto TrkA.....	20
Figure 3.1	Examples of mimetic dimers.....	25
Figure 3.2	Example of a “serine dimer” synthesized by Schreiber.....	25
Figure 3.3	Schematic of chemical domain shuffling and the structure of the potent inhibitor of A549 cells that emerged from screening.....	26
Figure 3.4	Dimer construction by modification of tetrameric A6B10C4.....	27
Figure 3.5	<i>In situ</i> construction of dimer <i>syn</i> -TZ2PA6.....	28

	Page
Figure 3.6	Dimerizing peptidomimetics using the Burgess methodology.....29
Figure 3.7	A possible solution to the solubility of the Burgess dimeric mimetics.....30
Figure 3.8	Schematic synthesis of triazole dendrimers.....31
Figure 3.9	Route to small PEG oligomers.....32
Figure 3.10	Route to first generation dendronized linear polymers.....33
Figure 3.11	Distances between various hot spots on NGF.....33
Figure 3.12	Measured distances of the various TEG and HEG linkers.....34
Figure 3.13	Structure of compound 5 , a substitute for compound A36
Figure 3.14	Structure of 3'-O-2-nitrobenzyl nucleotide. TP represents a triphosphate group. Modified 3'-O-protecting group incorporating a HEG unit.....45
Figure 3.15	A hypothetical relationship between charge and pH of a TEG linker.....46

LIST OF SCHEMES

	Page
Scheme 3.1 Original synthetic scheme to TEG and HEG linkers of variable lengths.....	36
Scheme 3.2 Modified synthetic scheme for synthesis of TEG linkers.....	37
Scheme 3.3 Synthetic route to compound 5	37
Scheme 3.4 Synthetic route to compound 4	38
Scheme 3.5 Synthetic route to compound 6	39
Scheme 3.6 Synthetic route to compound 7	39
Scheme 3.7 Synthetic route to compound 8	40
Scheme 3.8 Synthetic routes to compounds 9 and 10	41
Scheme 3.9 Synthetic routes to compounds 11 and 12	41
Scheme 3.10 Synthetic routes to compounds 13 , 14 , 15 , and 16	42
Scheme 3.11 Synthetic route to compound 17	42
Scheme 3.12 Synthetic routes to compounds 18 and 19	43
Scheme 3.13 Synthetic routes to compounds 20 and 21	44
Scheme 3.14 Synthetic routes to compounds 22 , 23 , and 24	45

LIST OF ABBREVIATIONS

BOC	<i>tert</i> -butoxycarbonyl
CHCl ₃	chloroform
CH ₂ Cl ₂	dichloromethane
DMAP	4-dimethylaminopyridine
DMF	<i>N, N</i> -dimethylformamide
EtOAc	ethyl acetate
EtOH	ethanol
HEG	hexaethylene glycol
<i>i</i> PrOH	isopropanol
MeCN	acetonitrile
MeOH	methanol
TBAF	tetrabutylammonium fluoride
TEA	triethylamine
TEG	triethylene glycol
TFA	trifluoroacetic acid
THF	tetrahydrofuran

CHAPTER I

INTRODUCTION TO PROTEIN-PROTEIN INTERACTIONS AND PEPTIDOMIMETICS

1.1 Protein-Protein Interactions

Proteins are ubiquitous macromolecules that play key roles in biological processes ranging from catalysis of chemical reactions to providing structural support of cells to the transcription of deoxyribonucleic acid (DNA). Central to the intrigue of proteins is how they interact with one another. Although the proteins primary, secondary, tertiary, and quaternary structural forms are important to how they interact with one another, only the primary and secondary structures are generally targets for mimicry. This thesis will focus on the mimicry of the proteins secondary structural forms, particularly the α -helix in the chapter II. Linus Pauling and Robert Corey, through their exhaustive x-ray diffractive studies of fibrous proteins, generalized the protein structures as falling into three secondary types: the α pattern, the β pattern, and the collagen pattern.¹

1.1.1 Protein Secondary Structures: α -Helices and β -Turns

The secondary motifs that seem to recur often in mediating protein-protein interactions are the α helices and β turns (Figure 1.1).^{2,3} The R-, L-, and 3.10 α -helices and the type I and type II β turns are of particular interest because of their well-known status in the literature. The R and L denote whether the helix is coiling to the right or left, respectively, and the 3.10 denotes 3 residues per turn of the helix, a total of 10 atoms from the oxygen of the carbonyl group (hydrogen bond donor) of the i residue to the hydrogen of the amide group (hydrogen bond acceptor) of the $i + 3$ group.⁴ A type I β turn has the carbonyl oxygen from the amide bond between the $i + 1$ and $i + 2$ oriented away from the observer while in a type II turn it is oriented toward the observer.⁵

This thesis follows the style of the *Journal of American Chemical Society*.

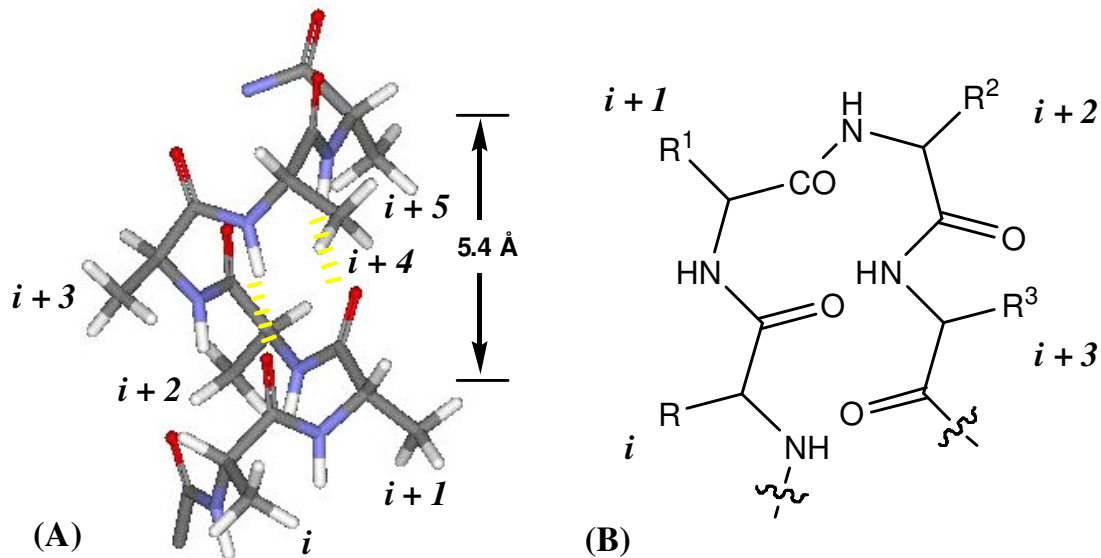


Figure 1.1 (A) General structure of an α helix (naturally occurring R- α helix shown). Each turn of the helix incorporates 3.6 residues. (B) General structure of a β turn.

1.1.2 “Hot Spots” at Protein-Protein Interfaces

Nussinov and coworkers define a protein-protein interface as an area, within a distance threshold, of interacting amino acid residues between at least two protein chains.⁶ Precisely which residues constitute an interface varies from study to study.⁷ Interface areas are calculated based on crystal structures of monomeric proteins and complexed proteins. In the complexed state, a certain percentage of the total area is “buried” by the interaction. This interface area was found by Janin and coworkers^{7,8} to be from 670 to 4890 Å² while Jones and Thornton⁷ discovered a slightly wider range, from 368 to 4761 Å². Within these interfaces there often exist critical binding points known as hot spots. Although no predictions can be made with regard to whether or not particular sites are hot spots, polar residues do tend to be conserved at these sites.^{6,9} X-ray crystallography revealed that hot spots are highly structural with side chains of amino acid residues from one surface fitting into the cavities and crevices on the opposite surface.¹⁰ These residues are so important in binding that when mutated to alanine cause a dramatic decrease in the binding constant, usually tenfold or higher.¹¹

1.2 Peptidomimetics

As the name implies, peptidomimetics are organic molecules that mimic the action of peptides. These molecules may structurally resemble peptides but are distinctly different in terms of their side chains or their molecular backbones. Since the mode of action for a small-molecule and a peptidomimetic is similar, confusion sometimes arises with regard to the classification of the molecule as being a peptidomimetic or simply a small organic molecular mimic. Nevertheless, interactions with proteins can be mediated by other molecules with intermediate molecular masses instead of the low molecular weights associated with small-molecules or peptidomimetics.

1.2.1 Small Molecules Mediating Protein-Protein Interactions

Mimicking or disrupting protein-protein interactions using small molecules is a well-known topic in the literature. Comprehensiveness of the subject is by no means the theme of this section. Instead, a few recent examples significant in the areas of cancer research and immunology will be presented. *In vitro* and *in vivo* evidence has shown that cancerous cells that metastasize depend on selectin-, integrin-, and chemokine-mediated vascular adhesion events.¹² It was recently discovered that the chemokine receptor CXCR4 was involved in attracting tumor metastases to the bone marrow, and that AMD3100, a small molecule antagonist, binds the receptor thereby preventing the spread of the tumor to the site.^{12,13} On a similar note, a mimic of the second mitochondria-derived activator of caspases (Smac), a protein involved in apoptosis, was just as effective as the native ligand at 10^5 to 10^6 -fold lower concentrations.¹⁴ The mannose-binding lectin (MBL) plays a very important role in the lectin complement pathway which is responsible for the development of the immune response in early childhood and the inflammatory response on oxidatively stressed endothelial cells.¹⁵ A decapeptide with the sequence SFGSGFGGGY was found to mimic the known ligand of MBL, *N*-acetyl-D-glucosamine (GlcNAc).¹⁵ Arguably one of the most extensively studied and important biological interactions are those between integrins and cell adhesion molecules (CAMs).¹⁶⁻¹⁸ Integrins are a large family of heterodimeric (consisting of an α subunit and a β subunit) surface receptors on cellular plasma membranes that mediate cell-matrix and cell-cell interactions.^{17,18} Thus far, the protein-protein interactions antagonized by

small molecules that involve integrins, intracellular adhesion molecules (ICAMs), and vascular cellular adhesion molecules (VCAMs) known are $\alpha_v\beta_3$ /vitronectin, $\alpha_v\beta_3$ /MMP2, VLA4/VCAM, and LFA-1/ICAM.^{19,20,21} BXT-51072, a glutathione peroxidase (GPx) mimic, has been shown to inhibit ICAM-1 and VCAM-1 expressions by tumor necrosis factor- α (TNF α).²² Since the discovery of the residues within ICAM-1 that are important for the interaction with LFA-1, Gadek and co-workers developed a LFA-1 antagonist with an IC₅₀ of 1.4 nM.²³ Figure 1.2 shows the structures of all the small molecules mentioned above.

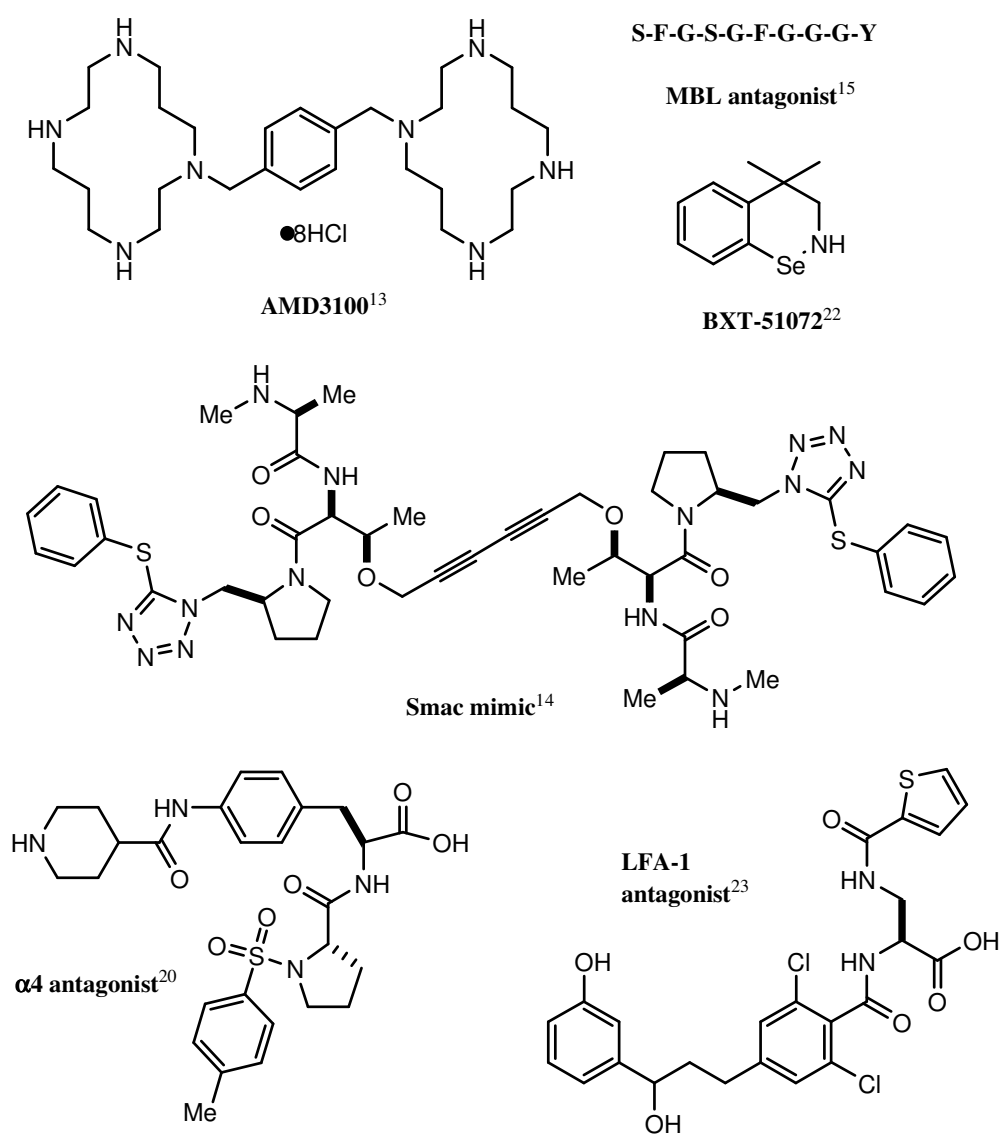


Figure 1.2 Small molecules that mimic or disrupt protein-protein interactions.

1.2.2 α -Helix and β -Turn Peptidomimetics

As mentioned earlier in the thesis, α helices and β turns are among the most abundant secondary structures that can be found mediating protein-protein interactions. As with all conceptual designs, the target protein serves as the model which fuels innovations. The target selected for the discussion in this thesis is nerve growth factor (NGF), a neurotrophin with some hot spots identified to be β turns and α helices.²⁴⁻²⁶ Details about the hot spots, its crystal structure and related neurotrophins will be covered in chapter II. This section will briefly touch upon the various published designs of α helix and β turn peptidomimetics. Figure 1.3 shows a couple of specific peptidomimetic examples that are neither α helix nor β turn mimics, but are potent inhibitors of herpes virus¹⁶ and adenovirus.²⁷ Figure 1.4 depicts examples of β turn peptidomimetics that

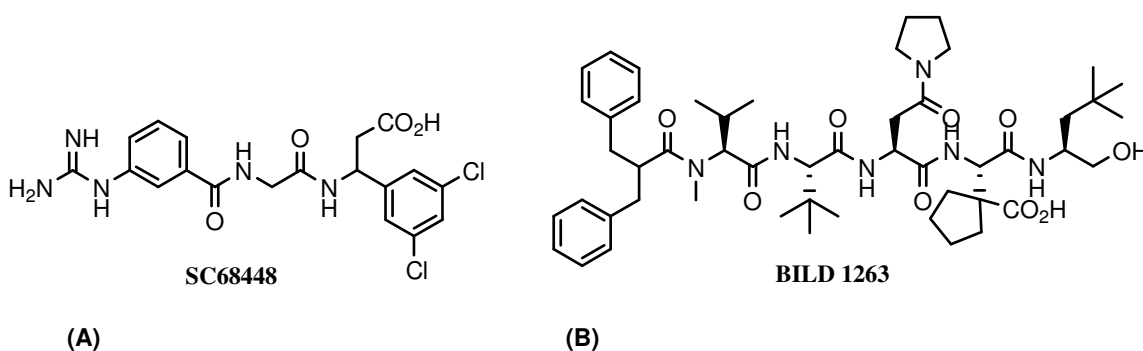


Figure 1.3 (A) Herpes virus ribonucleotide reductase inhibitor. (B) Adenovirus inhibitor.

have been published in the literature.²⁸⁻³⁵ Of particular interest is the Burgess design which provided useful lead compounds, **D3** and **MPT18**, each of which binds TrkA and

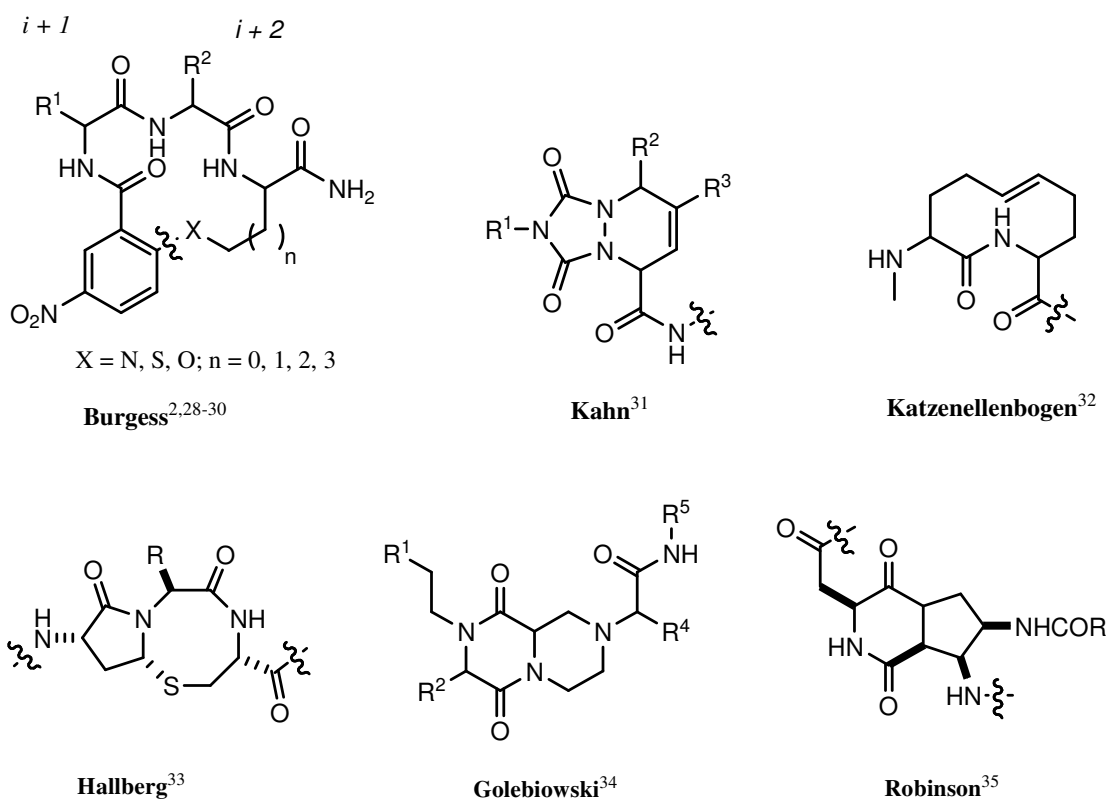


Figure 1.4 β turn peptidomimetic designs from various research groups.

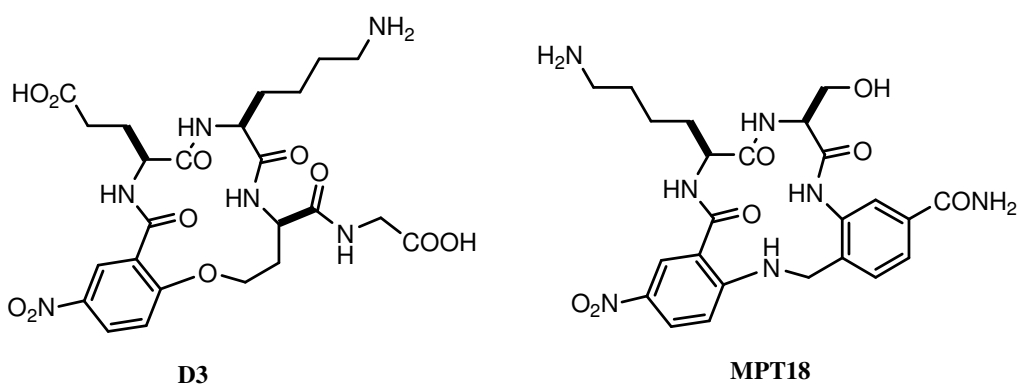


Figure 1.5 β turn peptidomimetics that bind tyrosine kinase A and C receptors.

TrkC respectively (Figure 1.5).^{25,30} Designing peptidomimetics to mimic the behavior of α helices are much more difficult as most of the designs are more prone to conform-

ational changes than those for β turns. Nevertheless, successful attempts have been made and published (Figure 1.6).^{3,36-41} The distances between the residues in the α -helices

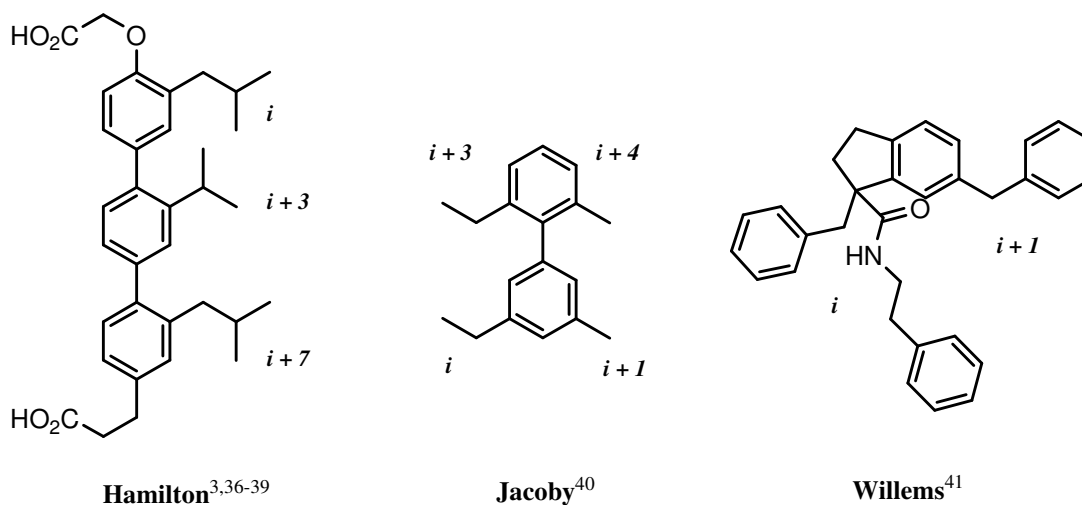


Figure 1.6 Terphenyl, biphenyl, and indane as α -helical mimetics.

Table 1.1 Distances between residue i and residue $i + n$ in an α -helix.

Residue, n	Distance from i , (\AA)
1	4.70
2	7.94
3	7.89
4	7.81
5	10.60
6	12.58
7	12.81
8	14.13
9	16.63
10	17.92

are unique in a sense that the distance between i and $i + n$ are not necessarily larger than the distance between i and $i + (n - 1)$. For instance, Table 1.1 shows that from i to $i + 3$

is 7.89 Å and from i to $i + 2$ is 7.94 Å for an α -helix. Since the distances vary slightly between R- and L- α helices, the distances shown in the table are averages. In addition, the helices were constructed using only alanine amino acids, and all the measurements were taken from the α carbons between the residues.

1.3 Summary

Mimicking protein-protein interactions poses a very challenging feat in medicinal chemistry. To be considered effective, a small-molecule or peptidomimetic must, at the least, interact with the protein in a way that is similar to the native ligand. Three factors need consideration before embarking on the task of designing such a molecule: the comparable binding orientation of the molecule with the native ligand, the synthetic feasibility of the designed molecule, and the binding strength.

Chapter II of this thesis will discuss the details of using molecular modeling to compare how a set of designed molecules, mimicking the *N*-terminus of NGF, interact with tyrosine kinase A (TrkA) receptor. Synthetic ease of the designed molecules were considered but not proven experimentally. Since the compounds were not synthesized, no binding constants were determined.

Chapter III will discuss the design and syntheses of linker molecules with variable lengths that have the capabilities of spanning the various distances between hot spots on a protein. Peptidomimetics could be attached to these linkers and then anchored to a core molecule, thereby creating bivalent molecules with potential for enhanced affinities.

CHAPTER II

PREDICTIVE COMPUTATIONAL STUDIES OF DESIGNED MOLECULES MIMICKING THE INTERACTION OF THE N-TERMINUS OF NGF AND TRKA

2.1 Introduction to Structure-Based Drug/Ligand Design

It is in no small part due to the structure-based design method that there are a plethora of drugs released nowadays on the market. With the emergence of more powerful computers not to mention the wealth of 3-D structural data of proteins currently available for meticulous scrutiny, the method has become almost a standard protocol in the pharmaceutical industry for designing novel drugs.^{42,43} Effort and research are now underway to “fine-tune” the simulation of ligand-protein interactions, a process known as docking, and compare the result to natural systems from which it tries to emulate.⁴⁴

2.1.1 Overview of the Docking Method

Assessing predictions of protein-protein interactions using the docking methodology is a complex and time-consuming process requiring collaborations between many research groups, such as the community-wide Critical Assessment of PRredicted Interactions (CAPRI) experiment.⁴⁵ For most docking algorithms, however, a docking calculation usually involves three basic steps: prepare the system, that is, assign receptor and ligand potentials and create a docking assembly; perform the calculation, fill in parameters, set energy cut-offs, and launch the job; and analyze the results.⁴⁵ In selecting what program to use, two factors need to be considered: parameterization and score functions.⁴²⁻⁴⁴ Parameterization refers to the set of parameters used to describe a molecule (such as bond lengths, bond angles, energy of bond types, etc.) and score functions refer to a set of conditions a program uses to either accept or reject a docking result, often comparing the free energy of binding (ΔG^0).⁴²⁻⁴⁴ There are many programs available to simulate docking, each one offers its unique approach and perspective. It is important to note that most programs are search algorithms, designed to scour for molecular structures in known databases, such as the Chemical Abstracts (CA), the American Chemicals Directory (ACD), or the National Cancer Institute (NCI),^{46,47} that seem to dock well onto the receptor.

2.1.2 Docking Programs

DOCK, CAVEAT, FLOG, GOLD, PRO_LIGAND, GROWMOL, and SPROUT are just some of the numerous programs currently available for *in silico* screening.^{48,49} Although covering all of them is beyond the scope of this thesis, a couple of programs are worth mentioning. Among them, DOCK is the most popular.^{46,50,51} Created by Kuntz, it is a rigid body docking method that does not consider protein and ligand flexibility.^{44,52} Given a receptor on a protein, DOCK generates hard spheres that conform to the shape of the receptor, identifies a scaffold by analyzing key contact points, and finally searches for a match in a known database (Figure 2.1).^{46,52} Unlike DOCK, the program CAVEAT⁵³

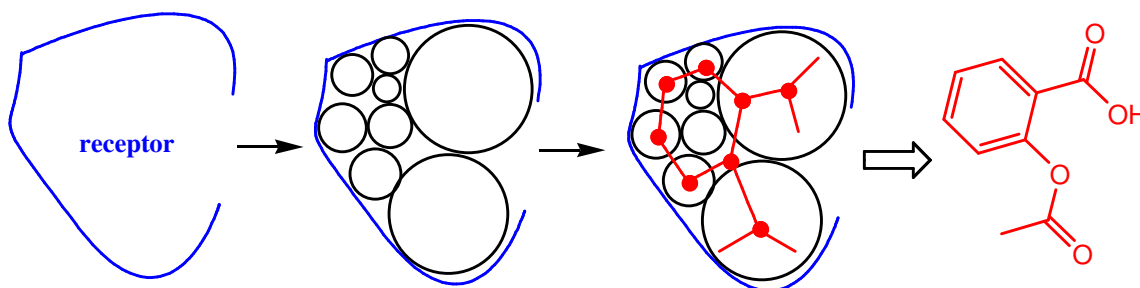


Figure 2.1 Schematic representation of DOCK operation.

operates initially on the assumption that the orientation and position of bonds take precedent over the placement of atoms.^{42,51} Like DOCK, it is a rigid body docking method, not accounting for the flexibilities of the protein and ligand.⁴² The mechanistic operation of CAVEAT is that it analyzes the receptor surface on a cell, establishes vectors that would correspond to bond orientations, and searches for compounds in the database with bonds matching the magnitude and direction of the vectors (Figure 2.2).^{42,53}

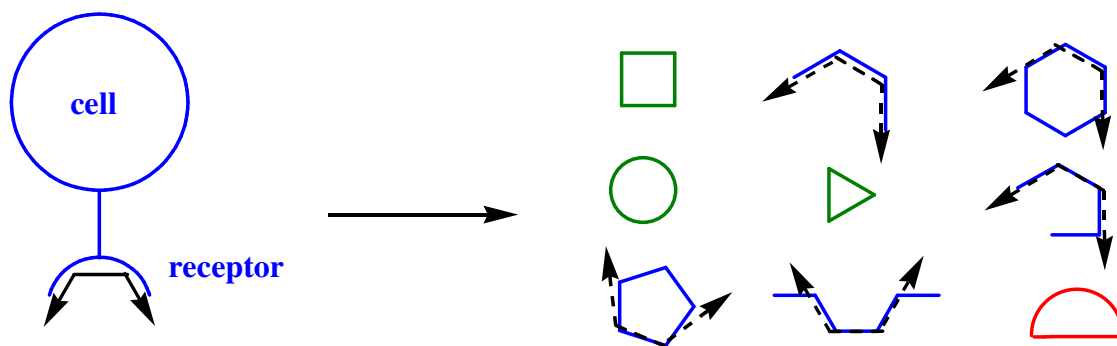


Figure 2.2 Schematic representation of CAVEAT operation. Compounds in blue are potential matches. The red compound is an exact match that the program overlooked.

Although CAVEAT is quite fast,⁴² a conspicuous drawback is that potential target matches can sometimes be overlooked.

2.1.3 Affinity

Jointly developed by Accelrys and the DuPont Merck Pharmaceutical Company, Affinity is a molecular mechanics/grid method that employs a full molecular force field, thus allowing for a more accurate representation of the receptor-ligand interaction.^{45,54,55} Other docking programs, such as DOCK, CAVEAT, and FLOG, are descriptor-based methods that utilize empirical rules taking into account only hydrogen bonding, hydrophobic interactions, and steric effects which, at times, may not be enough to describe an interaction accurately.⁴⁵ An attractive feature of Affinity is that it allows the user to rigidify the “bulk” of the protein while allowing only the binding site and ligand to move, minimizing the energy during the docking process with a combination of Monte Carlo (MC)^{45,56,57} and Simulated Annealing (SA)^{45,58} methods. In the MC method, the program takes a “random walk” to generate a new conformation, then either rejects or accepts it based on the energy as compared to the initial conformation.^{56,57} In the SA method, the program heats the molecules rapidly to a high temperature, usually 1000K, then cools them down slowly; with equilibration, there will be many “energetic states” to which the molecules will fall—many of which are local minima—but with the correct cooling rate one conformation will eventually “freeze out” which is the global minimum conformation.⁵⁸ In short, while holding the majority of the protein rigid, Affinity makes use of MC and SA methods to dock a given ligand onto a given receptor (Figure 2.3).

For simplicity the “bulk” of the protein being held rigid is not shown in the figure.

Affinity can only implement two force fields, Consistent

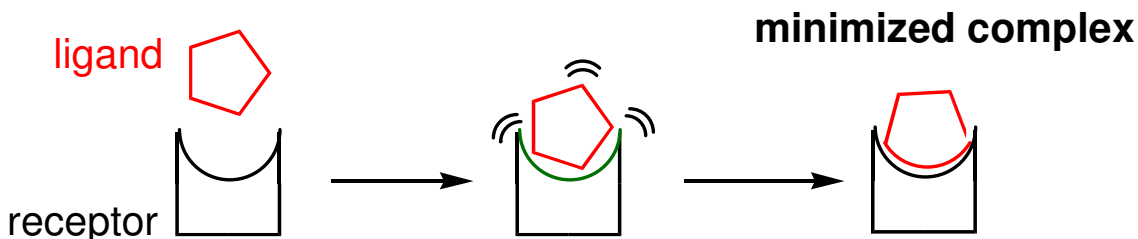


Figure 2.3 Schematic representation of Affinity operation.

Valence Force Field (CVFF) or Consistent Force Field, Second Generation (CFF91), in the docking procedure.⁴⁵ CVFF was the force field used in the docking procedure so only the functional form of the potential energy for CVFF is shown below (Figure 2.4).⁴⁵

$$\begin{aligned}
 E_{\text{pot}} = & \sum_b D_b [1 - e^{-\alpha(b-b_0)}] + \sum_{\theta} H_{\theta} (\theta - \theta_0)^2 + \sum_{\phi} H_{\phi} [1 + \text{sicos}(n\phi)] \\
 & \quad (1) \qquad \qquad \qquad (2) \qquad \qquad \qquad (3) \\
 & + \sum_{\chi} H_{\chi} \chi^2 + \sum_b \sum_{b'} F_{bb'} (b - b_0) (b' - b'_0) + \sum_{\theta} \sum_{\theta'} F_{\theta\theta'} (\theta - \theta_0) (\theta' - \theta'_0) \\
 & \quad (4) \qquad \qquad \qquad (5) \qquad \qquad \qquad (6) \\
 & + \sum_b \sum_{\theta} F_{b\theta} (b - b_0) (\theta - \theta_0) + \sum_{\phi} F_{\phi\theta\theta'} \cos\phi (\theta - \theta_0) (\theta' - \theta'_0) + \sum_{\chi} \sum_{\chi'} F_{\chi\chi'\chi\chi'} \\
 & \quad (7) \qquad \qquad \qquad (8) \qquad \qquad \qquad (9) \\
 & + \sum \varepsilon [(r^*/r)^{12} - 2 (r^*/r)^6] + \sum qq_i/\varepsilon r_{ij} \\
 & \quad (10) \qquad \qquad \qquad (11)
 \end{aligned}$$

Figure 2.4 The potential energy equation for CVFF.

The first nine terms are bonding terms, describing the vibrations of internal coordinates, and the tenth term and the eleventh term represent the 12-6 van der Waals and Coulombic electrostatics, respectively, both of which are nonbonding terms.⁴⁵ To establish a 3-D grid surrounding the movable atoms, the potential of the rigid atoms due to a grid point p

in space is calculated using the 12-6 van der Waals potentials (Figure 2.5).⁴⁵ Also shown in the figure is the procurement of the electrostatic potential at a point p in space.⁴⁵

$$\phi^A(p) = \sum_{j \in \text{rigid terms}} \frac{(A_{jj})^{1/2}}{r_{jp}^{12}}$$

$$\phi^B(p) = \sum_{j \in \text{rigid terms}} \frac{(B_{jj})^{1/2}}{r_{jp}^6}$$

} potentials for rigid atoms
due to a grid point p in space

$$\phi^{ES}(p) = \sum_{j \in \text{rigid terms}} \frac{q_j}{\epsilon r_{jp}}$$

} electrostatic potential
at point p in space

Figure 2.5 Potentials used to establish a 3-D grid around movable atoms in CVFF.

The A and B represent repulsive and dispersive parameters, respectively, while r_{jp} is the distance between atom j and point p in space.⁴⁵ ES is the electrostatic potential and q_j is the charge of atom j .⁴⁵

Although not as popular or fast as the programs mentioned earlier, Affinity has been used to dock inhibitors of proteins such as plasmepsin II⁵⁹ and telomerase.⁶⁰ Despite its limited uses in the literature, it is by no means ineffective; in fact, Affinity can be used to further study ligands designed in programs such as LUDI, reanalyze complexes docked with other programs, or perform relatively accurate *ab initio* docking.

2.2 Mimetics Designed to Mimic the *N*-Terminus of NGF

Several factors were kept in mind when designing peptidomimetics. One of the most obvious is the need to keep the molecules simple, thus synthetically facile should the need to make them arise. In addition, the designed compounds should take after molecular scaffolds often found in known drugs. Therefore, if the compounds were found to be active, then perhaps they will exhibit low toxicity and high bioavailability reducing the time spent in clinical trials.

2.2.1 Neurotrophins

Neurotrophins (NTs) are a family of highly homologous (~50% homology) growth factors that include nerve growth factor (NGF), brain-derived neurotrophic factor (BDNF), neurotrophin-3 (NT-3), and neurotrophin-4/5 (NT-4/5), and neurotrophin-6 (NT-6).⁶¹ X-ray crystallography revealed that these NTs share a common elongated shape with two pairs of twisted, antiparallel β -strands, three hairpin loops, and a cysteine-knot, formed by three disulfide bonds, to stabilize the conformation (Figure 2.6).⁶¹

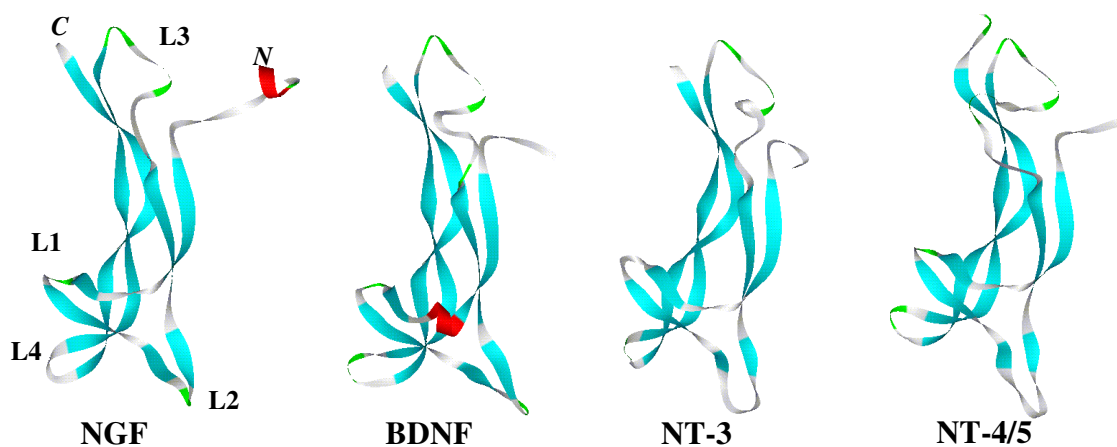


Figure 2.6 Neurotrophin monomers, excluding NT-6, with loops 1-4 (L1-L4).

These NTs are crucial in the development of axonal and dendritic growth, synaptic formations and connections, apoptosis of sensory neurons, and neurotransmitter release, thereby making them immensely important therapeutic targets for treating medical conditions such as pain, depression, obesity, learning, and memory.^{61,62} Despite their sequence homology, NTs elicit their action by binding to two classes of cell surface

receptors, the p75 neurotrophin receptor and the tyrosine kinase receptors.^{25,61} All mature NTs bind the common p75 receptor with low affinity ($K_d \sim 10^{-9}$ M) and bind the Trk receptors with higher affinity ($K_d \sim 10^{-11}$ M) and selectivity, that is NGF binds only to TrkA, BDNF and NT-4/5 bind only TrkB, and NT-3 has the propensity to bind to TrkC, though it can weakly bind to TrkA and TrkB (Figure 2.7).^{61,63,64} Binding to Trk receptors

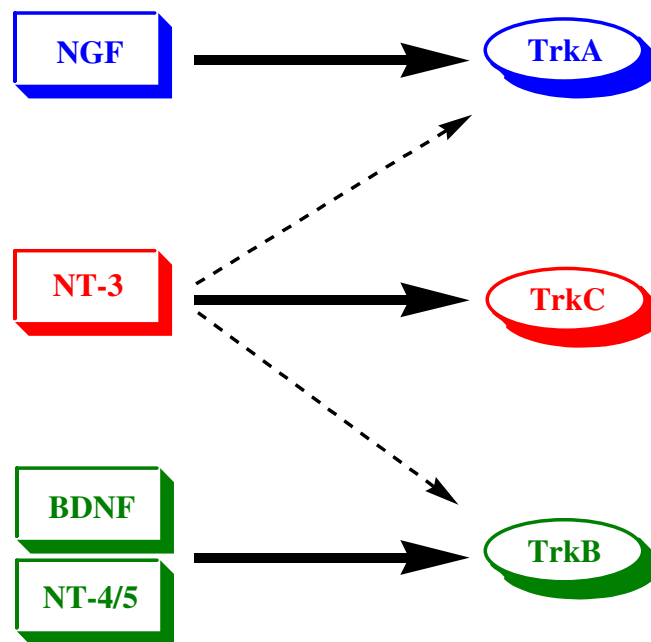


Figure 2.7 Interactions of neurotrophins with their specific tyrosine kinase receptors.

promote cell survival and normal differentiation, while binding to p75 causes apoptosis.^{61,65,66} Figure 2.8 shows the structures of the Trk receptors and p75.

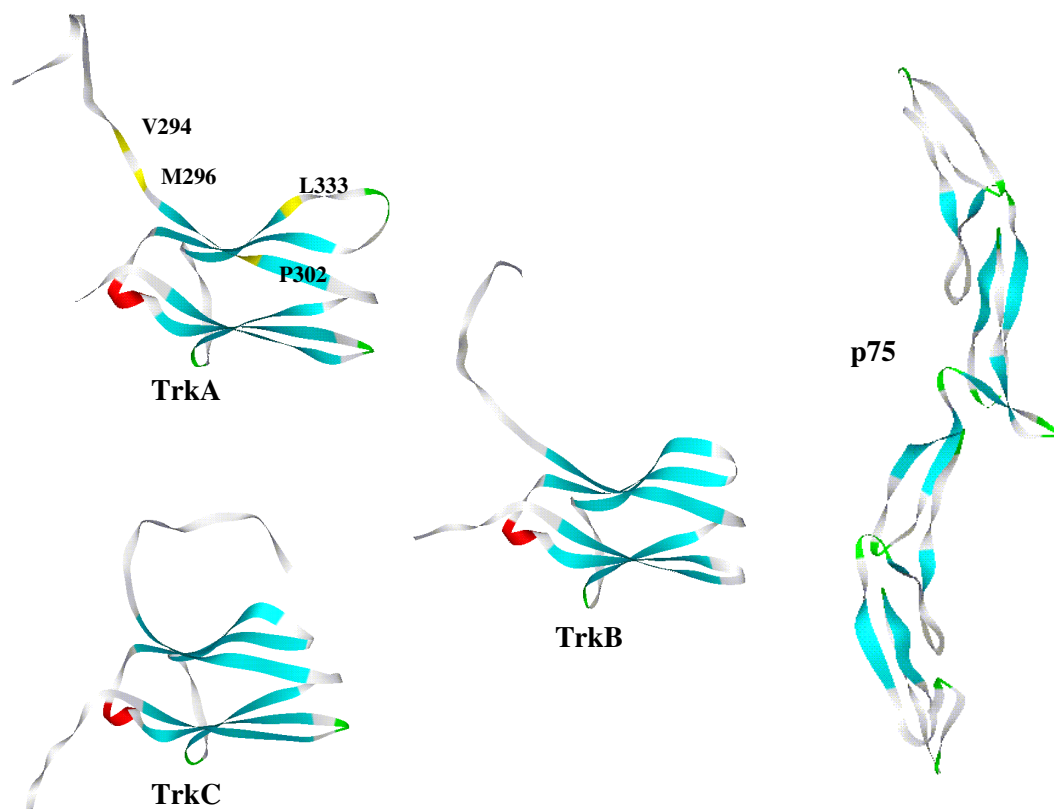


Figure 2.8 Structures of monomeric tyrosine kinase (Trk) receptors and monomeric p75 receptor. Residues shown in TrkA were found to be critical to binding NGF.

An interesting fact to note is that p75 inhibits apoptosis in its dimeric form, but once an NT dissociates it to monomer form, it induces apoptosis.⁶⁵ The focus of this thesis, however, is on NGF and TrkA; more specifically, the entire effort and emphasis will be on the *N*-terminus of NGF interacting with TrkA.

2.2.2 Small Molecules That Mimic or Disrupt NGF-TrkA Interactions

Small molecules that mimic or disrupt NGF-TrkA interactions are by no means absent in the literature. In addition to the Burgess TrkA agonist, **D3**, mentioned in chapter I of this thesis, Figure 2.9 shows some of the reported small molecules that mimic or disrupt NGF-TrkA interaction.^{25,67-70}

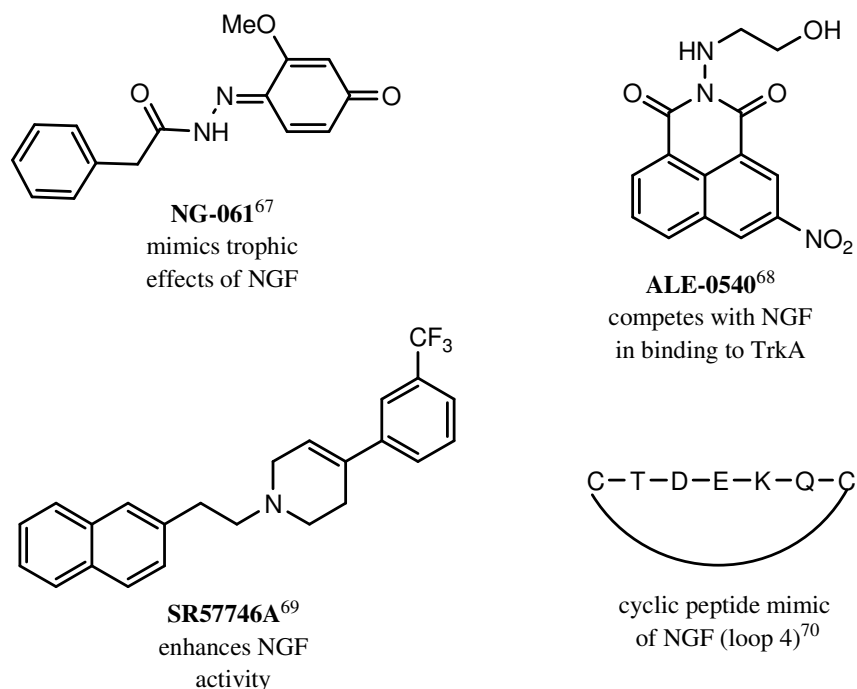


Figure 2.9 Small molecules that mimic or disrupt NGF-TrkA interaction.

2.2.3 Molecular Modeling of Designed Molecules Based on the α -Helix Scaffold

Accounting for nearly one-third of all known protein structures,⁷¹ the α -helix is definitely a vital structural motif for molecular design and organic syntheses. Its prominence can be seen at interfaces in viral/bacterial proteins such as HIV-1 gp41, *EcoR1*, and human papillomaviruses (HPVs); in transcription factors such as homodimers of bHLH TF E47, Jun, and cancer-linked ESX and Sur-2/DRIP130; and in cellular proteins such as HER2/neu, Bcl-X_L-Bak, and p53-MDM2.^{37,72-74} Alpha helical mimicry has been reviewed by Hamilton⁷³ and Fairlie.⁷⁵

NGF has many points of contact with its receptor TrkA (Figure 2.10).^{24,25} β -turn peptidomimetics have been synthesized and tested in the Burgess group for many of the turn regions, that is loops 1, 2, and 4.²⁵ However, no progress has been made towards mimicking the *N*-terminus of NGF, bearing in mind that it is a different secondary form.

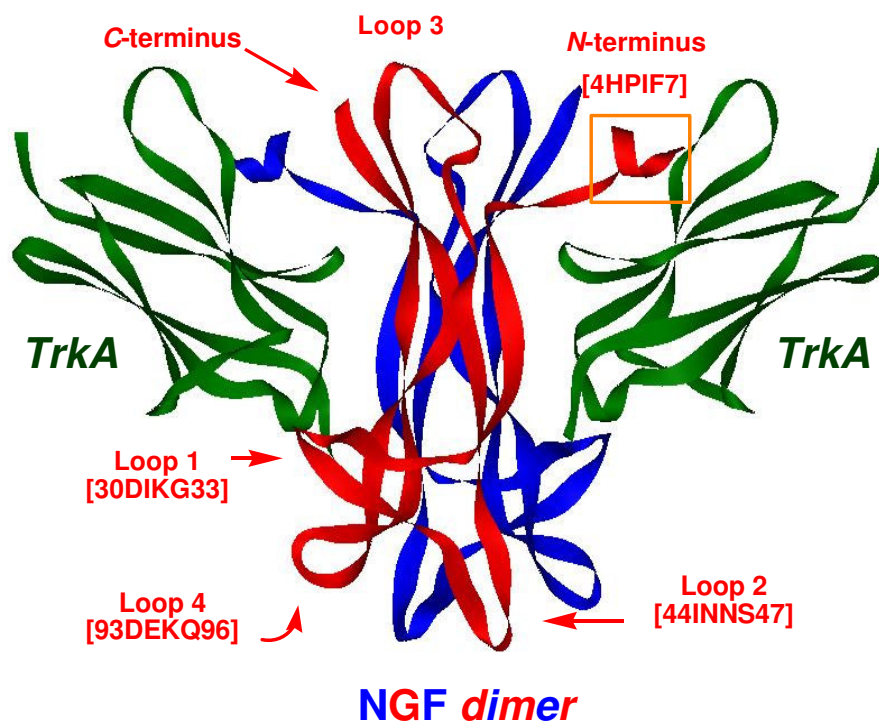


Figure 2.10 Structure of NGF dimer *partially* interacting with two TrkA receptors. The X-ray crystal showing the *complete* interaction has not been solved. The residues that are critical for binding as determined by mutagenesis are shown for loop 1, 2, 4, and the N-terminus.

Constraining molecules into helix-type conformations are difficult. Research groups have attempted to stabilize and constrain peptide mimics by using side-chain-to-side-chain covalent bonds, typically using linkages between residues i to $i + 4$ or residues i to $i + 7$,⁷⁶⁻⁷⁸ and even using metal ions.⁷⁹ In order to mimic NGF, the designed molecules must simulate histidine 4 (H4) and isoleucine 6 (I6) side-chains, since these are the most critical binding residues.²⁴ H4 forms hydrogen bonds with serine 304 (S304) of TrkA and I6 fills a hydrophobic “canyon” on the TrkA surface (Figure 2.11).²⁴ No special

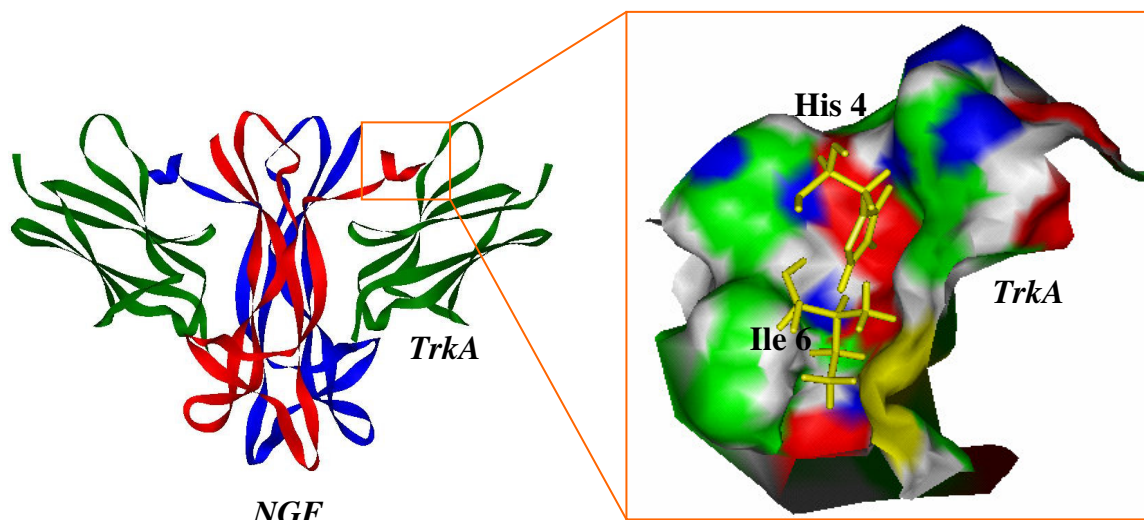


Figure 2.11 Crystallographic structure of the NGF-TrkA interaction at the *N*-terminus of NGF. The helix of NGF consists of four residues but only the residues of interest, histidine and isoleucine (yellow sticks), are shown. In the box, TrkA is represented by the Connolly surface.

attention was determined in advance to constrain the designed molecules into a helical conformation. Instead, the molecules proposed are limited to one degree of freedom about the central axis of rotation by the introduction of an alkyne functionality with a general notion that the steric hindrance between the side-chains will cause the molecule to adopt a helical conformation. Figure 2.12 shows the proposed molecules superimposed over the helical part of NGF and docked onto TrkA. Molecules **1** and **2** are indole derivatives. Indoles are attractive targets because they appear in many important natural products and are prominent in known drugs.⁸⁰ Cyclopentadienone **3**, furan **4**, and pyrazolidine **5** derivatives are strikingly simple structurally, almost drug-like. Biphenyl-type compounds **6** and **7**, utilizing triazines and pyrazolidines, were fathomed because of their structural intrigue and the synthetic routes to obtaining them could possibly be facile. Diketopiperazines and their derivatives are well known in the literature. Molecule **8** was proposed because the chemical routes to procure it are easily accessible. The figures show the proposed molecules superimposed over the helical part of NGF that

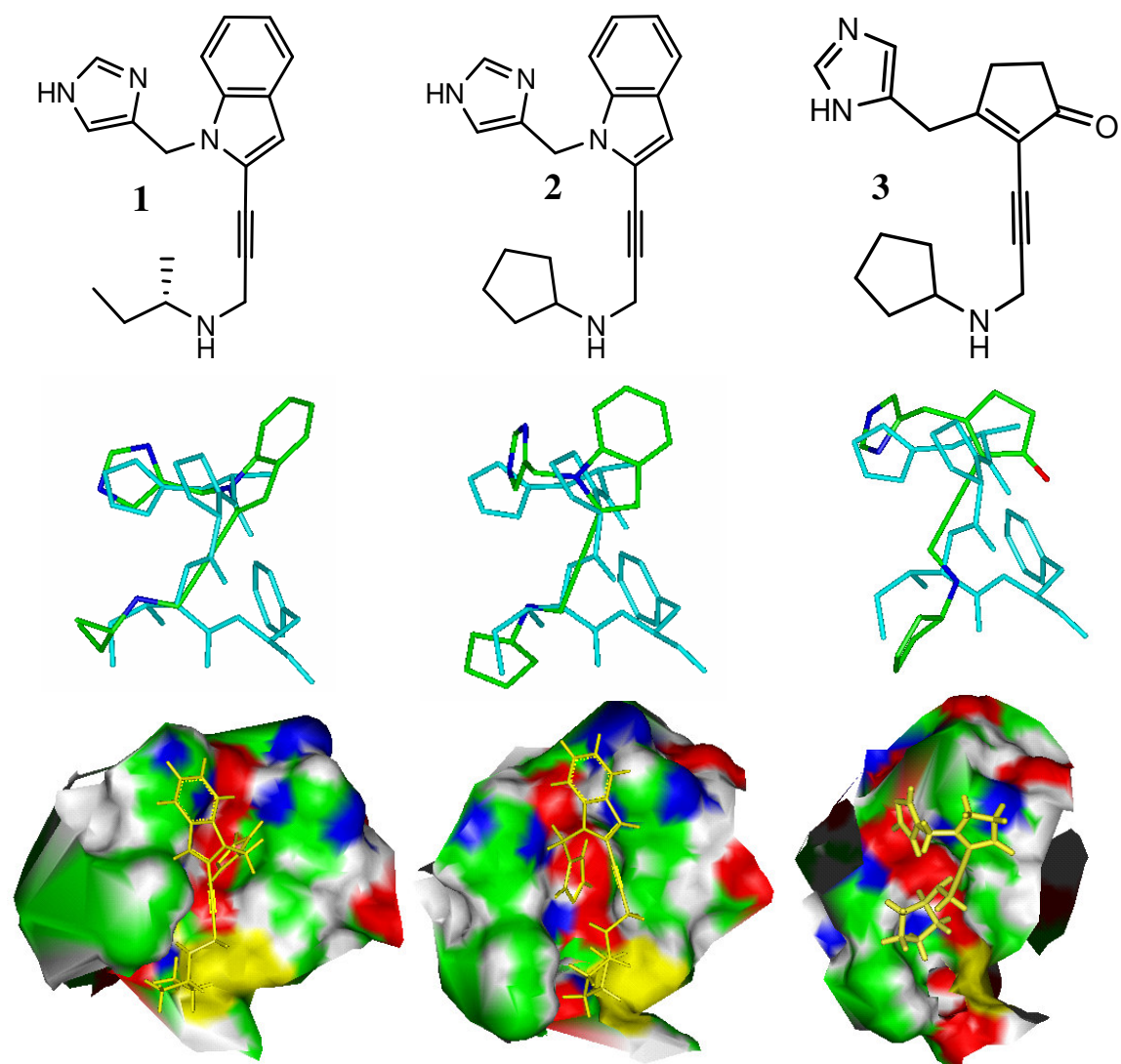


Figure 2.12 Designed molecules superimposed over the helical part of NGF containing H4 and I6 residues (blue sticks) and docked onto TrkA (Connolly surface).

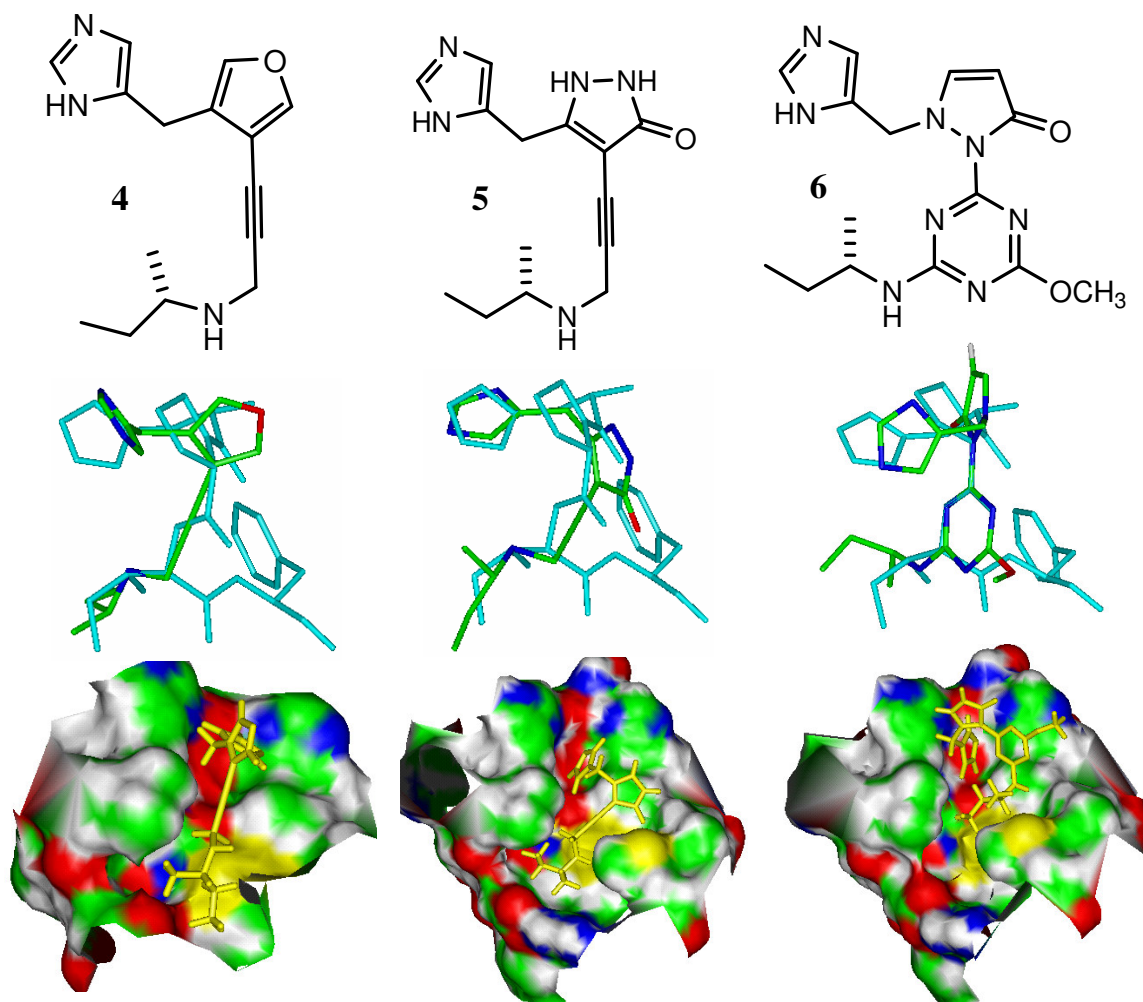


Figure 2.12 continued.

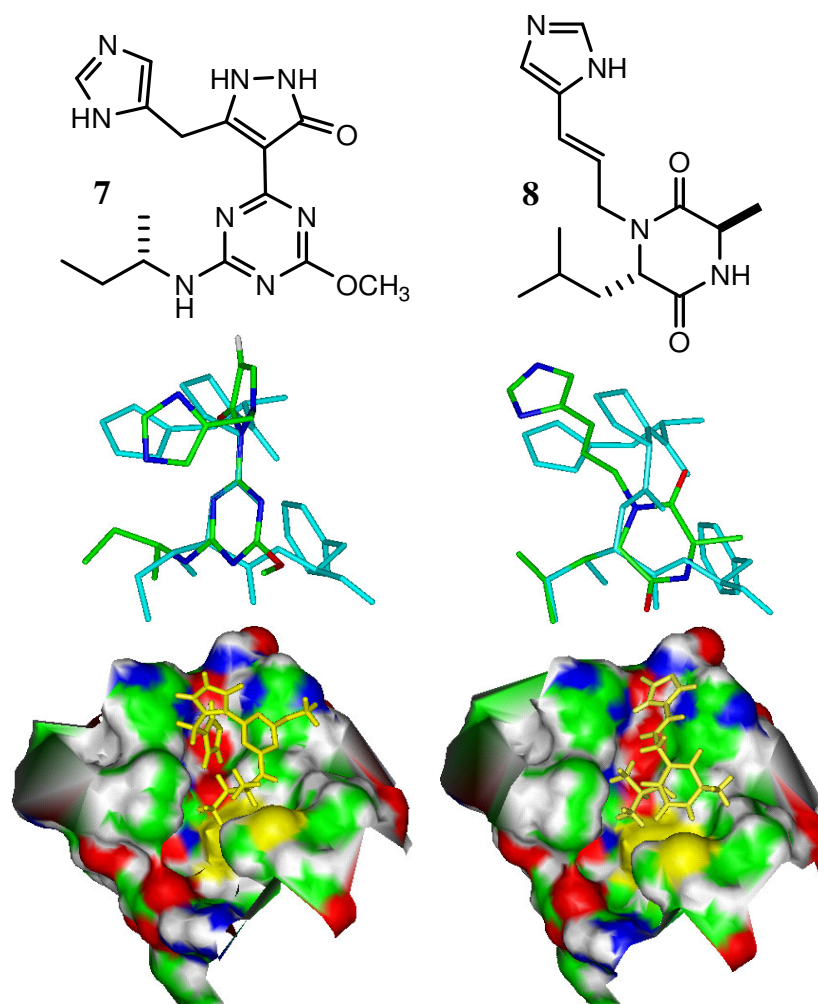


Figure 2.12 continued.

encompasses H4 and I6 (blue sticks). The docking calculations of the molecules onto TrkA were performed using Affinity in the InsightII package by Accelrys, Inc., running on a UNIX-based silicon graphic workstation. These calculations were executed in the gas phase ($\epsilon = 1$) with no predetermined cutoff values for the van der Waals and electrostatic interactions. All conformations were satisfactorily minimized with the maximum derivative of the potential energy less than 10^{-3} kcal/mol. Since solvent was not involved, the conformations that resulted must be used strictly in a predictive manner and not taken to be a representation of reality.

2.3 Results and Discussion

There are many factors that affect how strongly a certain protein would interact with another protein such as solvent accessible surface area (ASA), planarity, circularity, extent of hydrogen bonding, electrostatic and shape complementarities, and hydrophobicity.⁸¹ This thesis focuses more on electrostatic and shape complementarities. The minimized conformations are intended to be used in a qualitative sense rather than a quantitative sense, that is to say a decision about whether or not a designed molecule is a mimic depends upon how its docked image appear and not what the numbers say about it. With that in mind, the docking results could easily be interpreted. By comparing how well the side-chains of the designed molecules matched the side-chains of H4 and I6 of NGF in terms of both orientation and distance, compounds **1**, **2**, **4**, and **5** emerged as primed candidates. After analyzing the docked structures, only compound **1** arose as a potential α -helical mimic of the *N*-terminus of NGF, matching nearly perfectly with the crystal structure in Figure 2.11.

On an interesting exploratory tangent, the designed molecules above could be used in the program LigandFit from the Cerius² software suite.⁸² This algorithm differs from Affinity in that the entire receptor protein is held rigid while only the ligand is flexible.⁸² The uniqueness of the program lies in the fact that it can “predict” the hot spots by evaluating the terrain of a given protein surface, calculating whether or not the cavities and crevices are suitable for occupation.⁸² Therefore, the program has the potential of uncovering new sites of binding for a particular protein quickly without the need for experimentation. The designed molecules may be able to dock onto these new sites. However, preliminary work could not be carried out because the program was not yet available.

CHAPTER III

DESIGN AND SYNTHESSES OF LINKING MOLECULES

3.1 Multivalency in Biological Systems

Whitesides defines the term valency of a molecule as the number of connections that it can form with other molecules through ligand-receptor-type interactions.⁸³

Therefore, multivalent molecules have the capacity to interact at multiple sites which make them useful in mediating cellular and enzymatic interactions. After all, biological systems are complex entities. The communication circuitries needed to sustain and maintain such systems are themselves complex, usually requiring multivalent binding. Multivalent ligands are highly versatile—they can act as agonists or antagonists—and can bind to selected targets with higher specificity and affinity.^{84,85} Although there are many multivalent scaffolds in the literature, the most common ones are low-molecular weight displays (dimers, trimers, etc.), dendrimers, polymers, and liposomes.^{84,85} The focus of this thesis is on low-molecular weight displays, mainly bivalency through dimerization.

3.1.1 Dimerization Generalities

Dimerization, allosteric conformational change, and receptor aggregation are the key mechanisms by which information is transmitted from the cell surface across the plasma membrane.^{86,87} Receptors for growth or differentiation factors are often activated by dimerization.⁸⁷ It is no surprise then that this biological phenomenon has inspired synthetic organic chemists. In fact, successful designs and syntheses of dimeric mimetics of various proteins are common in the literature. Wrighton and co-workers demonstrated that a peptide mimetic of erythropoietin showed a 100-fold increase in binding affinity once it was dimerized.⁸⁸ Schreiber and co-workers synthesized a dimer FK1012 from the monomer FK506 to study T-cell receptor (TCR) signaling pathways.^{89,90} Figure 3.1 shows the structures of the erythropoietin mimetic and FK1012. While the chemistry was not as important as the biological significance when these compounds were contrived,

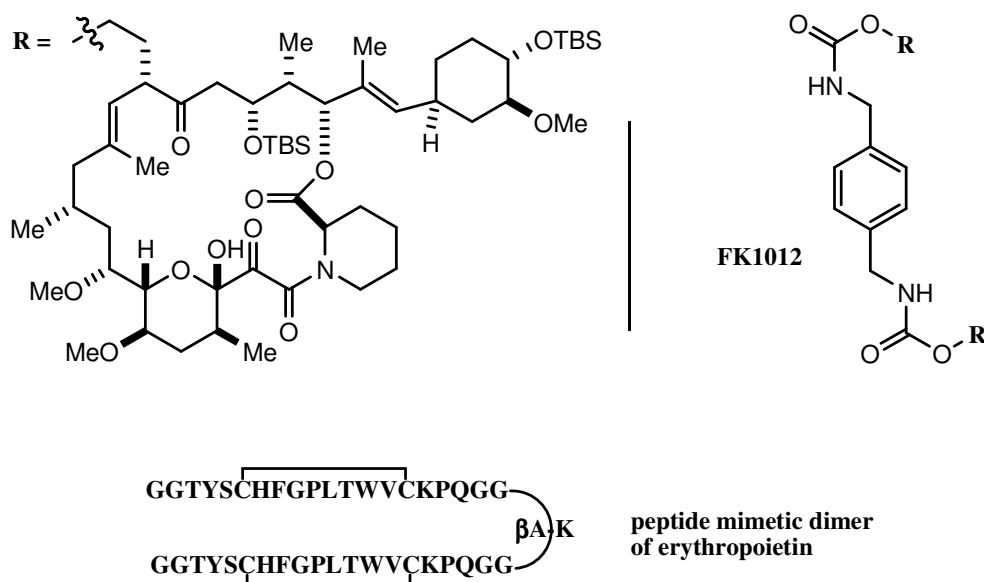


Figure 3.1 Examples of mimetic dimers. β A-K represents a β -alanine/lysine linker.

there are other examples in the literature where the emphasis is placed on the chemical means by which the dimers are constructed. Schreiber and co-workers synthesized homo- and heterodimers of Fmoc-amino acid and hydroxybenzaldehyde derivatives using cross-metathesis on solid support, a highly efficient and effective way to create libraries of diverse compounds (Figure 3.2).⁹¹ With the same goal of generating libraries

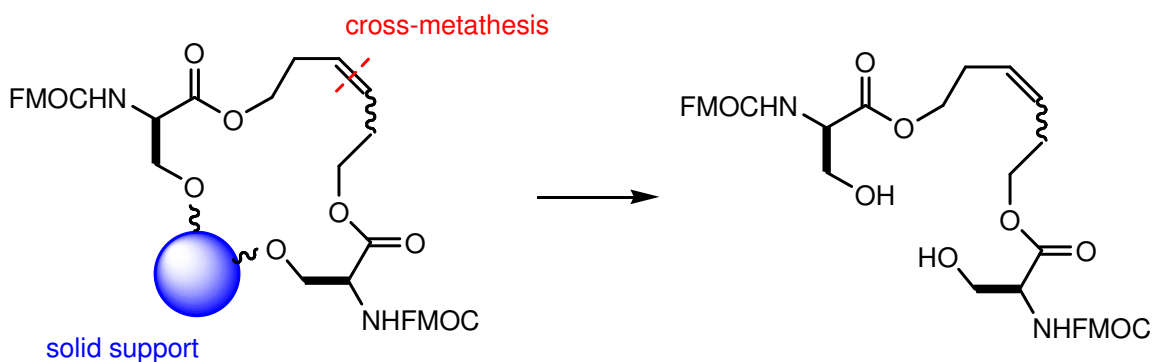


Figure 3.2 Example of a “serine dimer” synthesized by Schreiber.

for screening, Porco and co-workers recently produced a “oxime library” of heterodimers by ligating various alkoxyamine and carbonyl monomers through a process known as “chemical domain shuffling”.⁹² Biological screening against human small cell lung carcinoma (A549) cells revealed a dimer that inhibits growth with an IC_{50} value of $6.2 \mu\text{M}$ (Figure 3.3).⁹² Boger and co-workers screened libraries for antiangiogenic

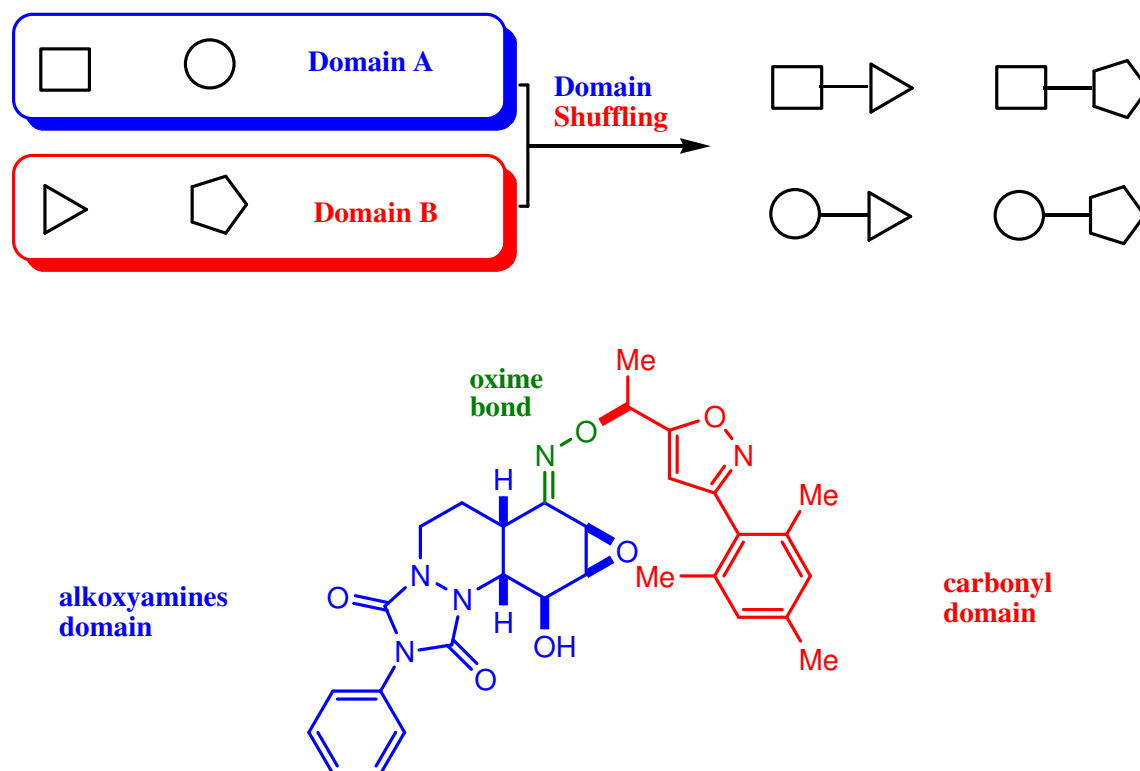


Figure 3.3 Schematic of chemical domain shuffling and the structure of the potent inhibitor of A549 cells that emerged from screening.

molecules that would be more potent once they were “streamlined” to dimers.⁹³ A dimer conceived from the tetramer A6B10C4 was discovered to have improved water-solubility and *in vivo* activity.⁹³ The chemistry utilized to make the modifications was standard amide-bond construction chemistry (Figure 3.4).⁹³ Deviating from the concept

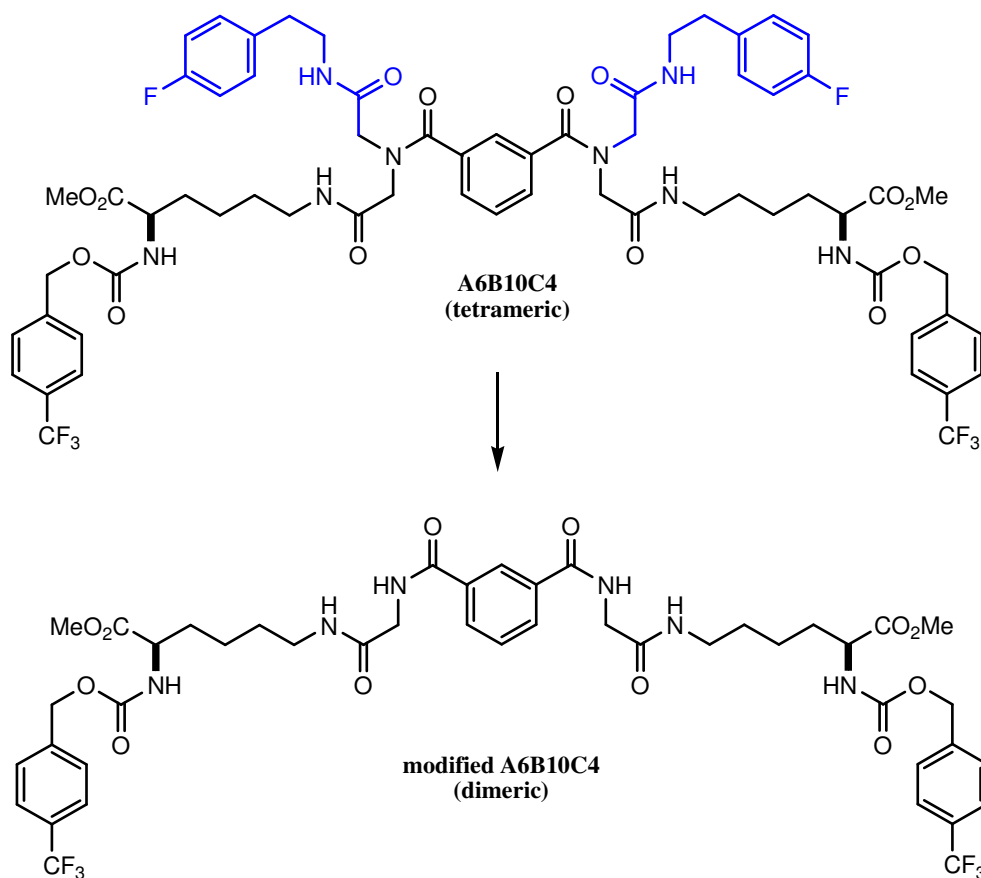


Figure 3.4 Dimer construction by modification of tetrameric A6B10C4.

of target-guided synthesis pioneered by Rideout almost 20 years ago, Sharpless and co-workers screened for bivalent inhibitors by synthesizing them *in situ* from their monomeric parts.⁹⁴ Monomeric alkyne and azides were situated into the active site—one monomeric partner at the peripheral site and the other partner at the active center—of *Electrophorus electricus* acetylcholinesterase (AChE) and “clicked” together by incubating at room temperature for 6 days.⁹⁴ The result from the screen yielded *syn*-TZ2PA6, an AChE inhibitor with a K_d value of 77 fM in *Torpedo californica* and a K_d value of 410 fM in murine AChE (Figure 3.5).⁹⁴

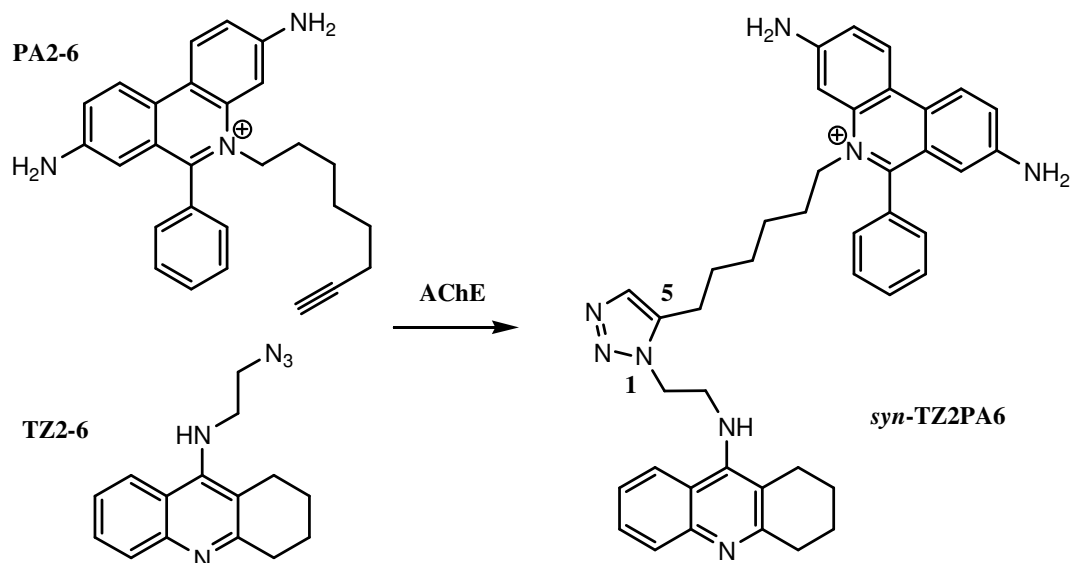


Figure 3.5 *In situ* construction of dimer *syn*-TZ2PA6. Initially, monomer TZ2-6 would be placed in the active center and PA2-6 would be placed in the peripheral site of the AChE binding site. “*Syn*” refers to the 1,5-regioisomer (*anti* would be the 1,4-isomer).

3.1.2 Burgess Method: Dimerizing Peptidomimetics Using Triazine as a Scaffold

Cyanuric chloride (2,4,6-trichloro-1,3,5-triazine) is an attractive compound from a synthetic standpoint. The chlorine atoms could easily be substituted successively with nucleophiles by varying the temperature.⁹⁵ In fact, the simple chemistry allows easy generation of libraries, whether by solid-phase or solution-phase.⁹⁶⁻⁹⁸ Burgess and co-workers have further demonstrated the utility of the triazine scaffold by the generation of a library of bivalent peptidomimetics to screen for binding of TrkA and TrkC.⁹⁹ The syntheses were performed on solid-support using peptidomimetic monomers made in the group.⁹⁹ Designed to be mimics of NGF and NT-3, the dimers were equipped with a fluorescein label to increase the solubility of the compounds and allow them to be detected easily by fluorescence activated cell sorting (FACS) assays.⁹⁹ Although there were many hits from the screening, two homodimers emerged as having the highest fluorescence, dimers consisting only of I and dimers consisting only of II (Figure 3.6).⁹⁹

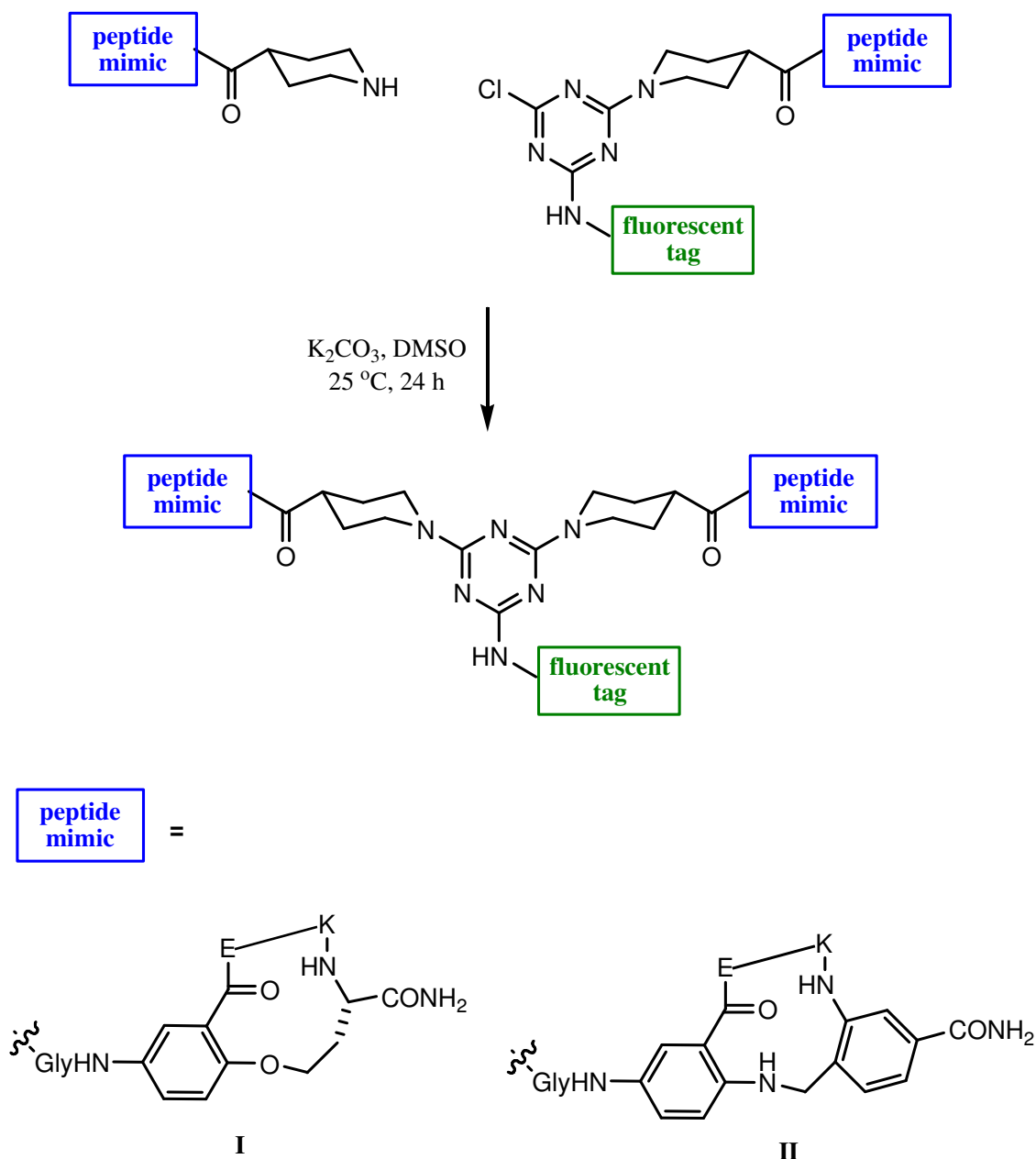


Figure 3.6 Dimerizing peptidomimetics using the Burgess methodology. Homodimers of I bind TrkC, while homodimers of II bind TrkA.

3.2 Triethylene and Hexaethylene Glycol-Based Linking Molecules

Even though the fluorescein label helped the solubility of the dimeric peptide mimetics, solubility still remains a problem. Low water-solubility causes difficulties in creating an assay to test them in addition to rendering them nearly useless as potential

pharmacophores in the drug discovery effort. Attempts to modify the fluorescent tag by adding water-soluble functional groups such as sulfonic acids, carboxylic acids, and hydroxyl groups were unsuccessful and chemically impractical. Not only were the modified fluorescent tags difficult to synthesize, they often exhibited unexpected and unwanted behavior—such as decomposition or lowered water solubility—when anchored to the triazine core. Therefore, alternative approaches using triethylene glycols and hexaethylene glycols were explored to circumvent this problem.

3.2.1 Triethylene Glycols (TEGs) and Hexaethylene Glycols (HEGs)

Triethylene glycols and hexaethylene glycols have been widely-used molecules with applications that greatly vary in scope. Ma and co-workers used both TEGs and HEGs as linker molecules in synthesizing RNA miniduplexes that retained their binding activities while being more resistant to higher temperatures, that is their denaturing temperature (T_m) increased by 24–31 °C.¹⁰⁰ TEGs have been used in the synthesis of π -extended chromophores, with strong absorption in the UV/Vis region, that have a myriad of applications in materials science.¹⁰¹ On the other hand, HEGs have been used as linkers in the construction of non-nucleoside molecules that behave like RNA catalysts.¹⁰² More recently, HEG uses have extended into the syntheses of copolymers¹⁰³ and double hairpin helicates that bind divalent metal ions like copper.¹⁰⁴ Water-solubility may increase up to 27-fold if TEGs or HEGs are incorporated into a desired system.^{105,106} Thus, it is a plausible solution to the solubility problem discussed earlier (Figure 3.7).

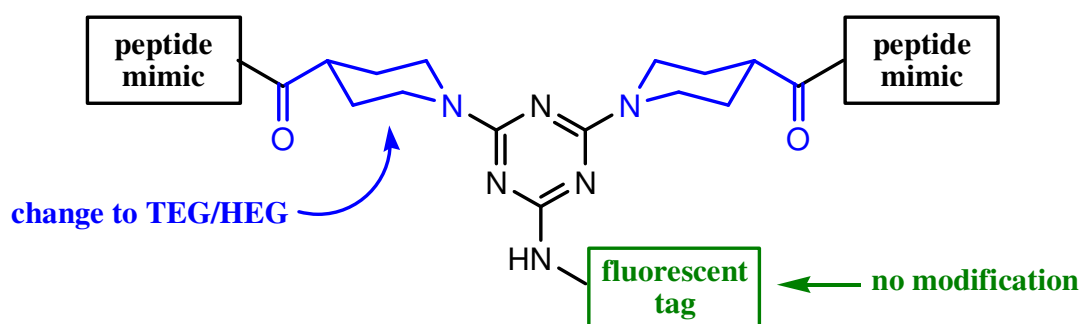


Figure 3.7 A possible solution to the solubility of the Burgess dimeric mimetics.

3.2.2 Linker Designs

Organic chemistry has many cycloaddition reactions involving heteroatoms at its disposal, such as hetero–Diels–Alder and 1,3-dipolar cycloadditions. In their review of click chemistry, Sharpless and co-workers regarded the Huisgen dipolar cycloaddition of azides and alkynes as the “cream of the crop”.¹⁰⁷ The recent interest can be attributed to the fact that 1,2,3-triazole derivatives have a wide range of applications, such as fungicides, herbicides, optical brightening agents, corrosion retardants, and pharmaceuticals.¹⁰⁸ The reaction is robust, taking place in either aqueous or organic environments with a pH range from 4 to 12, and regioselective in the presence of copper(I), giving only 1,4-disubstituted 1,2,3-triazoles.¹⁰⁹ Even with a series of publications adroitly demonstrating its simplicity and efficiency, Sharpless and co-workers silenced any remaining critics with an elegant and imaginative synthesis of triazole dendrimers, perhaps the most significant impact with click chemistry recently published (Figure 3.8).¹¹⁰ Hii and co-workers recently developed a way to desymmetrize

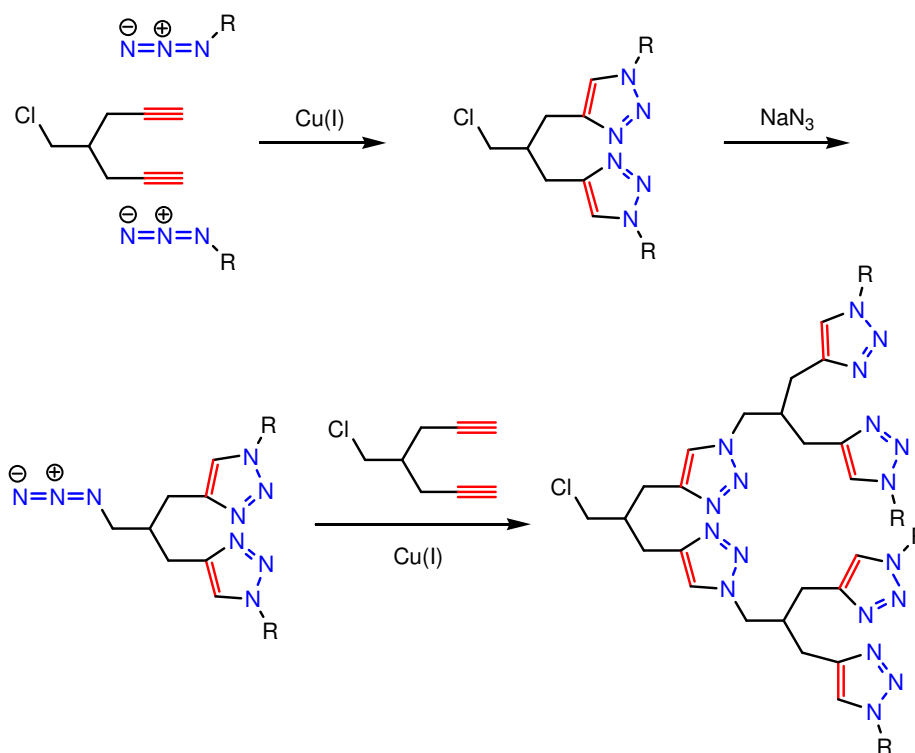


Figure 3.8 Schematic convergent synthesis of triazole dendrimers.

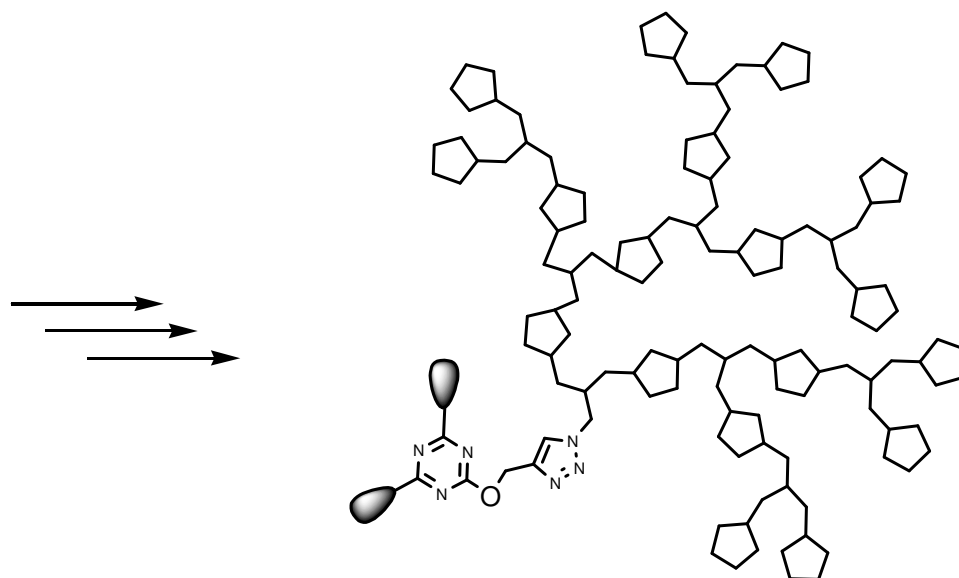


Figure 3.8 continued.

TEG and HEG glycols, which they then applied to the syntheses of PEG chains of variable lengths (Figure 3.9).¹¹¹ Frechet and co-workers utilized poly(vinylacetylene)

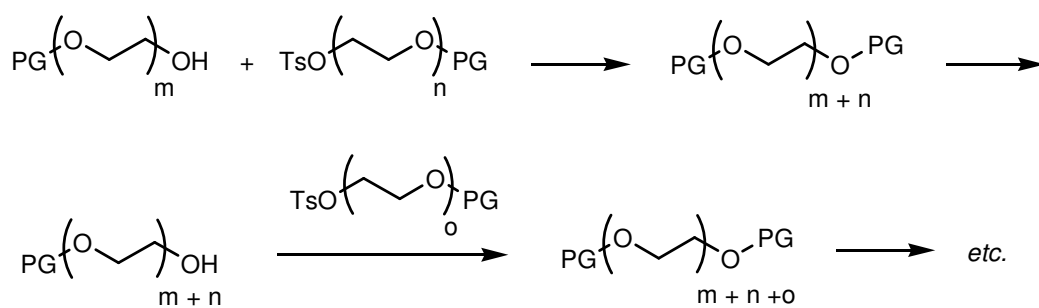


Figure 3.9 Route to small PEG oligomers.

and click chemistry to synthesize linear “dendrimer-like” polymers.¹¹² They were able to repeat the click reactions making up to, but not including, fourth generation dendrons (Figure 3.10).¹¹²

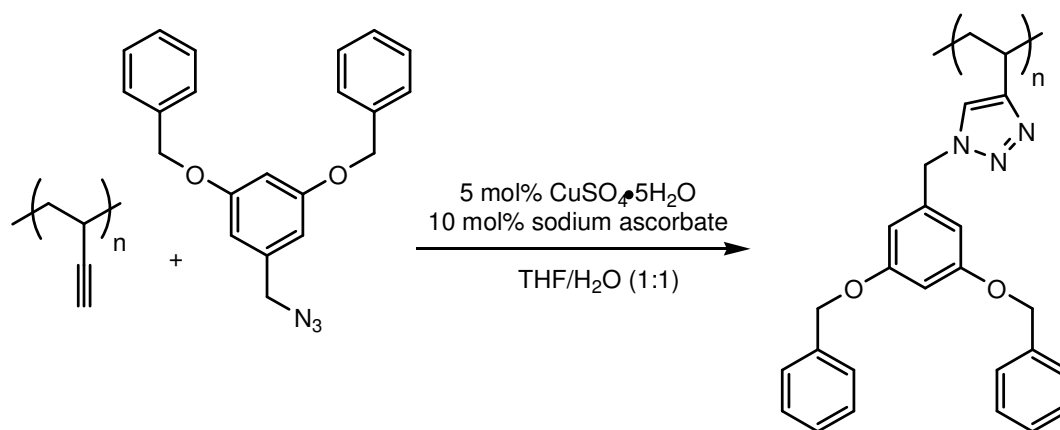


Figure 3.10 Route to first generation dendronized linear polymers.

With the recent trend in mind, the linkers were fathomed to be variable lengths of TEG and HEG components constructed utilizing iterative “click” reactions. Since these are designed to use in bivalent peptidomimetics mimicking neurotrophins, the various distances between the hot spots on the proteins were considered (Figure 3.11). Linkers must be able to span the minimum distance of about 20 Å to a maximum of about 60 Å.

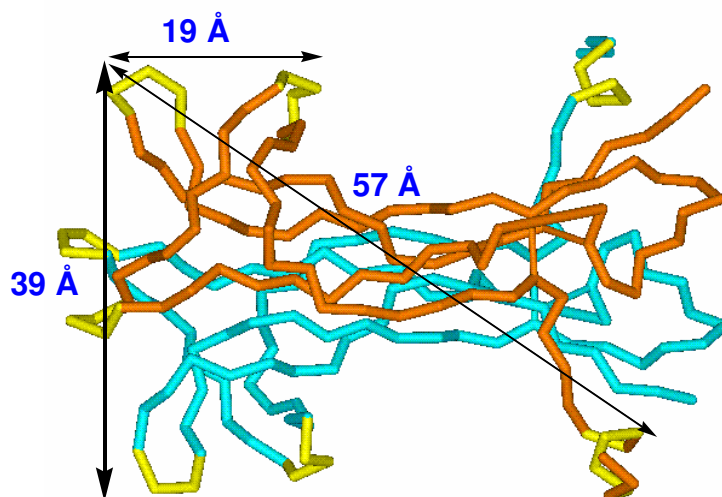


Figure 3.11 Distances between various hot spots (highlighted in yellow) on NGF.

Although the linkers are not meant to be implemented as they are shown below, they are plausible starting points for the actual linkers that will be incorporated into the bivalent peptidomimetics (Figure 3.12). The TEG linkers seem to match the distances on NGF

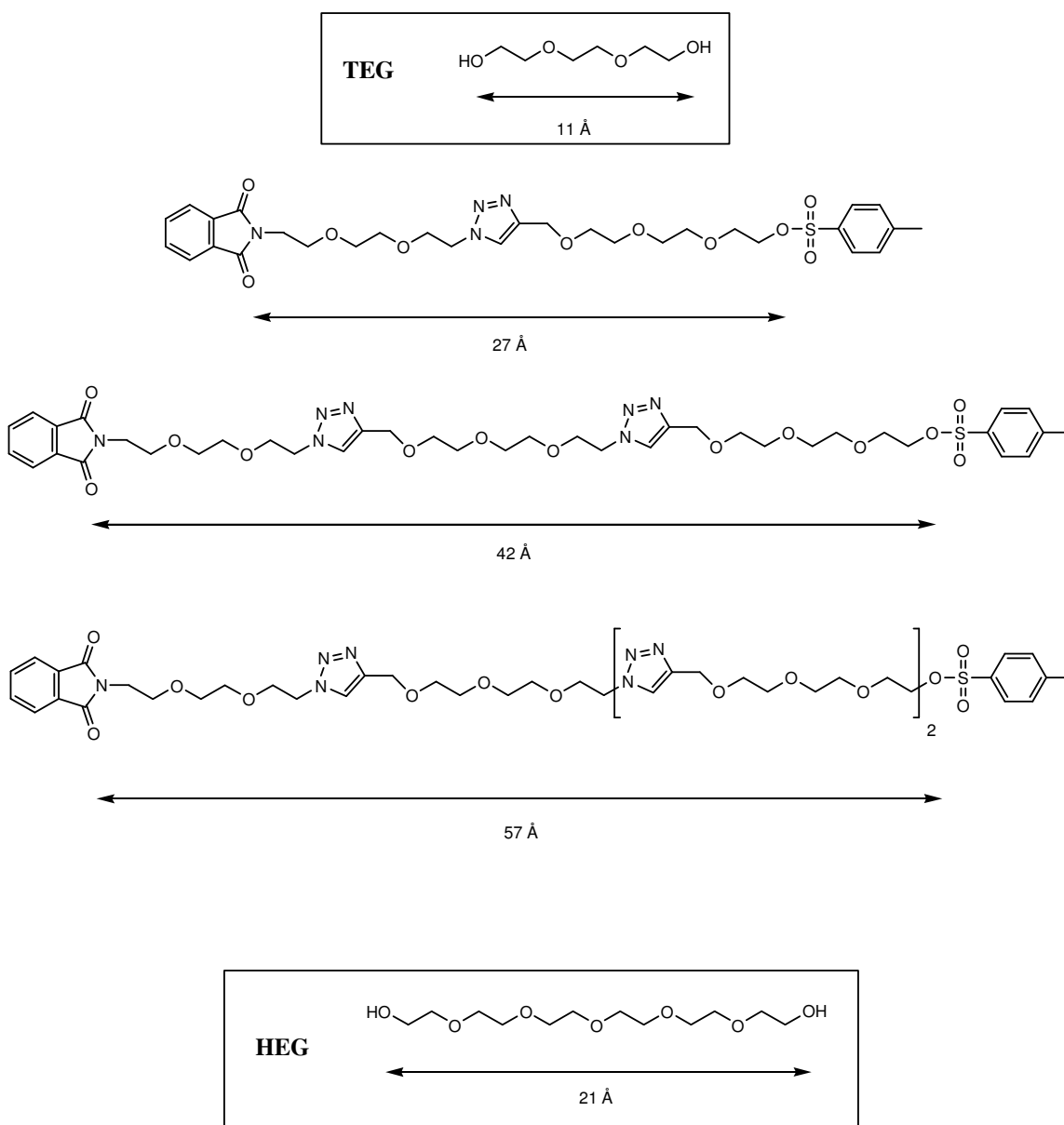


Figure 3.12 Measured distances of the various TEG and HEG linkers.

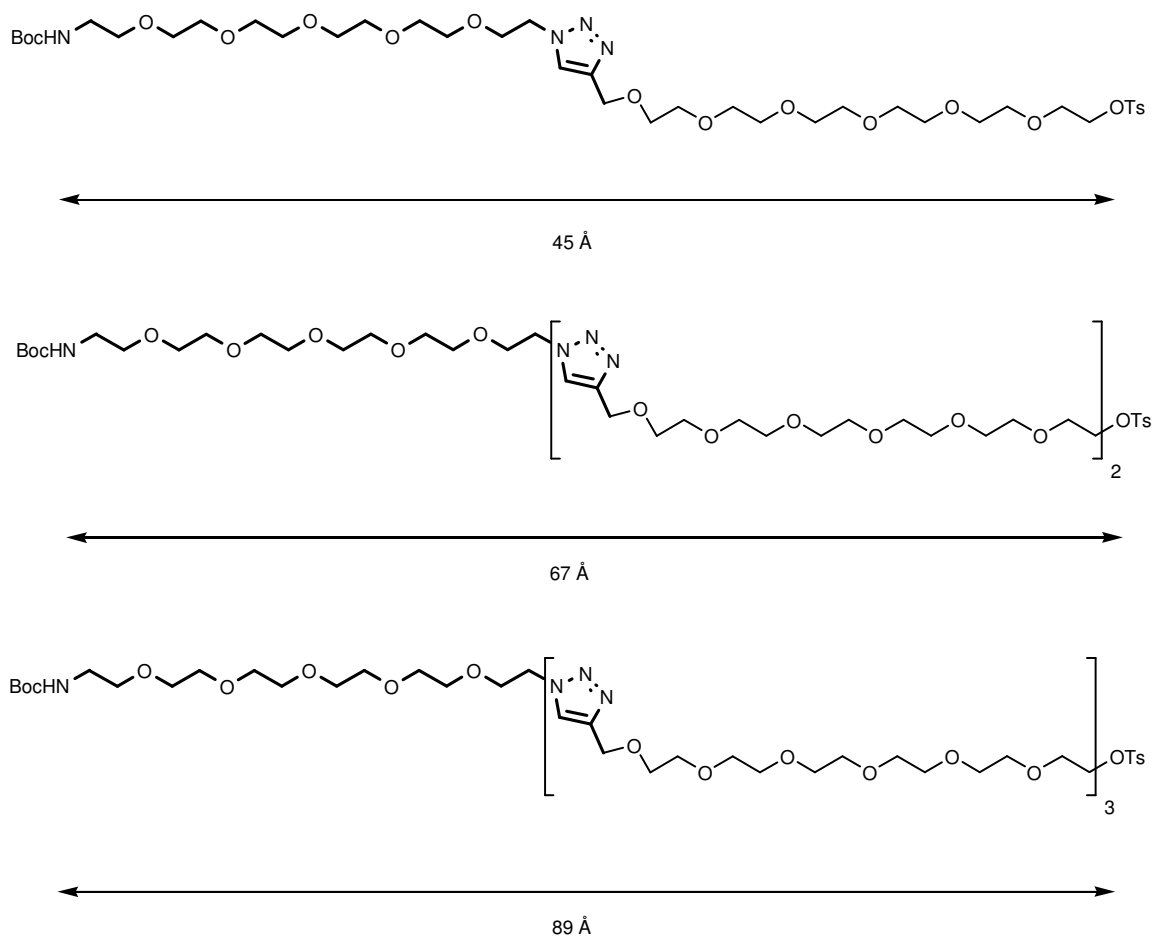
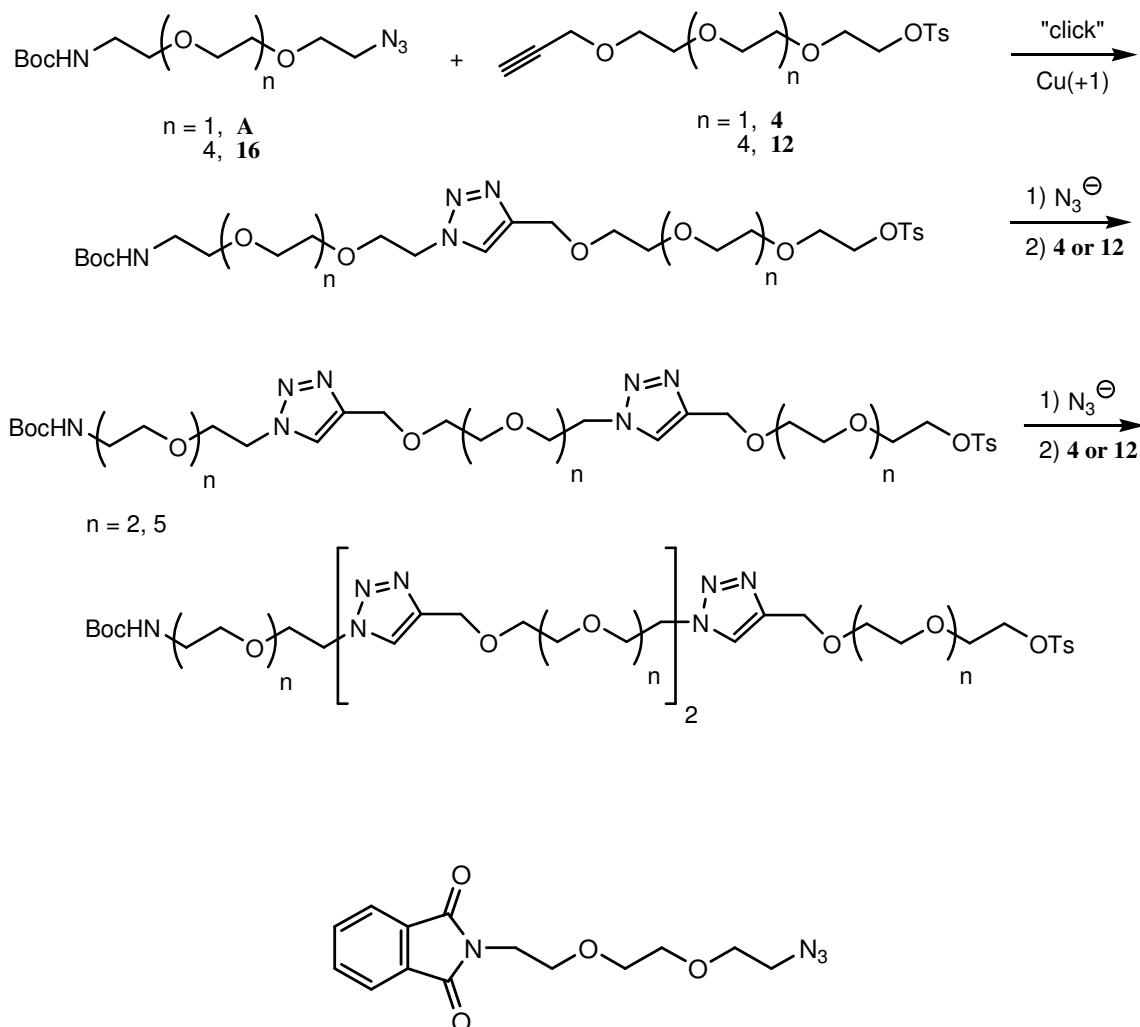


Figure 3.12 continued.

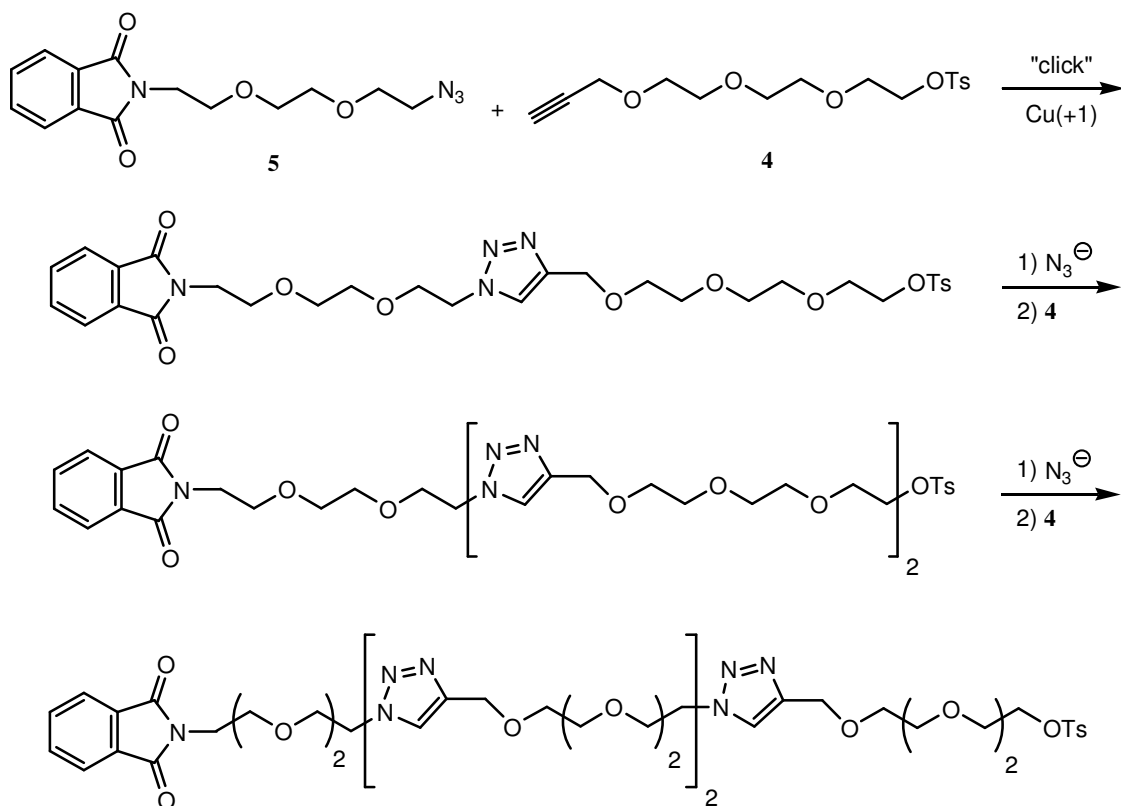
well, while HEG linkers are too long. An important fact to keep in mind about these linkers is the extended form may not be the preferred conformation, therefore HEG linkers might prove to be more useful than they originally seem.

3.2.3 Syntheses of Linkers

Retrosynthetic analysis of the various linkers indicated the starting materials should be compounds **A**, **4**, **12**, and **16** (Scheme 3.1). However, Dr. Genliang Lu discovered that compound **A** was difficult to synthesize on a large scale and the purity was poor. Thus, it was substituted with a more UV active compound **5** (Figure 3.13).

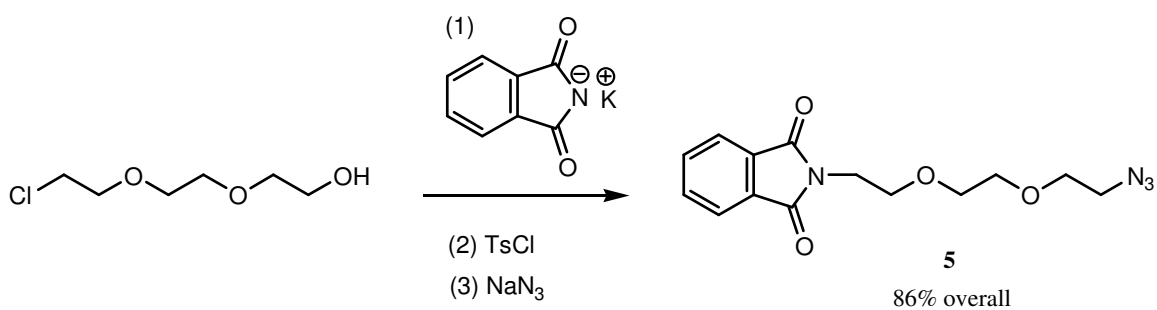
Scheme 3.1 Original synthetic scheme to TEG and HEG linkers of variable lengths.**Figure 3.13** Structure of compound **5**, a substitute for compound **A**.

Compound **5** is a more synthetically attractive compound than **A** because it could easily be visualized under the UV lamp, thus avoiding the need for chemical stains when monitoring reactions, and it is easier to purify chromatographically because of the relatively non-polar isoindoline-1,3-dione component. With the new modification, the original synthetic scheme was changed to accommodate the TEG linker synthesis (Scheme 3.2). Even though compound **12** could be modified to maintain consistency,

Scheme 3.2 Modified synthetic scheme for synthesis of TEG linkers.

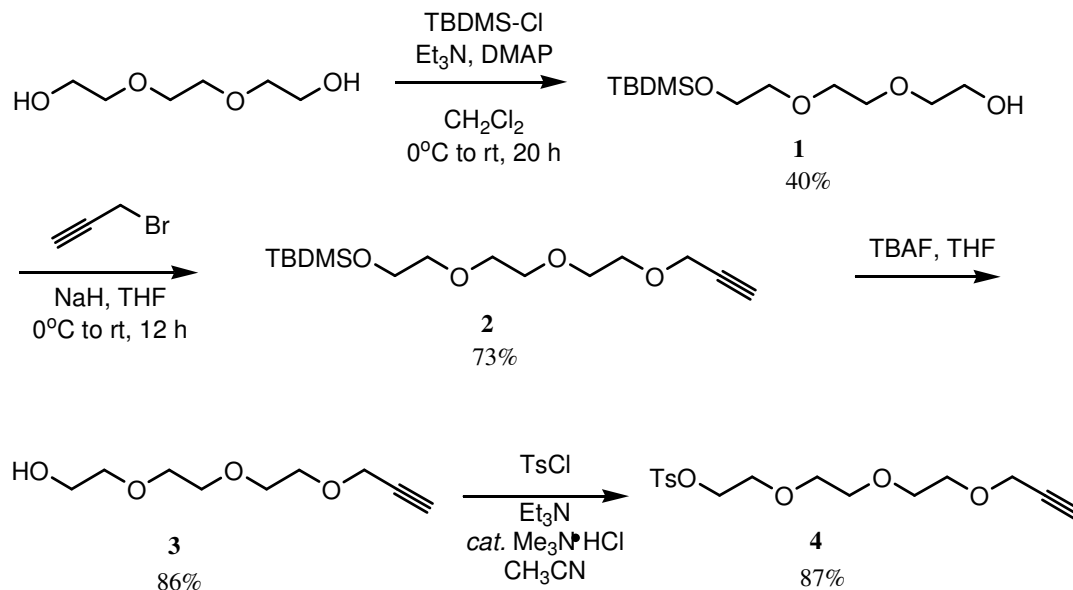
compound **A** was modified when work had already begun on the HEG linker following the original scheme.

The iterative syntheses of the TEG linkers begin with the syntheses of compounds

Scheme 3.3 Synthetic route to compound **5**.

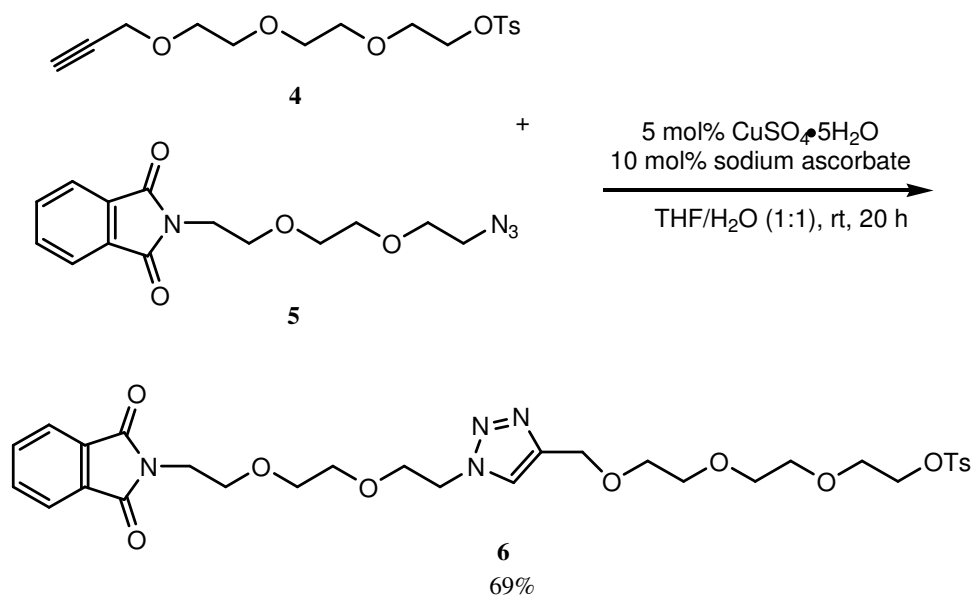
4 and **5**. Dr. Lu performed the synthesis of compound **5**, which begins with nucleophilic substitution of the chlorine on 2-(2-(2-chloroethoxy)ethoxy)ethanol with the commercially-available potassium salt of isoindoline-1,3-dione, tosylation of the hydroxyl group, and displacement of the tosylate by an azide nucleophile afforded the product with an overall yield of 86% (Scheme 3.3). Compound **4** was synthesized in four steps beginning with monoprotection of TEG using TBDMS-Cl, alkylation using propargyl bromide, deprotection of the silyl group using TBAF, and finally tosylation of the free hydroxyl group to yield the desired product (Scheme 3.4).¹¹³⁻¹¹⁵ Combining **4**

Scheme 3.4 Synthetic route to compound **4**.



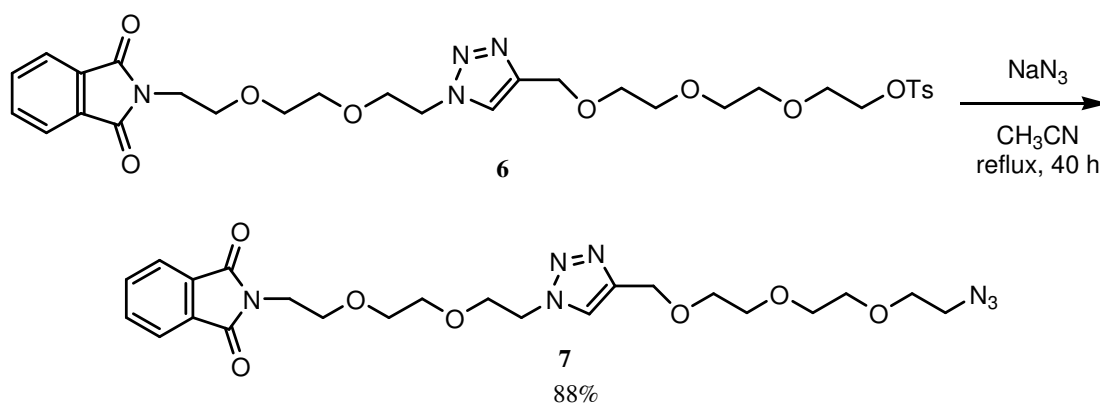
and **5** in the presence of copper(II) with the reducing agent sodium ascorbate yielded the desired compound **6** (Scheme 3.5).¹¹² The click condition was chosen based on a conceptually similar use in the literature by Frechet and co-workers with their synthesis of dendronized linear polymers.¹¹² Another condition used was the generation of Cu(I) *in situ* by the comproportionation of Cu(0) and Cu(II) in *t*-BuOH and water (1:1)¹¹⁶ which produced the triazole product with no improvement in yield. For the sake of consistency

Scheme 3.5 Synthetic route to compound **6**.

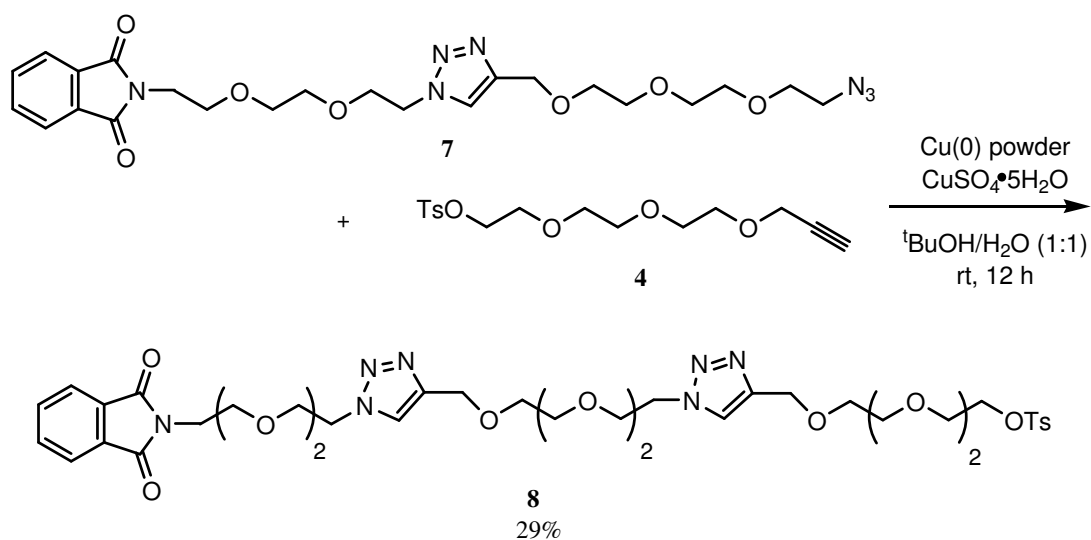


and to potentially avoid any side reactions with the sodium ascorbate reductant, the Fokin method was used for the all subsequent click reactions. Compound **6** was converted to **7** simply by refluxing sodium azide in acetonitrile (Scheme 3.6).¹¹⁷ Compound **7** was then reacted with compound **4** to yield compound **8** (Scheme 3.7).¹¹⁶ The dramatic decrease in

Scheme 3.6 Synthetic route to compound **7**.

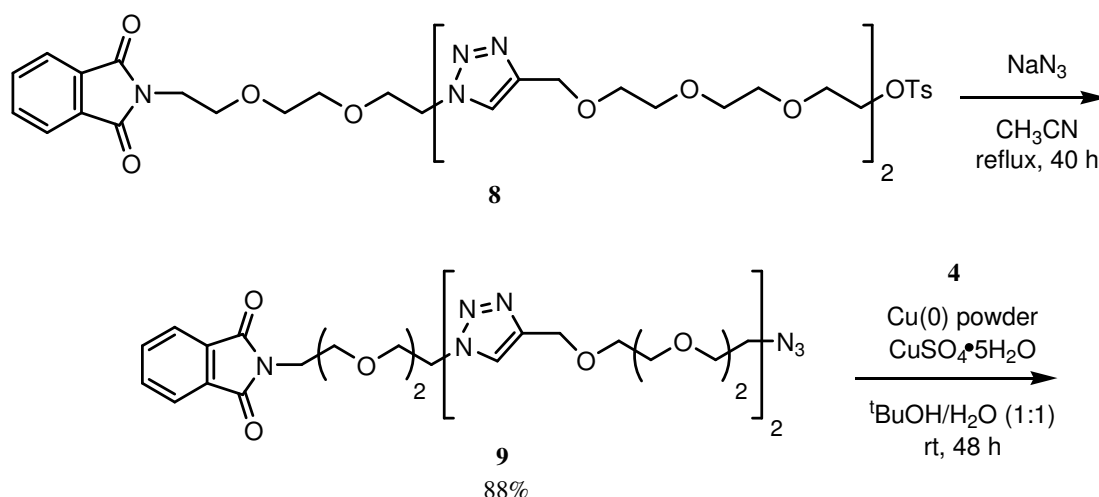


Scheme 3.7 Synthetic route to compound **8**.

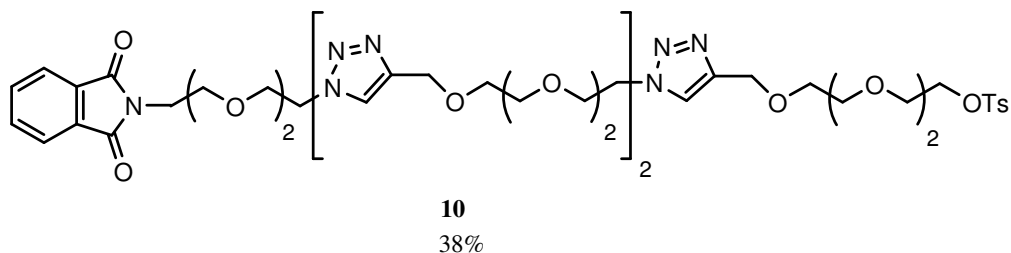


yield can be attributed to the difficulty collecting all the product during the purification step. In addition, as the shear size and bulkiness of the reagents increase, the azide and alkyne functionalities are more shielded from each other, thereby preventing the cycloaddition process.¹¹² Compounds **9** and **10** were synthesized using the previous reaction conditions for the syntheses of compounds **7** and **8**, respectively, with the exception for the synthesis of **10** which ran for 48 hours (Scheme 3.8).^{116,117}

Scheme 3.8 Synthetic routes to compounds **9** and **10**.

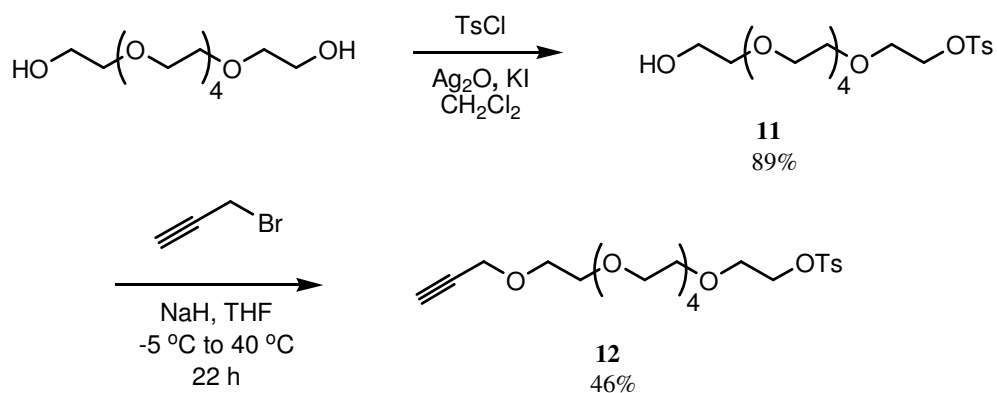


Scheme 3.8 continued.



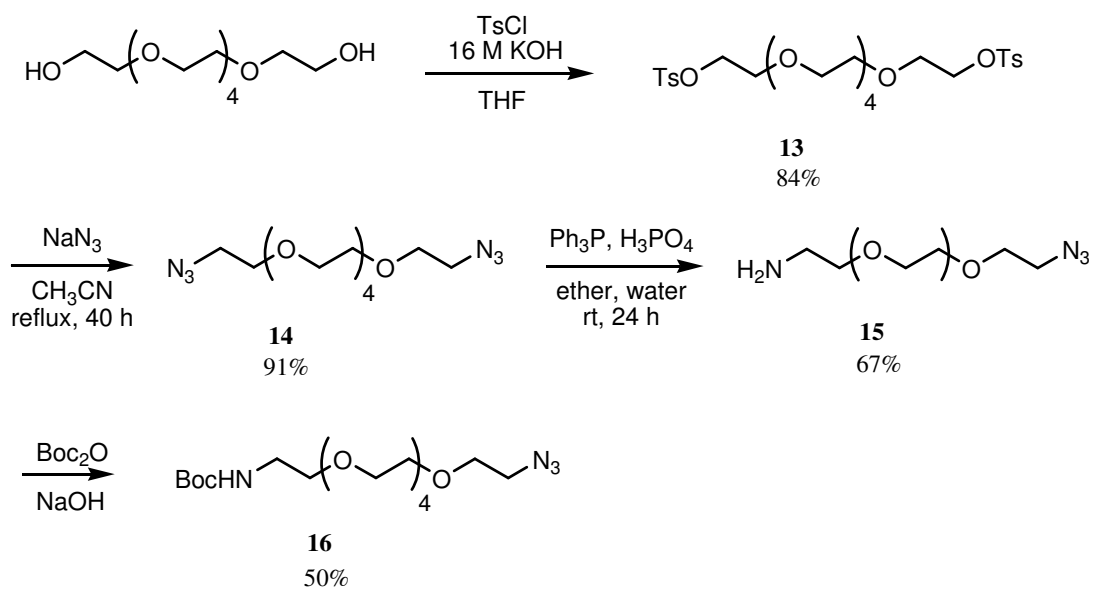
The iterative syntheses of HEG linkers begin with the syntheses of compounds **12** and **16**. Compound **12** was obtained in two steps: monotosylation of HEG using the Hii¹¹¹ method and alkylation with propargyl bromide (Scheme 3.9).¹¹³ The

Scheme 3.9 Synthetic routes to compounds **11** and **12**.



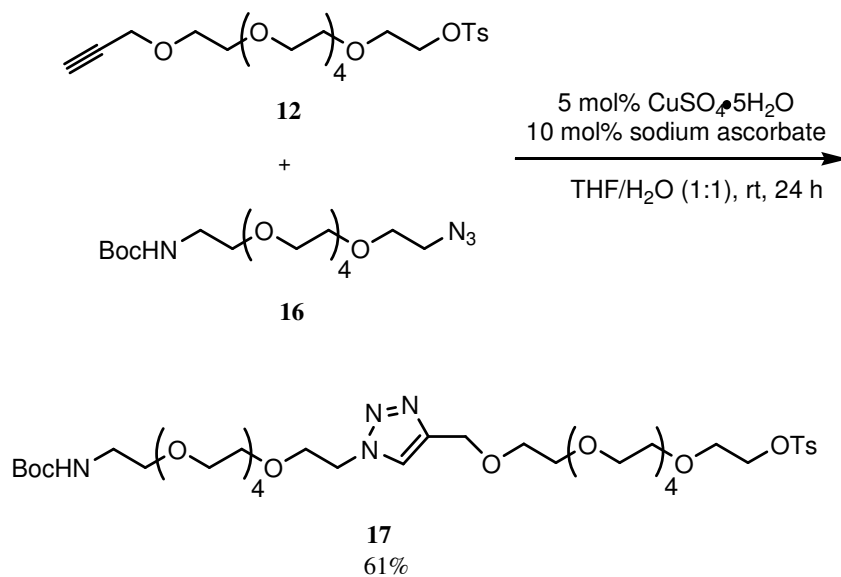
monotosylation developed by Hii was adopted because it was a mild, high-yielding, and high-purity procedure, avoiding the classical approach of using pyridine. The synthesis of **16** required four steps. HEG was ditosylated to give **13**.¹¹⁸ The tosylates were then displaced with azides to give **14**.^{113,119} Monoreduction of one azide functionality gave **15**¹²⁰ and protection of the amine group with *tert*-butylcarbonate (BOC)¹²¹ afforded the desired starting material **16** (Scheme 3.10). Compounds **12** and **16** were reacted using the

Scheme 3.10 Synthetic routes to compounds **13**, **14**, **15**, and **16**.



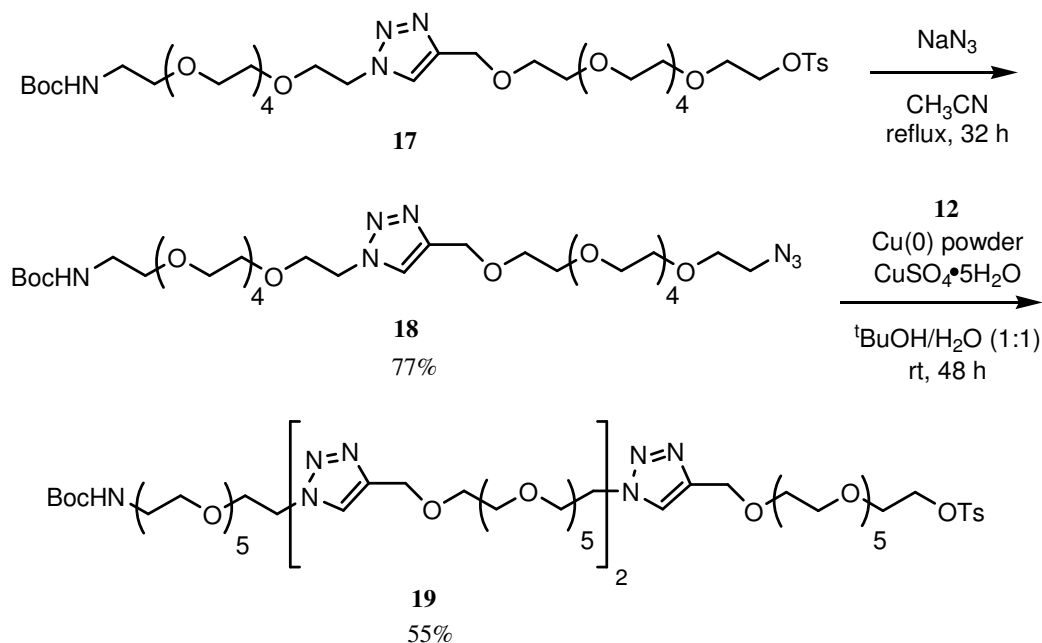
same conditions as in the first click reaction of the TEG linker synthesis for the sake of consistency (Scheme 3.11).¹¹² Note that the yields for **6** and **17** are comparable.

Scheme 3.11 Synthetic route to compound **17**.



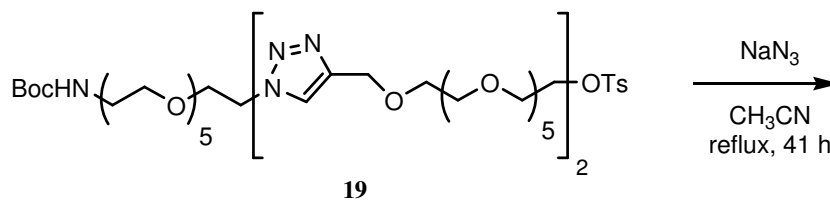
Compound **17** was refluxed with sodium azide in acetonitrile¹¹⁷ to give **18**, which was used to react with **12** in the presence of Cu(I) generated by comproportionation of Cu(0) and Cu(II)¹¹⁶ to give **19** (Scheme 3.12). Finally, the tosylate on **19** was substituted with

Scheme 3.12 Synthetic routes to compounds **18** and **19**.

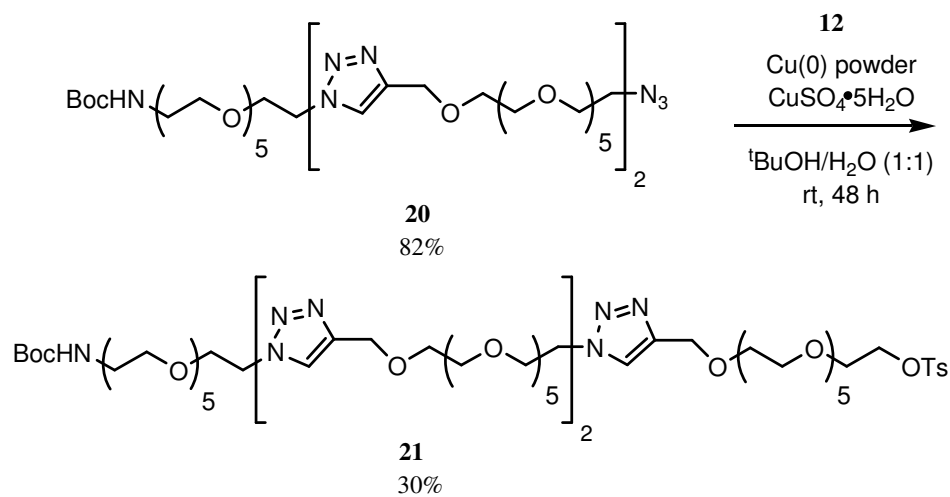


an azide¹¹⁷ to give **20**, which was reacted with **12** in the presence of Cu(I)¹¹⁶ to give the third iterative HEG linker **21** (Scheme 3.13). The yield obtained for **21** is similar to that

Scheme 3.13 Synthetic routes to compounds **20** and **21**.



Scheme 3.13 continued.



obtained for **10**. In general, the purities and yields for TEG linkers are better than those for HEG linkers.

3.2.4 Application of TEG/HEG Units to 3'-O-Protected Nucleotide Triphosphates

One of the many methods currently available for DNA sequencing is the Base Addition Sequencing Scheme (BASS). Crucial to this technique is a set of four nucleotide bases blocked at the 3' position that are fluorescent and labile.¹²² Burgess and co-workers had synthesized a library of 3'-O-labile nucleotide protecting groups and discovered that the nucleotide with the *o*-nitrobenzyl functionality had significant incorporation and could easily be removed by irradiating at 350 nm.¹²² The other protecting groups were not incorporated and some had solubility problems.¹²² A plausible solution would be to modify the nitrobenzyl template using TEG or HEG units to improve water-solubility (Figure 3.14). Compound **24** emerged as an initial target, which could easily be modified later by changing the HEG unit. The synthesis of **24**

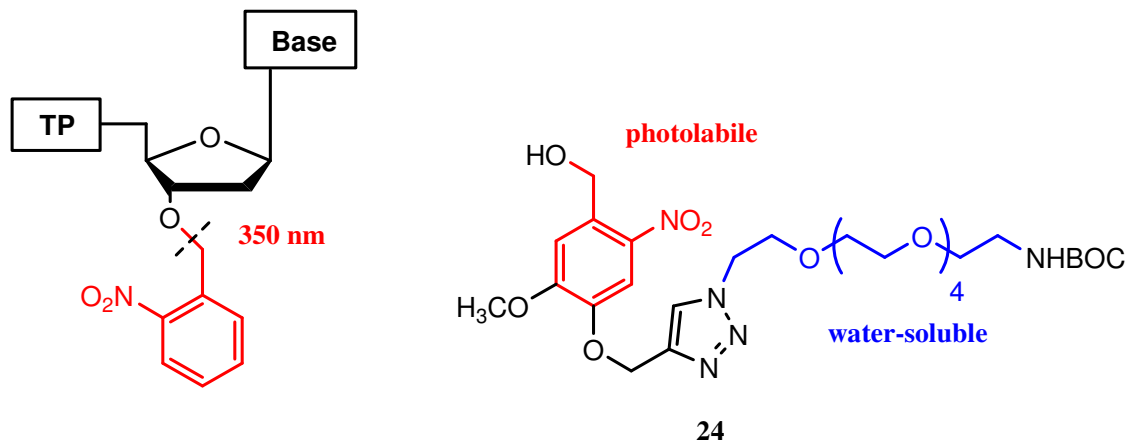
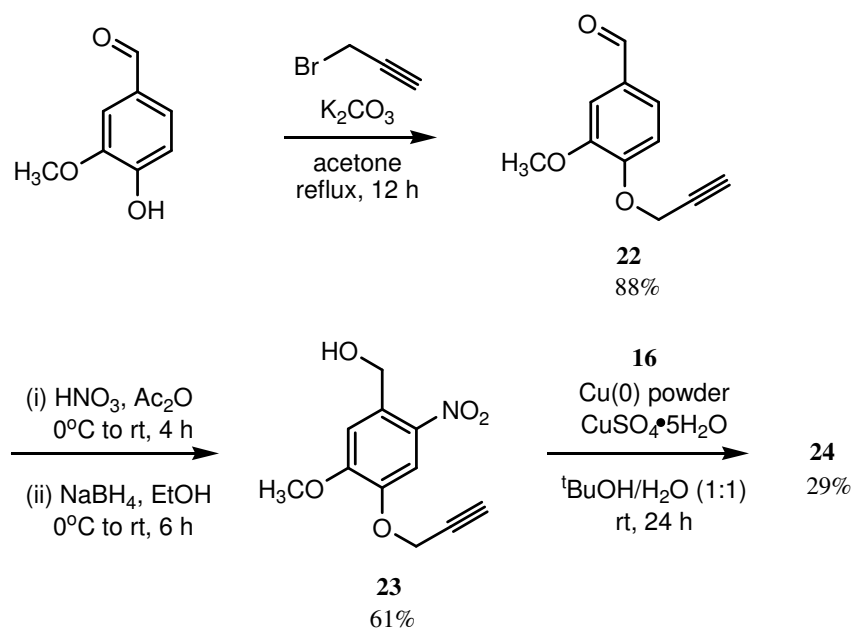


Figure 3.14 Structure of a 3'-O-2-nitrobenzyl nucleotide (left). TP represents a triphosphate group. Modified 3'-O-protecting group incorporating a HEG unit (right).

begins with the alkylation of vanillin using propargyl bromide to give **22**,¹²³ then stepwise nitration and reduction of the aldehyde¹²² to give **23**. Compound **23** was then reacted with **16** using Cu(0) and Cu(II)¹¹⁶ to yield **24** (Scheme 3.14).

Scheme 3.14 Synthetic routes to compounds **22**, **23**, and **24**.



3.2.5 Application of TEG/HEG Units to Isoelectric Point (pI) Markers

A potentially interesting application of the TEG and HEG linkers is in isoelectric focusing (IEF). IEF is a method by which proteins are separated and characterized by their overall net charges, which are zeroes at their respective pIs.¹²⁴ Unlike the standard SDS-PAGE technique, the pH in IEF is not kept constant.¹²⁴ Instead, the proteins move against a pH-gradient until they reach a certain pH where their charges are zero (pH = pI).¹²⁴ Therefore, to characterize and separate proteins or other amphoteric analytes, the pH at the focusing point must be known.¹²⁵ Often reference standards, such as pI makers, are used to help determine the pH.¹²⁵ Low-molecular mass compounds¹²⁵ and peptides¹²⁶ have been used as pI markers. Although triazoles ($pK_a \sim 14$)¹²⁷ can be protonated relatively easily with weak to mild acids in aqueous solutions, 1,4-substituted triazoles require much stronger acidic conditions for protonation.¹²⁸ Abboud and co-workers experimentally determined that 1-methyl-4-phenyltriazole had a pK_{BH^+} of 0.05 in aqueous media.¹²⁸ Therefore, only very strong acids such as hydrobromic acid ($pK_a \sim -9$), perchloric acid ($pK_a \sim -10$), and trifluoromethanesulfonic acid ($pK_a \sim -3$) can completely protonate 1,4-substituted triazole derivatives. Nonetheless, Figure 3.15

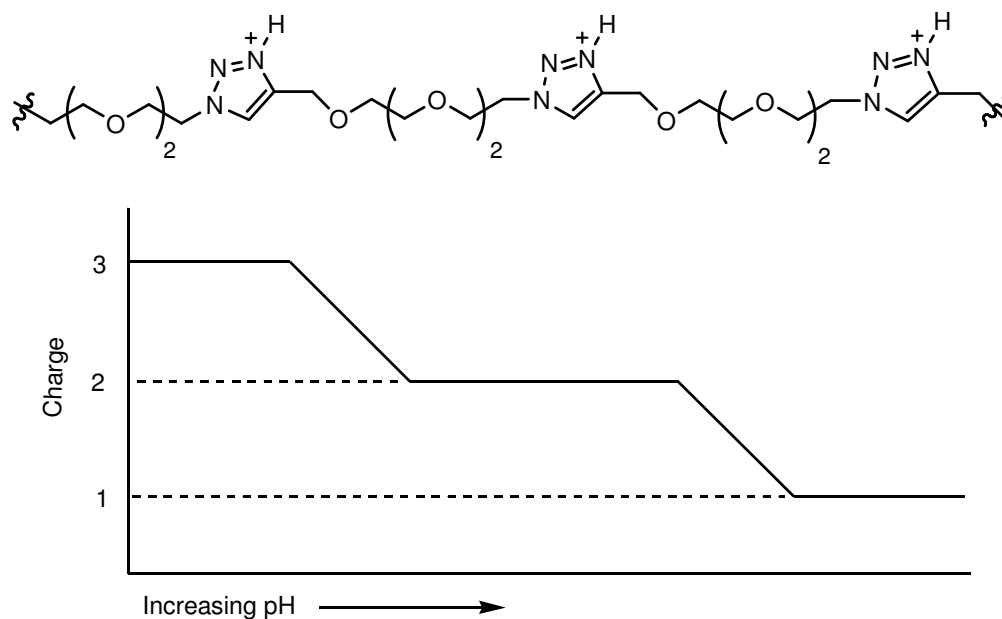


Figure 3.15 A hypothetical relationship between charge and pH of a TEG linker.

shows a hypothetical situation in which a TEG linker—with the appropriate modifications—can serve as a pI marker. In a strongly acidic medium, all three triazoles would be protonated. As the pH is increased, the charge on the linker decreases. Thus, a relationship between charge on the linker and pH of the aqueous environment can be established. Even though the linkers are far from being useful pI markers for protein purification applications, with some modifications and exploratory experimentations, they may become conceptual realities.

3.3 Results and Discussion

Indeed, the utilities of the TEG and HEG linkers extend beyond the realm of serving as merely water-soluble spacers in bivalent peptidomimetic constructions. Although the yields (and the purities, especially for the HEG linkers) from the syntheses of the linker molecules are not quite up to par as reported in the literature for the click reactions, they are tolerable nevertheless. Gauging the purities of these linkers by NMR could be misleading. Some of these compounds may seem clean by NMR, but not so by HPLC. For example, the ^1H NMR spectrum for compound **16** seems to suggest high purity but that is not the case by HPLC, which indicates an 82% purity. Despite the slight setback, these linker molecules, however, could be obtained in gram-quantities. TEG and HEG are relatively cheap, commercially-available starting materials. Simply scaling-up the click reactions would provide enough TEG and HEG linkers for exploring whatever applications a creative mind may conjure.

CHAPTER IV

CONCLUSION

A small set of molecules designed to mimic the *N*-terminus of NGF has been studied computationally. They were all docked successfully onto TrkA. However, successful docking does not simply imply they are all primed candidates and should be synthesized and tested. Likewise, those that did not “fit” well should not be blindly discarded. Modifications to the structures can be made and the compounds studied again. Designing new mimics is a very time-consuming process. α -helices are not trivial targets to mimic for two reasons. First, the attribute of the “helix conformation” is difficult to “design” into a molecule mimic because it is not a low energy conformation. Molecules do not have the propensity to adopt it unless restraints are in place. Second, the designs available in the literature are few and relatively complex with various restraints to hold the molecule in a helix conformation. As research continues in this area, every molecular design should be cherished and regarded as special.

A set of TEG and HEG linkers for use in constructing bivalent peptidomimetics has been synthesized. These linkers serve dual roles. First, they can increase the water-solubility of the bivalent peptidomimetics and, second, they can act as spacer units spanning the distances between the critical hot spots on proteins. In addition, their water-soluble attribute can be applied in making 3'-O-nucleotide protecting groups and pI markers. These linkers can be obtained relatively easy and in large amounts. Generally speaking, the purities for most of the linkers are good, more so for the TEG linkers than the HEG linkers. Considering that the starting units for TEG and HEG linker syntheses are not consistent, the purity for HEG linkers can be improved by using the isoindoline-1,3-dione moiety instead of the BOC for compound **16**. Also, the synthetic scheme of **12** can be modified to give a purer compound—perhaps monoprotection/deprotection like in the synthesis of **4**. Whether making nucleotide protecting groups or pI markers or optimizing conditions to get purer linkers, further work in this area, it seems, is inevitable.

REFERENCES

- (1) Zubay, G. L. *Biochemistry*, 4th ed.; Wm. C. Brown Publishers: Dubaque, Iowa, 1998.
- (2) Park, C.; Burgess, K. J. *Comb. Chem.* **2001**, *3*, 257-266.
- (3) Orner, B. P.; Ernst, J. T.; Hamilton, A. D. *J. Am. Chem. Soc.* **2001**, *123*, 5382-5383.
- (4) (a) Marchesini, S. Secondary Protein Structure: 3.10 helix. <http://www.med.unibs.it/~marchesi/310.html> (accessed 9/29/05). (b) Janes, R. W. First Year: Basic Biochemistry. <http://www.qmul.ac.uk/~ugbt760/bas02new.doc> (accessed 9/29/05)
- (5) A Server for b-Turn Types Prediction. <http://bioinformatics.uams.edu/raghava/beteturns/method.html> (accessed 9/29/05).
- (6) Hu, Z.; Ma, B.; Wolfson, H.; Nussinov, R. *Proteins: Structure, Function, and Genetics* **2000**, *39*, 331-342.
- (7) Stites, W. E. *Chem. Rev.* **1997**, *97*, 1233-1250.
- (8) Conte, L. L.; Chothia, C.; Janin, J. *J. Mol. Biol.* **1999**, *285*, 2177-2198.
- (9) Ma, B.; Elkayam, T.; Wolfson, H.; Nussinov, R. *PNAS* **2003**, *100*, 5772-5777.
- (10) Arkin, M. R.; Wells, J. A. *Nature Reviews: Drug Discovery* **2004**, *3*, 301-317.
- (11) DeLano, W. L. *Curr. Opin. Struc. Bio.* **2002**, *12*, 14-20.
- (12) Sipkins, D. A.; Wei, X.; Wu, J. W.; Runnels, J. M.; Cote, D.; Means, T. K.; Luster, D. A.; Scadden, D. T.; Lin, C. P. *Nature* **2005**, *435*, 969-974.
- (13) AMD3100: CXCR4 Chemokine Receptor Antagonist. <http://www.sigmaaldrich.com/img/assets/13760/amd3100.pdf> (accessed 9/29/05).
- (14) Li, L.; Thomas, R. M.; Suzuki, H.; De Brabander, J. K.; Wang, X.; Harran, P. G. *Science* **2004**, *305*, 1471-1474.
- (15) Montalto, M. C.; Collard, C. D.; Buras, J. A.; Reenstra, W. R.; McClaine, R.; Gies, D. R.; Rother, R. P.; Stahl, G. L. *J. Immunol.* **2001**, *166*, 4148-4153.
- (16) Cochran, A. G. *Chemistry & Biology.* **2000**, *7*, R85-R94.
- (17) Berman, A. E.; Kozlova, N. I.; Morozovich, G. E. *Biochemistry (Moscow)* **2003**, *68*, 1284-1299.

- (18) Newham, P.; Humphries, M. J. *Molecular Medicine Today* **1996**, *96*, 304-313.
- (19) Gadek, T. R.; Nicholas, J. B. *Biochem. Pharm.* **2003**, *65*, 1-8.
- (20) Jackson, D. Y. *Curr. Pharm. Des.* **2002**, *8*, 1229-1253.
- (21) Boturyn, D.; Coll, J.-L.; Garanger, E.; Favrot, M.-C.; Dumy, P. *J. Am. Chem. Soc.* **2004**, *126*, 5730-5739.
- (22) D'Alessio, P.; Moutet, M.; Coudrier, E.; Darquenne, S.; Chaudiere, J. *Free Radical Biology & Medicine* **1998**, *24*, 979-987.
- (23) Gadek, T. R.; Burdick, D. J.; McDowell, R. S.; Stanley, M. S.; Marsters, J. C., Jr.; Paris, K. J.; Oare, D. A.; Reynolds, M. E.; Ladner, C.; Zioncheck, K. A.; Lee, W. P.; Gribbling, P.; Dennis, M. S.; Skelton, N. J.; Tumas, D. B.; Clark, K. R.; Keating, S. M.; Beresini, M. H.; Tilley, J. W.; Presta, L. G.; Bodary, S. C. *Science* **2002**, *295*, 1086-1089.
- (24) Wiesmann, C.; Ultsch, M. H.; Bass, S. H.; de Vos, A. M. *Nature* **1999**, *401*, 184-188.
- (25) Pattarawarapan, M.; Burgess, K. *J. Med. Chem.* **2003**, *46*, 5277-5291.
- (26) Burgess, K. *Acc. Chem. Res.* **2001**, *34*, 826-835.
- (27) Hippenmeyer, P. J.; Ruminski, R. P.; Rico, J. G.; Sharon, H.; Lu, D.; Griggs, D. W. *Antiviral Research* **2002**, *55*, 169-178.
- (28) Lee, H. B.; Zaccaro, M. C.; Pattarawarapan, M.; Roy, S.; Saragovi, H. U.; Burgess, K. *J. Org. Chem.* **2004**, *69*, 701-713.
- (29) Reyes, S. J.; Burgess, K. *Tetrahedron: Asymmetry* **2005**, *16*, 1061-1069.
- (30) Maliartchouk, S.; Feng, Y.; Ivanisevic, L.; Debeir, T.; Cuello, A. C.; Burgess, K.; Saragovi, H. U. *Mol. Pharm.* **2000**, *57*, 385-391.
- (31) Ogbu, C. O.; Qabar, M. N.; Boatman, P. D.; Urban, J.; Meara, J. P.; Ferguson, M. D.; Tulinsky, J.; Lum, C.; Babu, S.; Blaskovich, M. A.; Nakanishi, H.; Ruan, F.; Cao, B.; Minarik, R.; Little, T.; Nelson, S.; Nguyen, M.; Gall, A.; Kahn, M. *Bioorg. Med. Chem. Lett.* **1998**, *8*, 2321.
- (32) Fink, B. E.; Kym, P. R.; Katzenellenbogen, J. A. *J. Am. Chem. Soc.* **1998**, *120*, 4334.
- (33) Johannesson, P.; Lindeberg, G.; Tong, W.; Gogoll, A.; Karlen, A.; Hallberg, A. *J. Med. Chem.* **1999**, *42*, 601.

- (34) Golebiowski, A.; Klopfenstein, S. R.; Chen, J. J.; Shao, X. *Tet. Lett.* **2000**, *41*, 4841-4844.
- (35) Pfeifer, M. E.; Moehle, K.; Linden, A.; Robinson, J. *Helv. Chim. Acta* **2000**, *83*, 444.
- (36) Kutzki, O.; Park, H. S.; Ernst, J. T.; Orner, B. P.; Hamilton, A. D. *J. Am. Chem. Soc.* **2002**, *124*, 11838-11839.
- (37) Ernst, J. T.; Becerril, J.; Park, H. S.; Yin, H.; Hamilton, A. D. *Angew. Chem. Int. Ed.* **2003**, *42*, 535-539.
- (38) Yin, H.; Lee, G.; Sedey, K. A.; Rodriguez, J. M.; Wang, H.-G.; Sebti, S. M.; Hamilton, A. D. *J. Am. Chem. Soc.* **2005**, *127*, 5463-5468.
- (39) Yin, H.; Lee, G.; Kutzki, O.; Park, H. S.; Orner, B. P.; Ernst, J. T.; Wang, H.-G.; Sebti, S. M.; Hamilton, A. D. *J. Am. Chem. Soc.* **2005**, *127*, 10191-10196.
- (40) Jacoby, E. *Bioorg. Med. Chem. Lett.* **2002**, *12*, 891-893.
- (41) Horwell, D. C.; Howson, W.; Nolan, W. P.; Ratcliffe, G. S.; Rees, D. C.; Willems, H. *Tetrahedron* **1995**, *51*, 203-216.
- (42) Marrone, T. J.; Briggs, J. M.; McCammon, J. A. *Annu. Rev. Pharmacol. Toxicol.* **1997**, *37*, 71-90.
- (43) Joseph-McCarthy, D. *Pharmacology & Therapeutics* **1999**, *84*, 179-191.
- (44) McConkey, B. J.; Sobolev, V.; Edelman M. *Curr. Sci.* **2002**, *83*, 845-856.
- (45) (a) Affinity, December 1998. Molecular Simulations, Inc.: San Diego, 1998. (b) Janin, J. *Protein Science* **2005**, *14*, 278-283.
- (46) MacKerell, A.D., Jr. Pharmaceutical Chemistry. http://www.pharmacy.umaryland.edu/courses/PHAR531/lectures/compchem_1.html (accessed 9/29/05)
- (47) Ajay, W.; Walters, P.; Murcko, M. *J. Med. Chem.* **1998**, *41*, 3314.
- (48) Luo, Z.; Wang, R.; Lai, L. *J. Chem. Inf. Comput. Sci.* **1996**, *36*, 1187.
- (49) Schneider, G.; Bohm, H. J. *Drug Discovery Today* **2002**, *7*, 64.
- (50) Kuntz, I. D. The Official UCSF Dock Web-site. <http://www.cmpharm.ucsf.edu/> (accessed 9/29/05)
- (51) Martin, Y. C. *J. Med. Chem.* **1992**, *35*, 2145-2154.

- (52) Kuntz, I. D. *Science* **1992**, *257*, 1078-1082.
- (53) Lauri, G.; Bartlett, P. A. *J. Comput.-Aided Mol. Design* **1994**, *8*, 51-66.
- (54) Luty, B. A.; Wasserman, Z. R.; Stouten, P. F. W.; Hodge, C. N.; Zacharias, M.; McCammon, J. A. *J. Comp. Chem.* **1995**, *16*, 454-464.
- (55) Stouten, P. F. W.; Froemmel, C.; Nakamura, H.; Sander, C. *Molecular Simulation* **1993**, *10*, 97-120.
- (56) Chang, G.; Guida, W. C.; Still, W. C. *J. Am. Chem. Soc.* **1989**, *111*, 4379-4386.
- (57) Saunders, M.; Houk, K. N.; Wu, Y.; Still, W. C.; Lipton, M.; Chang, G.; Guida, W. C. *J. Am. Chem. Soc.* **1990**, *112*, 1419-1427.
- (58) Wilson, S. R.; Cui, W.; Moskowitz, J. W.; Schmidt, K. E. *Tet. Lett.* **1988**, *29*, 4373-4376.
- (59) Nezami, A.; Luque, I.; Kimura, T.; Kiso, Y.; Freire, E. *Biochemistry* **2002**, *41*, 2273-2280.
- (60) Read, M. A.; Wood, A. A.; Harrison, J. R.; Gowan, S. M.; Kelland, L. R.; Dosanjh, H. S.; Neidle, S. *J. Med. Chem.* **1999**, *42*, 4538-4546.
- (61) Wiesmann, C.; de Vos, A. M. *Cell. Mol. Life Sci.* **2001**, *58*, 748-759.
- (62) Zampieri, N.; Chao, M. V. *Science* **2004**, *304*, 833-834.
- (63) Urfer, R.; Tsoulfas, P.; O'Connell, L.; Presta, L. G. *Biochemistry* **1997**, *36*, 4775-4781 and references therein.
- (64) Saragovi, H. U.; Zaccaro, M. C. *Curr. Pharm. Design* **2002**, *8*, 2201-2216.
- (65) He, X.-L.; Garcia, K. C. *Science* **2004**, *304*, 870-875.
- (66) Kaplan, D. R.; Miller, F. D. *Curr. Opin. Neurobio.* **2000**, *10*, 381-391.
- (67) Ito, M.; Sakai, N.; Ito, K.; Mizobe, F.; Hanada, K. *J. Antibiotics* **1999**, *52*, 224-230.
- (68) Owolabi, J. B.; Rizkalla, G.; Tehim, A.; Ross, G. M.; Riopelle, R. J. *J. Pharm. Expt. Ther.* **1999**, *289*, 1271-1276.
- (69) Labie, C.; Lafon, C.; Marmouget, C.; Saubusse, P.; Fournier, J. *British J. Pharm.* **1999**, *127*, 139-144.

- (70) LeSauteur, L.; Cheung, N. K. V.; Lisbona, R.; Saragovi, H. U. *Nature Biotech.* **1996**, *14*, 1120-1122.
- (71) Shepherd, N. E.; Abbenante, G.; Fairlie, D. P. *Angew. Chem. Int. Ed.* **2004**, *43*, 2687-2690.
- (72) Calvo, J. C.; Choconta, K. C.; Diaz, D.; Orozco, O.; Bravo, M. M.; Espejo, F.; Salazar, L. M.; Guzman, F.; Patarroyo, M. E. *J. Med. Chem.* **2003**, *46*, 5389-5394.
- (73) Peczuh, M. W.; Hamilton, A. D. *Chem. Rev.* **2000**, *100*, 2479-2494.
- (74) Asada, S.; Choi, Y.; Uesugi, M. *J. Am. Chem. Soc.* **2003**, *125*, 4992-4993.
- (75) Fairlie, D. P.; West, M. L.; Wong, A. K. *Curr. Med. Chem.* **1998**, *5*, 29-62.
- (76) Jackson, D. Y.; King, D. S.; Chmielewski, J.; Singh, S.; Schultz, P. G. *J. Am. Chem. Soc.* **1991**, *113*, 9391-9392.
- (77) Phelan, J. C.; Skelton, N. J.; Braisted, A. C.; McDowell, R. S. *J. Am. Chem. Soc.* **1997**, *119*, 455-460.
- (78) Yu, C.; Taylor, J. W. *Bioorg. Med. Chem.* **1999**, *7*, 161-165.
- (79) Ruan, F.; Chen, Y.; Hopkins, P. B. *J. Am. Chem. Soc.* **2002**, *124*, 11838-11839.
- (80) Nicolaou, K. C.; Snyder, S. A. *Classics in Total Synthesis II*. Wiley-VCH: Weinheim, Germany, 2003, pp. 365-378.
- (81) Jones, S.; Thornton, J. M. *Proc. Natl. Acad. Sci.* **1996**, *93*, 13-20.
- (82) Accelrys, Inc., Cerius2 Modeling Environment, Release 4.0, Accelrys, Inc.: San Diego, 1999.
- (83) Mammen, M.; Choi, S.-K.; Whitesides, G. M. *Angew. Chem. Int. Ed.* **1998**, *37*, 2755-2794.
- (84) Bertozzi, C. R.; Kiessling, L. L. *Science* **2001**, *291*, 2357-2364.
- (85) Gestwicki, J. E.; Cairo, C. W.; Strong, L. E.; Oetjen, K. A.; Kiessling, L. L. *J. Am. Chem. Soc.* **2002**, *124*, 14922-14933.
- (86) Austin, D. J.; Crabtree, G. R.; Schreiber, S. L. *Chem. & Biol.* **1994**, *1*, 131-136.
- (87) Seed, B. *Chem. & Biol.* **1994**, *1*, 125-129.

- (88) Wrighton, N. C.; Balasubramanian, P.; Barbone, F. P.; Kashyap, A. K.; Farrell, F. X.; Jolliffe, L. K.; Barrett, R. W.; Dower, W. J. *Nature Biotech.* **1997**, *15*, 1261-1265.
- (89) Ho, S. N.; Biggar, S. R.; Spencer, D. M.; Schreiber, S. L.; Crabtree, G. R. *Nature* **1996**, *382*, 822-826.
- (90) Pruschy, M. N.; Spencer, D. M.; Kapoor, T. M.; Miyake, H.; Crabtree, G. R.; Schreiber, S. L. *Chem. & Biol.* **1994**, *1*, 163-172.
- (91) Blackwell, H. E.; Clemons, P. A.; Schreiber, S. L. *Org. Lett.* **2001**, *3*, 1185-1188.
- (92) Su, S.; Acquilano, D. E.; Arumugasamy, J.; Beeler, A. B.; Eastwood, E. L.; Giguere, J. R.; Lan, P.; Lei, X.; Min, G. K.; Yeager, A. R.; Zhou, Y.; Panek, J. S.; Snyder, J. K.; Schaus, S. E.; Porco, J. A., Jr. *Org. Lett.* **2005**, *7*, 2751-2754.
- (93) Boger, D. L.; Goldberg, J.; Silletti, S.; Kessler, T.; Cheresch, D. A. *J. Am. Chem. Soc.* **2001**, *123*, 1280-1288.
- (94) Manetsch, R.; Krasinski, A.; Radic, Z.; Raushel, J.; Taylor, P.; Sharpless, K. B.; Kolb, H. C. *J. Am. Chem. Soc.* **2004**, *126*, 12809-12818.
- (95) Katritzky, A. R.; Oniciu, D. C.; Ghiviriga, I.; Barcock, R. A. *J. Chem. Soc. Perkin Trans.* **1995**, *2*, 785-792.
- (96) Stankova, M.; Lebl, M. *Mol. Diversity* **1996**, *2*, 75-80.
- (97) Johnson, C. R.; Zhang, B.; Fantauzzi, P.; Hocker, M.; Yager, K. M. *Tetrahedron* **1998**, *54*, 4097-4106.
- (98) Bork, J. T.; Lee, J. W.; Khersonsky, S. M.; Moon, H.-S.; Chang, Y.-T. *Org. Lett.* **2003**, *5*, 117-120.
- (99) Pattarawarapan, M.; Reyes, S.; Xia, Z.; Burgess, K. *J. Med. Chem.* **2003**, *46*, 3565-3567.
- (100) Ma, M. Y.-X.; Reid, L. S.; Climie, S. C.; Lin, W. C.; Kuperman, R.; Sumner-Smith M.; Barnett, R. W. *Biochemistry* **1993**, *32*, 1751-1758.
- (101) Pasini, D.; Righetti, P. P.; Zema, M. *Org. Biomol. Chem.* **2004**, *2*, 1764-1769.
- (102) Benseler, F.; Fu, D.-J.; Ludwig, J.; McLaughlin, L. W. *J. Am. Chem. Soc.* **1993**, *115*, 8483-8484.
- (103) Blasquez, E.; Mustarelli, P.; Pasini, D.; Righetti, P. P.; Tomasi, C. *J. Mater. Chem.* **2004**, *14*, 2524-2529.

- (104) Constable, E. C.; Hougen, I. A.; Housecroft, C. E.; Neuburger, M.; Schaffner, S.; Whall, L. A. *Inorg. Chem. Comm.* **2004**, *7*, 1128-1131.
- (105) Newkome, G. R.; Kotta, K. K.; Mishra, A.; Moorefield, C. N. *Macromolecules* **2004**, *37*, 8262-8268.
- (106) Warnecke, A.; Kratz, F. *Bioconjugate Chem.* **2003**, *14*, 377-387.
- (107) Kolb, H. C.; Finn, M. G.; Sharpless, K. B. *Angew. Chem. Int. Ed.* **2001**, *40*, 2004-2021.
- (108) Abu-Orabi, S. T. *Molecules* **2002**, *7*, 302-314.
- (109) Rostovtsev, V. V.; Green, L. G.; Fokin, V. V.; Sharpless, K. B. *Angew. Chem. Int. Ed.* **2002**, *41*, 2596-2599.
- (110) Wu, P.; Feldman, A. K.; Nugent, A. K.; Hawker, C. J.; Scheel, A.; Voit, B.; Pyun, J.; Frechet, J. M. J.; Sharpless, K. B.; Fokin, V. V. *Angew. Chem. Int. Ed.* **2004**, *43*, 3928-3932.
- (111) Loiseau, F. A.; Hii, K. K.; Hill, A. M. *J. Org. Chem.* **2004**, *69*, 639-647.
- (112) Helms, B.; Mynar, J. L.; Hawker, C. J.; Frechet, J. M. J. *J. Am. Chem. Soc.* **2004**, *126*, 15020-15021.
- (113) Hansen, T. M.; Engler, M. M.; Forsyth, C. J. *Bioorg. Med. Chem. Lett.* **2003**, *13*, 2127-2130.
- (114) Corey, E. J.; Venkateswarlu, A. *J. Am. Chem. Soc.* **1972**, *94*, 6190-6191.
- (115) Yoshida, Y.; Sakakura, Y.; Aso, N. A.; Okada, S.; Tanabe, Y. *Tetrahedron* **1999**, *55*, 2183-2192.
- (116) Appukkuttan, P.; Dehaen, W.; Fokin, V. V.; Eycken, E. V. *Org. Lett.* **2004**, *6*, 4223-4225.
- (117) Zych, A. J.; Iverson, B. L. *J. Am. Chem. Soc.* **2000**, *122*, 8898-8909.
- (118) Chen, Y.; Baker, G. L. *J. Org. Chem.* **1999**, *64*, 6870-6873.
- (119) Iyer, S. S.; Anderson, A. S.; Reed, S.; Swanson, B.; Schmidt, J. G. *Tet. Lett.* **2004**, *45*, 4285-4288.
- (120) Schwabacher, A. W.; Lane, J. W.; Schiesher, M. W.; Leigh, K. M.; Johnson, C. W. *J. Org. Chem.* **1998**, *63*, 1727-1729.

- (121) Biltresse, S.; Descamps, D.; Henneuse-Boxus, C.; Marchand-Brynaert, J. J. *Polymer Sci.: Part A: Polymer Chem.* **2002**, *40*, 770-781.
- (122) Welch, M. B.; Martinez, C. I.; Zhang, A. J.; Jin, S.; Gibbs, R.; Burgess, K. *Chem. Eur. J.* **1999**, *5*, 951-960.
- (123) Ukhin, L. Y.; Suponitskii, K. Y.; Kartsev, V. G. *Chem. Nat. Compounds* **1998**, *39*, 482-488.
- (124) Analytix. http://www.sigmaaldrich.com/img/assets/4242/fl_analytix2_2003.pdf (accessed 9/29/05).
- (125) Slais, K. *J. Chrom. A* **1994**, *661*, 249-256.
- (126) Shimura, K.; Zhi, W.; Matsumoto, H.; Kasai, K. *Anal. Chem.* **2000**, *72*, 4747-4757.
- (127) Ripin, D. H.; Evans, D. A. pK_a's of Nitrogen Acids, Chem 206 notes, Harvard University, Massachusetts, 2005.
- (128) Abboud, J.-L. M.; Foces-Foces, C.; Notario, R.; Trifonov, R. E.; Volovodenko, A. P.; Ostrovskii, V. A.; Alkorta, I.; Elguero, J. *Eur. J. Org. Chem.* **2001**, *16*, 3013-3024.

APPENDIX A

CHAPTER II EXPERIMENTAL PROCEDURES

Docking Protocol. Docking calculations were performed on a Silicon Graphics O₂ workstation with an IRIX 6.3 operating system using *InsightII* suite of programs developed by Accelrys. Simulations were carried out using the CVFF method.

The receptor was loaded in PDB format and hydrogens were displayed. The pH was set to 7 and charged. Water was unmerged and removed from the receptor. The force field potentials were fixed and checked for any incomplete valencies. The receptor file was then saved as a .CAR file.

The ligand was loaded and saved as a .CAR file.

The receptor and ligand were loaded onto the same screen. The docking assembly was created with the “Associate” menu option. The assembly was given a name. The site where the ligand will be placed and docked was defined under the “Subset” and “Interface” menu options. The radius of the subset was defined to be 10 squared angstroms.

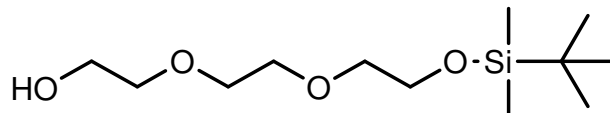
The side-chains on the ligand molecules were each oriented in a way that is the most similar to the crystal structure H4 and I6 of NGF interacting with TrkA. Docking was carried out in the “Docking” and “Affinity” options in the MSI module. A grid for the “bulk” atoms was first carried out, then the potential energy of the docking assembly was minimized with a minimum of 1000 steps. The best minimized complex was selected and displayed.

The radius of the subset—*i.e.* the site on TrkA where the ligand molecule was docked—was converted to a Connolly surface, which is basically a potential surface, smoothed by rolling a water molecule along the desired area. The calculation takes place under the “Molecule” and “Surface” menu options.

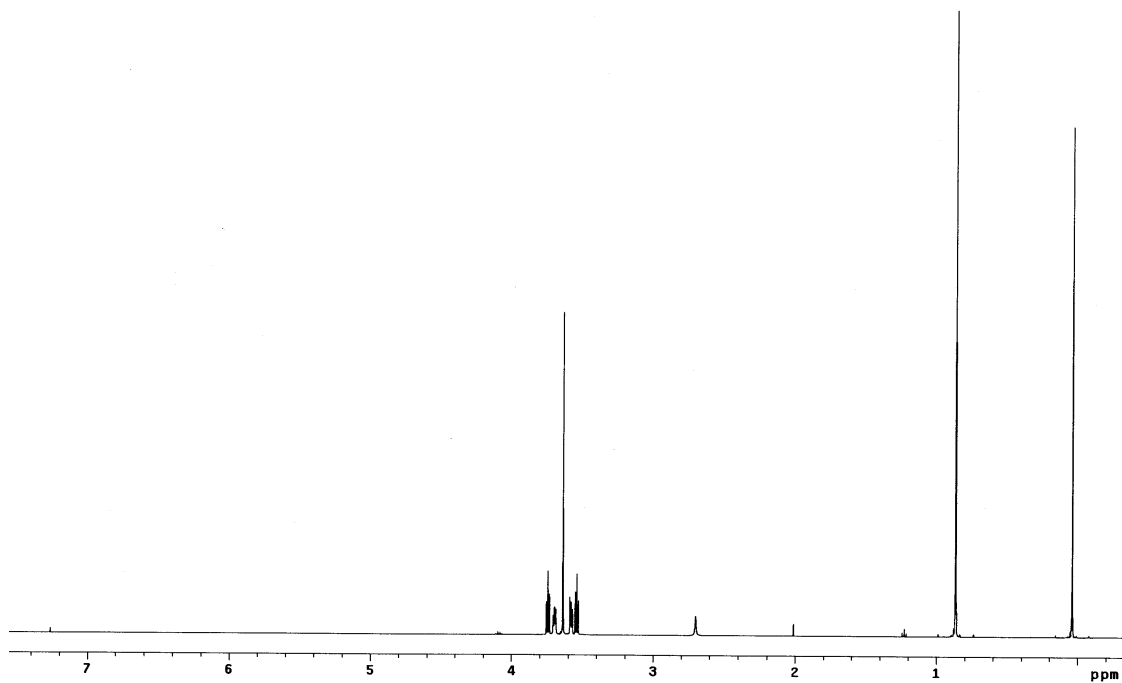
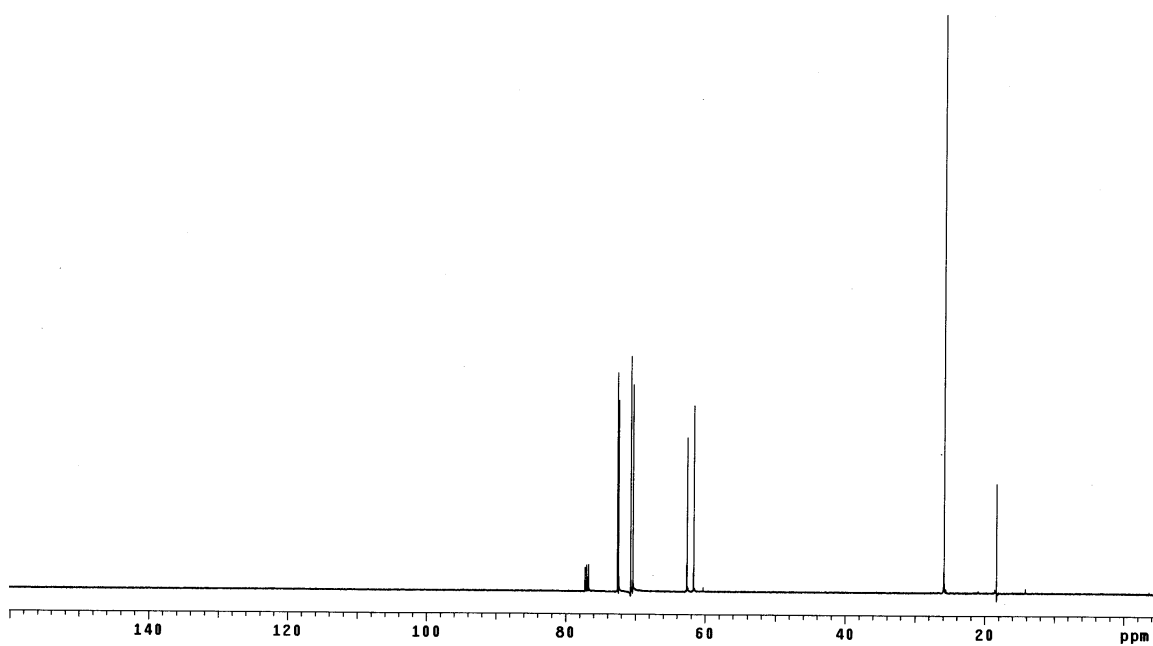
APPENDIX B

CHAPTER III EXPERIMENTAL PROCEDURES

General Methods. Melting points were determined in capillary tubes with a MEL-TEMPH apparatus by Laboratory Devices and are uncorrected. Nuclear Magnetic Resonance (NMR) spectra were recorded with a Mercury-300 (^1H at 300 MHz, ^{13}C NMR at 75 MHz) or Inova-500 (^1H at 500 MHz, ^{13}C NMR at 125 MHz) NMR spectrometers. Chemical shifts are reported in units of parts per million (ppm) relative to solvent (CDCl_3 : 7.27 ppm for ^1H and 77.0 ppm for ^{13}C). Fourier Transform-Infrared (FT-IR) spectra were recorded with a Nicolet Impact 410 IR instrument using NaCl plates. Mass spectra were obtained from the Laboratory for Biological Mass Spectrometry at Texas A&M University. Thin layer chromatography was performed using silica gel 60 F254 plates. Flash chromatography was performed using ultra pure silica gel (40-63 μm particle size, 230-400 mesh). Ether, THF, MeOH, CH_2Cl_2 , and triethylamine were distilled from appropriate drying agents. Analytical HPLC were run on a Scientific Systems, Inc. system (232C Gradient solvent module, 222C Pump) with a UV detector using a GraceVydac (cat. #101TP54, 4.6 x 250 mm) unbonded silica column. Gradient elution was used (A = hexane or CHCl_3 , B = $^i\text{PrOH}$) with a constant flow rate of 1.0 mL/min. Analytical HPLC were also run on a Beckman Coulter System Gold 125 Solvent Module and Sedex 55 Detector using a GraceVydac (cat. #218TP54, 4.6 x 250 mm) Protein and Peptide C18 column. Gradient elution was used (A = water, B = MeCN, both with 0.1% v/v TFA) with a constant flow rate of 1.0 mL/min.

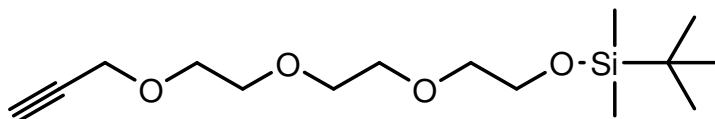
Compound 1**2-(2-(2-(2-*tert*-Butyldimethylsilyloxy)ethoxy)ethoxy)ethanol**¹¹³**Procedure:**

Triethylene glycol (20.0 g, 133 mmol) and *tert*-butyldimethylsilyl chloride (22.1 g, 146 mmol) were dissolved in 250 mL distilled CH₂Cl₂. The mixture was cooled to 0 °C in an ice bath. TEA (20.4 mL, 146 mmol) was added gradually followed by the addition of DMAP (1.62 g, 13.2 mmol). The mixture was allowed to warm slowly to room temperature with stirring for 20 h. The reaction mixture was washed with 0.1 M HCl (2 x 300 mL). The acidic extracts were pooled and extracted with CH₂Cl₂ (1 x 200 mL). The combined organic extracts were evaporated under reduced pressure and purified by flash chromatography eluting first with 1:4 EtOAc/hexane then with 4:1 EtOAc/hexane to afford **1** as a colorless oil (14.2 g, 40%). ¹H NMR (CDCl₃, 500 MHz): δ (ppm) 0.04 (s, 6H), 0.87 (s, 9H), 2.70 (br, 1H), 3.55 (t, *J* = 3.0 Hz, 2H), 3.58 (t, *J* = 7.0 Hz, 2H), 3.64 (s, 4H), 3.70 (t, *J* = 4.8 Hz, 2H), 3.75 (t, *J* = 5.5 Hz, 2H); ¹³C NMR (CDCl₃, 125 MHz): δ (ppm) 18.3, 25.8, 61.6, 62.6, 70.4, 70.7, 72.4, 72.6.

 ^1H NMR ^{13}C NMR

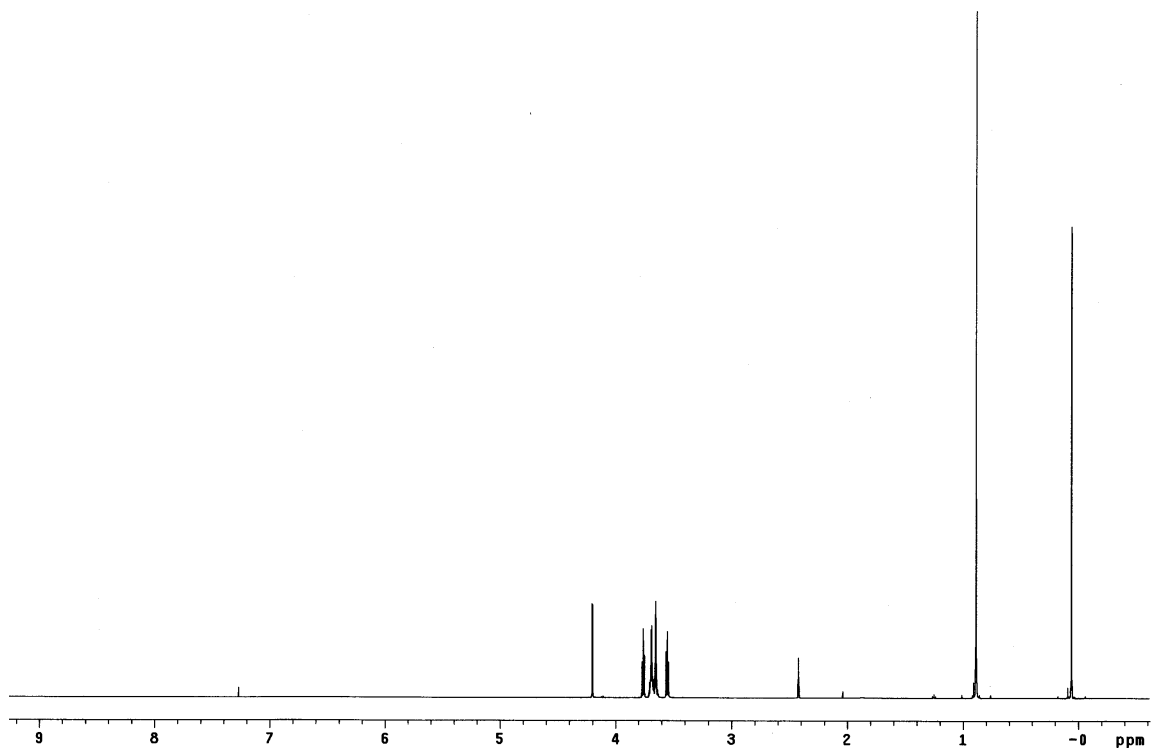
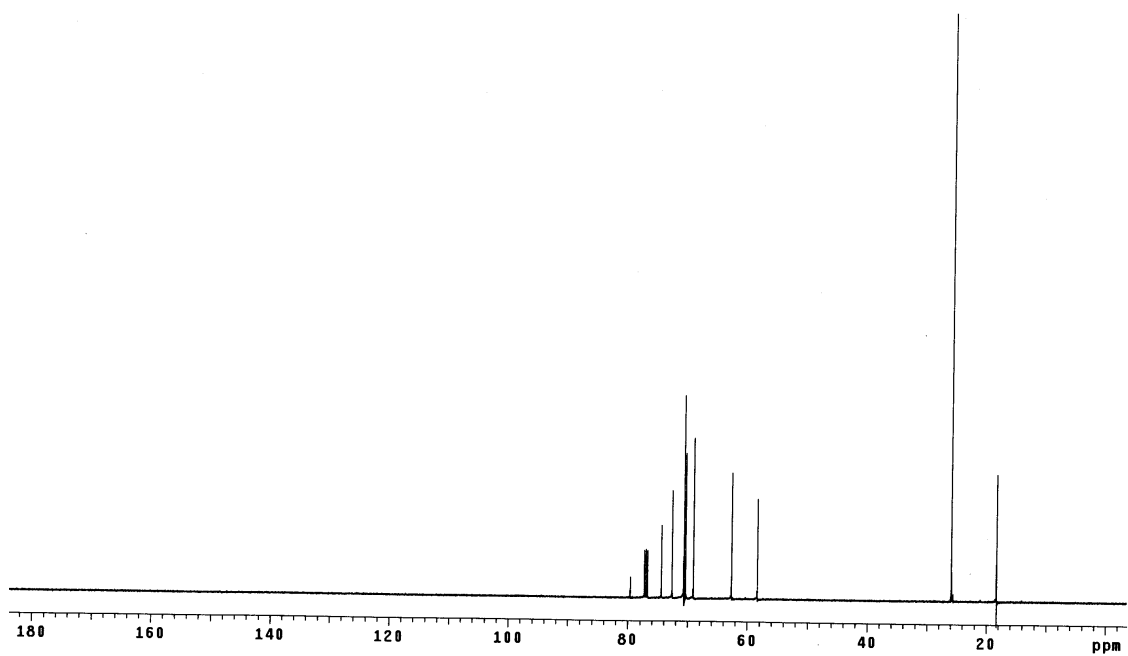
Compound 2

2-(2-(2-(Prop-2-ynyloxy)ethoxy)ethoxy)ethoxy)tert-butyldimethylsilane¹¹³



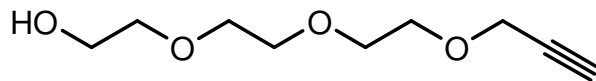
Procedure:

Sodium hydride (2.54 g, 63.5 mmol) was added scoop-wise to a solution containing compound **1** (14.0 g, 52.9 mmol) and 75 mL distilled THF at 0 °C under N₂. After the evolution of hydrogen gas had ceased, the reaction flask was capped and propargyl bromide (11.8 g, 79.3 mmol) was syringed into the mixture slowly. The reaction mixture was allowed to warm gradually to room temperature with stirring under N₂ for 12 h. Deionized water (200 mL) was then added to the mixture and extracted with CH₂Cl₂ (3 x 100 mL). The organic extracts were pooled, dried over Na₂SO₄, filtered and evaporated *in vacuo*. The resulting residue was purified by flash chromatography using 1:5 EtOAc/hexane, yielding **2** as a colorless oil (11.7 g, 73%). ¹H NMR (CDCl₃, 500 MHz): δ (ppm) 0.06 (s, 6H), 0.89 (s, 9H), 2.42 (t, *J* = 2.5 Hz, 1H), 3.55 (t, *J* = 5.3 Hz, 2H), 3.64-3.70 (m, 8H), 3.76 (t, *J* = 5.5 Hz, 2H), 4.20 (d, *J* = 2 Hz, 2H); ¹³C NMR (CDCl₃, 125 MHz): δ (ppm) 18.3, 25.9, 58.3, 62.7, 69.0, 70.4, 70.6, 70.7, 72.6, 74.4, 79.6.

 ^1H NMR ^{13}C NMR

Compound 3

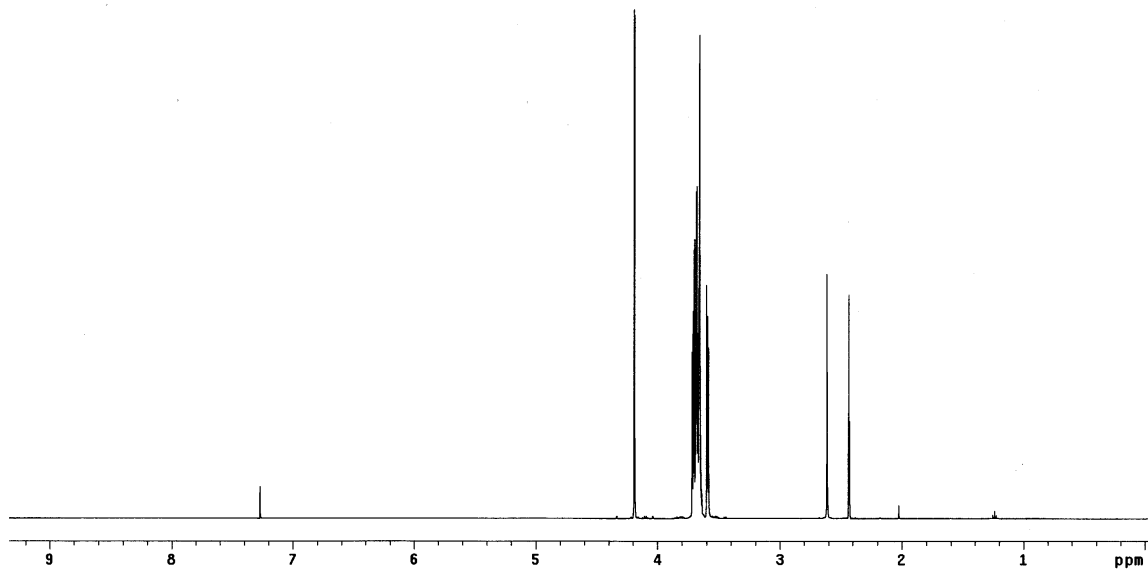
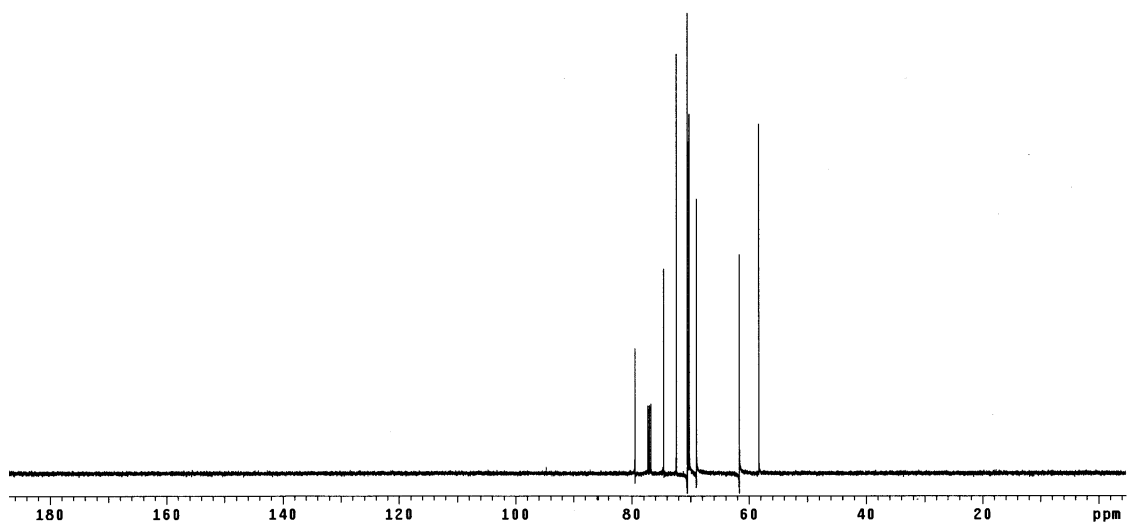
2-(2-(2-(Prop-2-ynyloxy)ethoxy)ethoxy)ethanol¹¹³



Procedure:

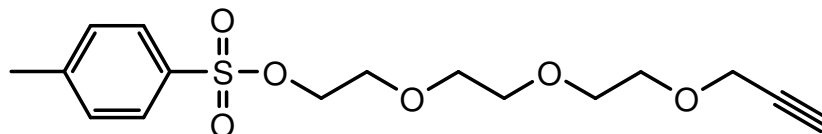
Method A: TBAF (77.0 mL, 77.0 mmol) was added to a solution containing compound **2** (11.7 g, 38.5 mmol) and 120 mL distilled THF at 0 °C under N₂. After the addition was completed, the ice-bath was removed and the solution stirred at room temperature for 1 h. The reaction mixture was then evaporated *in vacuo*, yielding a wine-red oil which was purified by flash chromatography using EtOAc to afford **3** as a yellow oil (6.27 g, 86%).

Method B: Sodium hydride (1.44 g, 36.0 mmol) was added scoop-wise to a solution containing triethylene glycol (15.0 g, 100. mmol) and 75 mL distilled THF at 0 °C. After the bubbling had ceased, the reaction flask was capped and the solution stirred under N₂ for 0.5 h at 0 °C. Propargyl bromide (7.44 g, 50.0 mmol) in 5 mL distilled THF was added slowly to the reaction flask via a syringe. The mixture was warmed gradually to room temperature with stirring for 16 h. DI water (150 mL) was added and extracted with CH₂Cl₂ (3 x 75 mL). The organics were pooled, dried over Na₂SO₄ and concentrated under reduced pressure. The residue was purified by flash chromatography eluting with 3:2 EtOAc/hexane to afford **3** as a yellow oil (4.01 g, 59%). ¹H NMR (CDCl₃, 500 MHz): δ (ppm) 2.43 (t, *J* = 2.5 Hz, 1H), 2.61 (s, 1H), 3.59 (t, *J* = 2.8 Hz, 2H), 3.60-3.70 (m, 8H), 3.71 (t, *J* = 3.0 Hz, 2H), 4.19 (d, *J* = 2.5 Hz, 2H); ¹³C NMR (CDCl₃, 125 MHz): δ (ppm) 58.3, 61.6, 69.0, 68.9, 70.2, 70.3, 72.4, 74.5, 79.5.

 ^1H NMR ^{13}C NMR

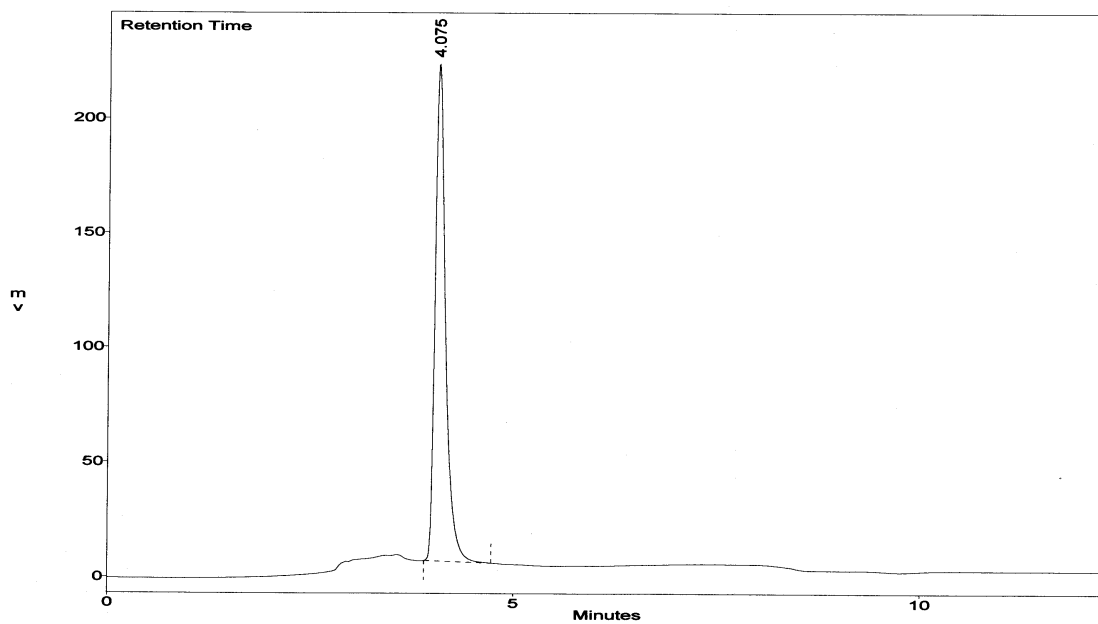
Compound 4

2-(2-(2-(Prop-2-ynoxy)ethoxy)ethoxy)ethyl 4-methylbenzenesulfonate

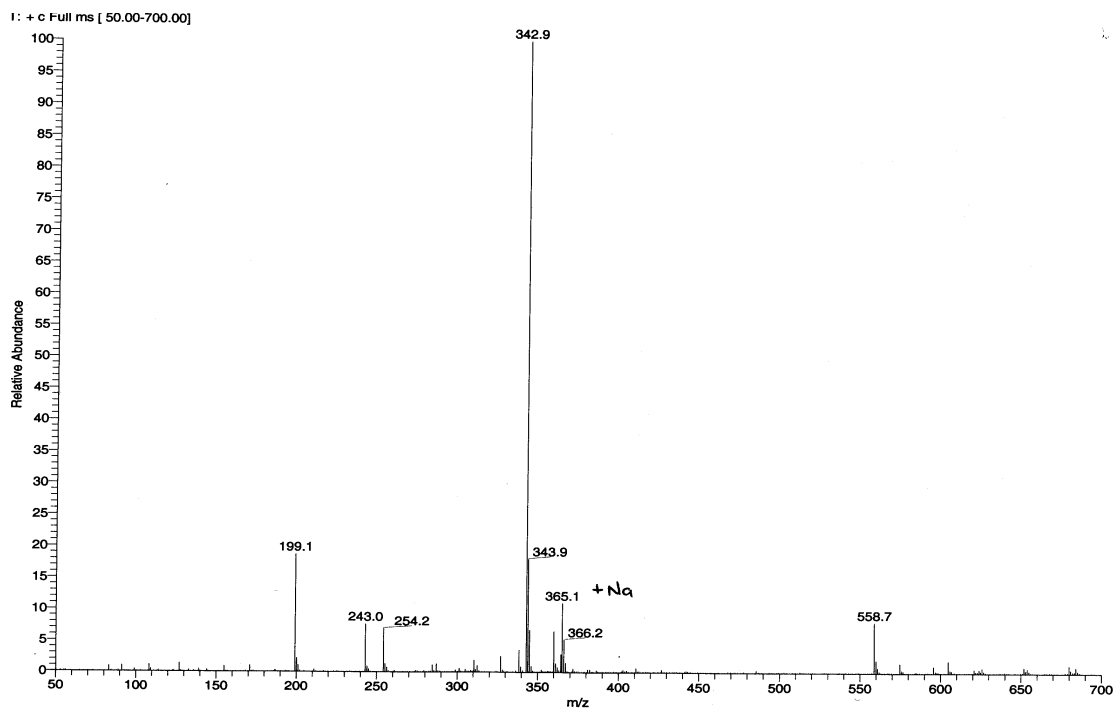


Procedure:

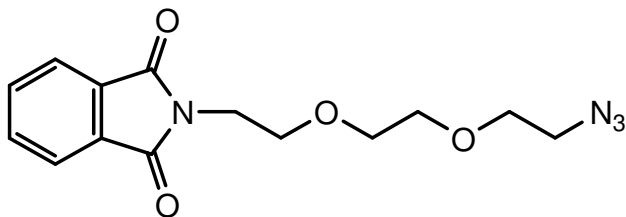
Compound **3** (10.3 g, 54.6 mmol), TEA (19.0 mL, 136 mmol), and trimethylamine hydrochloride (522 mg, 5.46 mmol) were dissolved in 140 mL MeCN at 0 °C. *p*-Toluenesulfonyl chloride (20.8 g, 109 mmol) was added and the reaction mixture stirred at 0 °C for 50 minutes, then at room temperature for 30 minutes. DI water (180 mL) was added and extracted with EtOAc (3 x 150 mL). The combined organics were dried over MgSO₄, filtered, and concentrated *in vacuo*. The resulting residue was purified by flash chromatography eluting first with 1:3 EtOAc/hexane then with 1:1 EtOAc/hexane, yielding **4** as a yellow oil (16.2 g, 87%). ¹H NMR (CDCl₃, 500 MHz): δ (ppm) 2.43 (t, *J* = 2.5 Hz, 1H), 2.45 (s, 3H), 3.59 (s, 4H), 3.64-3.65 (m, 2H), 3.67-3.69 (m, 4H), 4.15 (t, *J* = 5.0 Hz, 2H), 4.19 (d, *J* = 2 Hz, 2H), 7.34 (d, *J* = 8.5 Hz, 2H), 7.79 (d, *J* = 8.5 Hz, 2H); ¹³C NMR (CDCl₃, 125 MHz): δ (ppm) 21.6, 58.3, 68.6, 69.1, 70.4, 70.5, 70.7, 74.5, 79.6, 127.9, 129.8, 132.9, 144.7; MS (APCI, *m/z*) 365.1 for [M+Na]⁺.



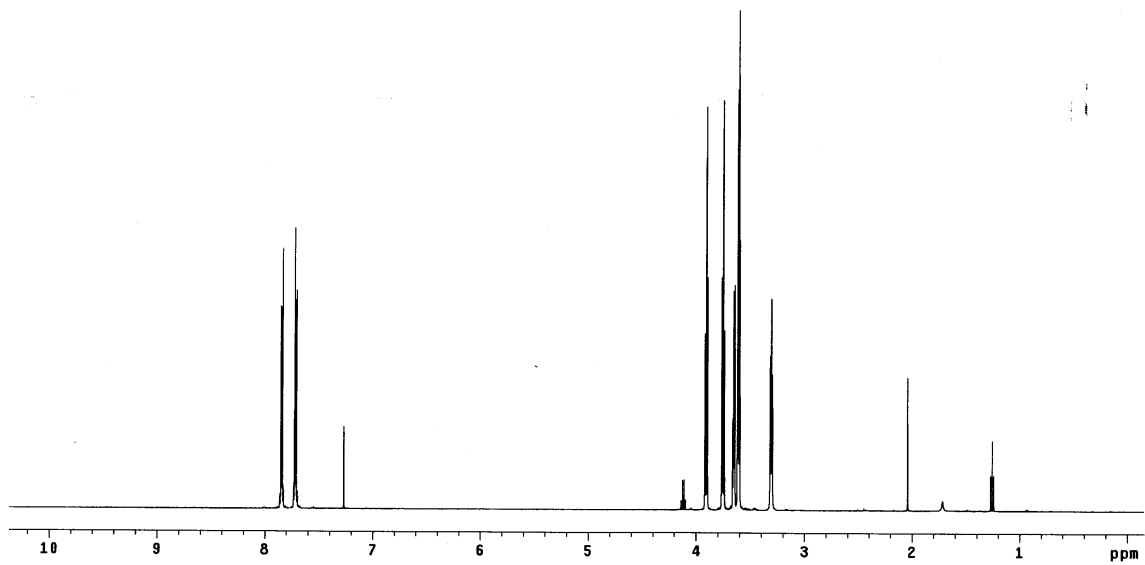
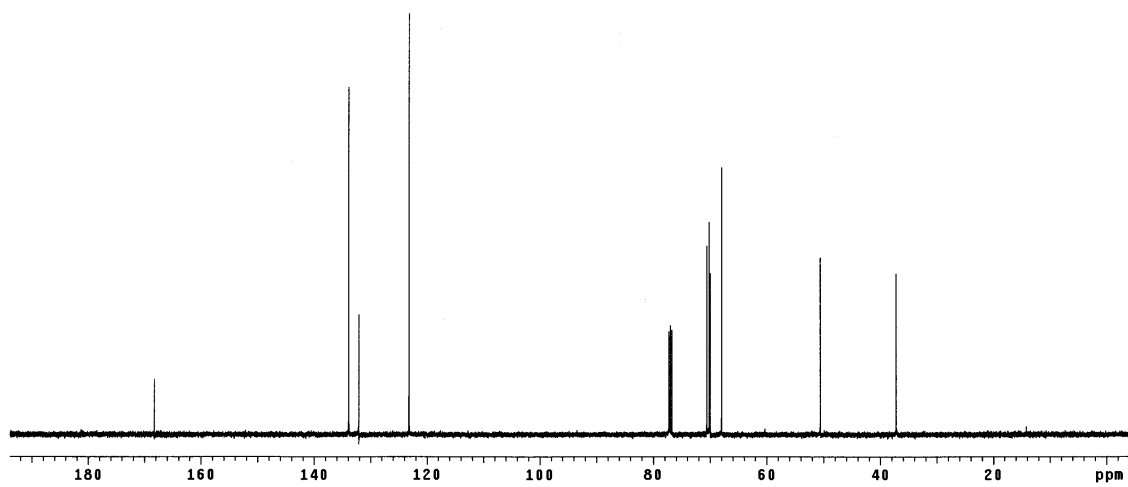
HPLC

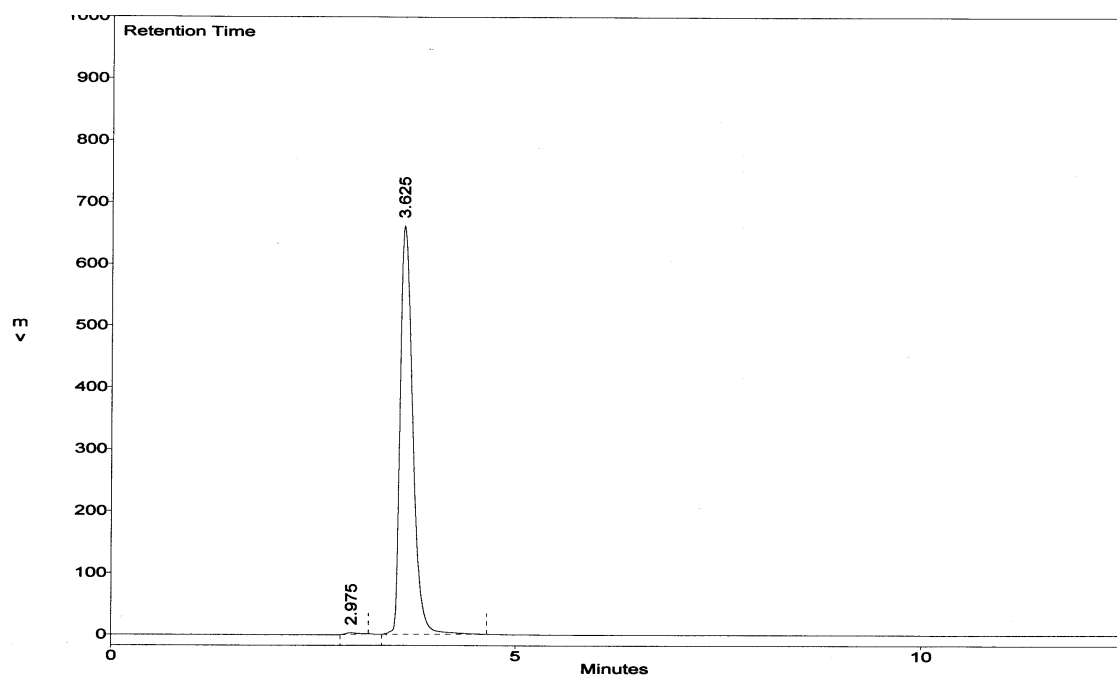


MS

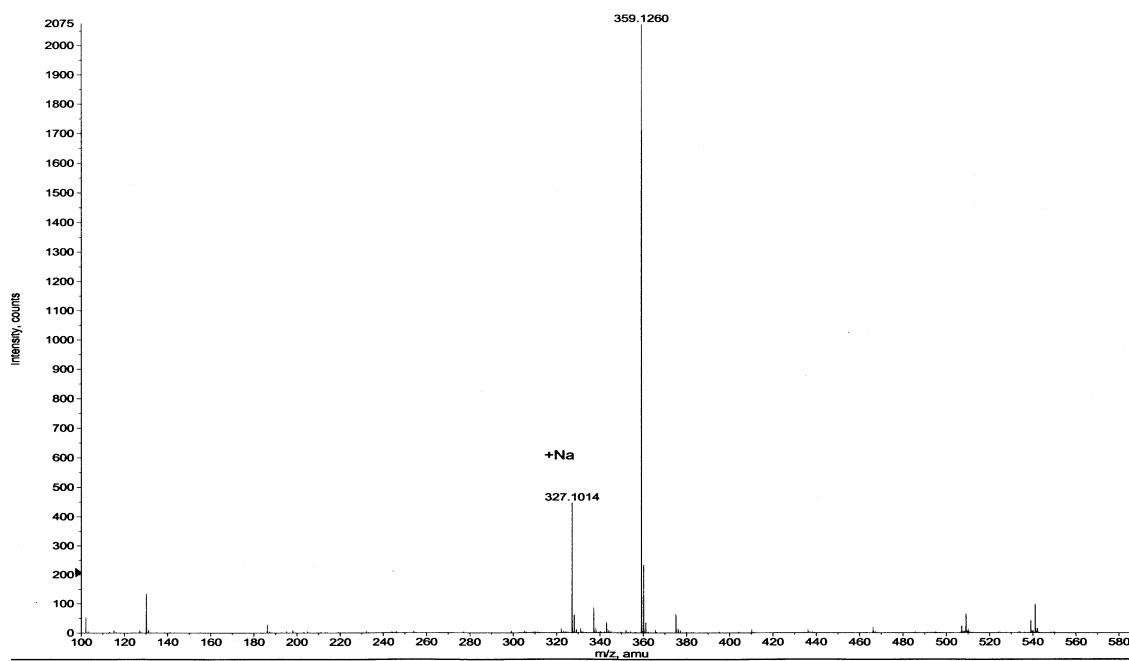
Compound 5**2-(2-(2-(2-Azidoethoxy)ethoxy)ethyl)isoindoline-1,3-dione****Procedure:**

Compound was obtained from Dr. Genliang Lu and purified by column chromatography eluting with 2:3 EtOAc/hexane to afford **5** as a light-yellow oil. ^1H NMR (CDCl_3 , 500 MHz): δ (ppm) 3.30 (t, $J = 5.3$ Hz, 2H), 3.61 (dt, $J = 6.0$ Hz, 5.3 Hz, 4H), 3.65 (dt, $J = 5.0$ Hz, 4.3 Hz, 2H), 3.75 (t, $J = 5.6$ Hz, 2H), 3.90 (t, $J = 5.5$ Hz, 2H), 7.72 (dd, $J = 7.0$ Hz, 3.5 Hz, 2H), 7.85 (dd, $J = 6.0$ Hz, 3.0 Hz, 2H); ^{13}C NMR (CDCl_3 , 125 MHz): δ (ppm) 37.2, 50.6, 68.0, 70.0, 70.1, 70.6, 123.2, 132.1, 133.9, 168.2; MS (APCI/ESI, m/z) 327.1 for $[\text{M}+\text{Na}]^+$.

 ^1H NMR ^{13}C NMR



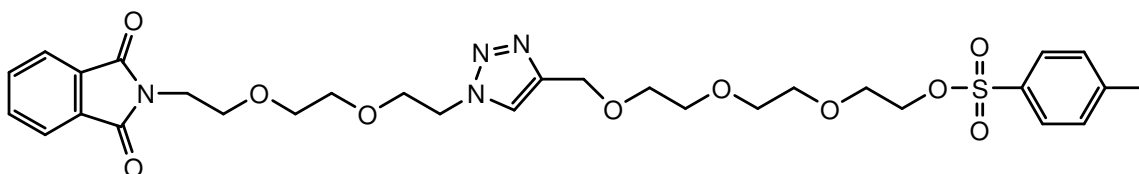
HPLC



MS

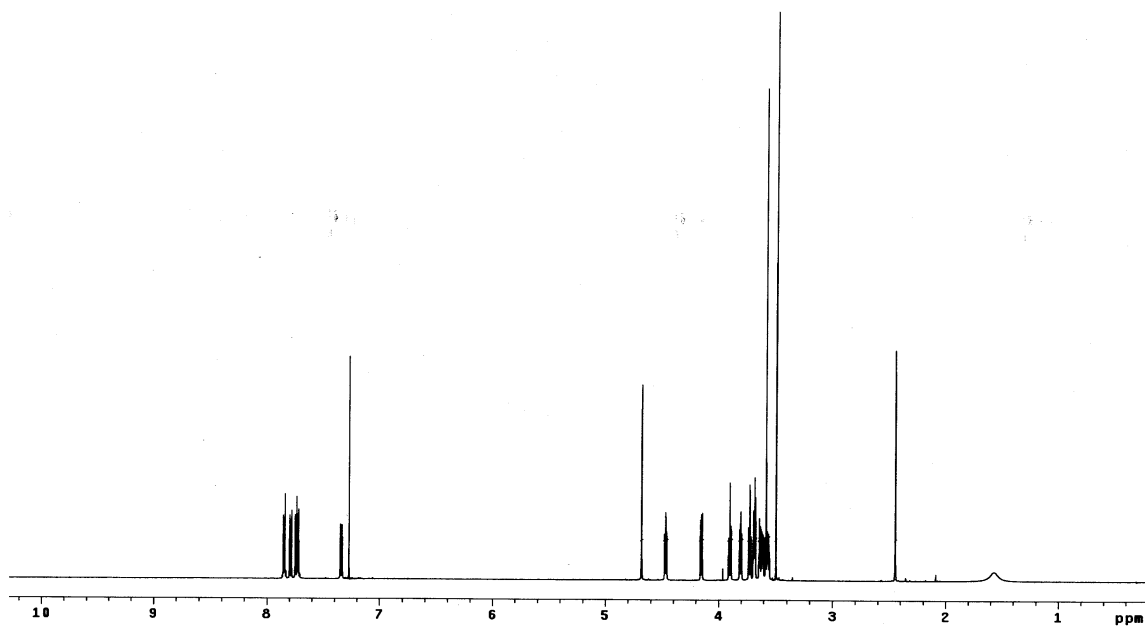
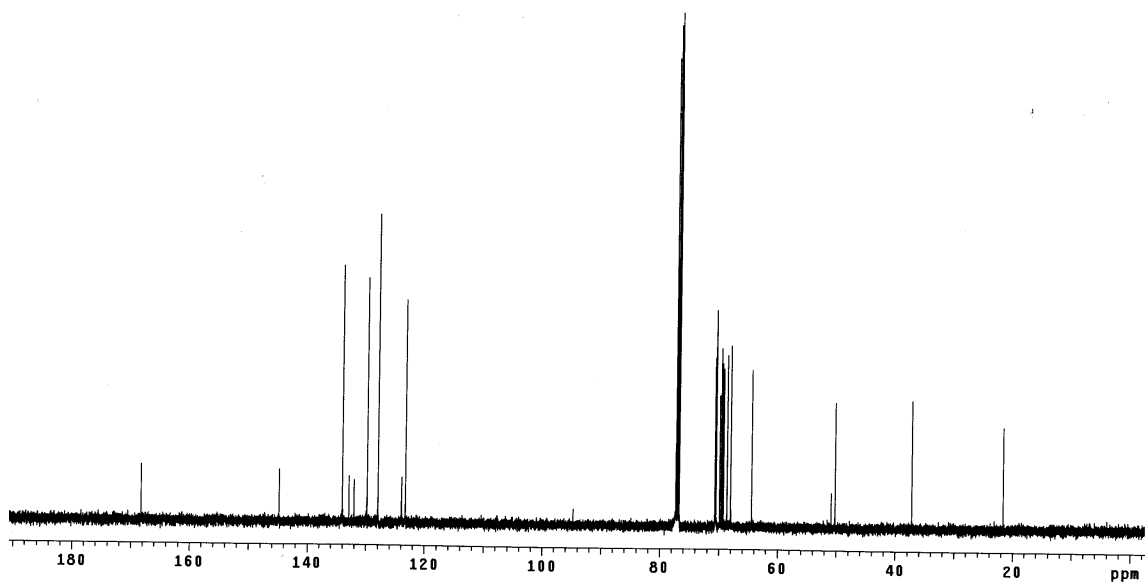
Compound 6

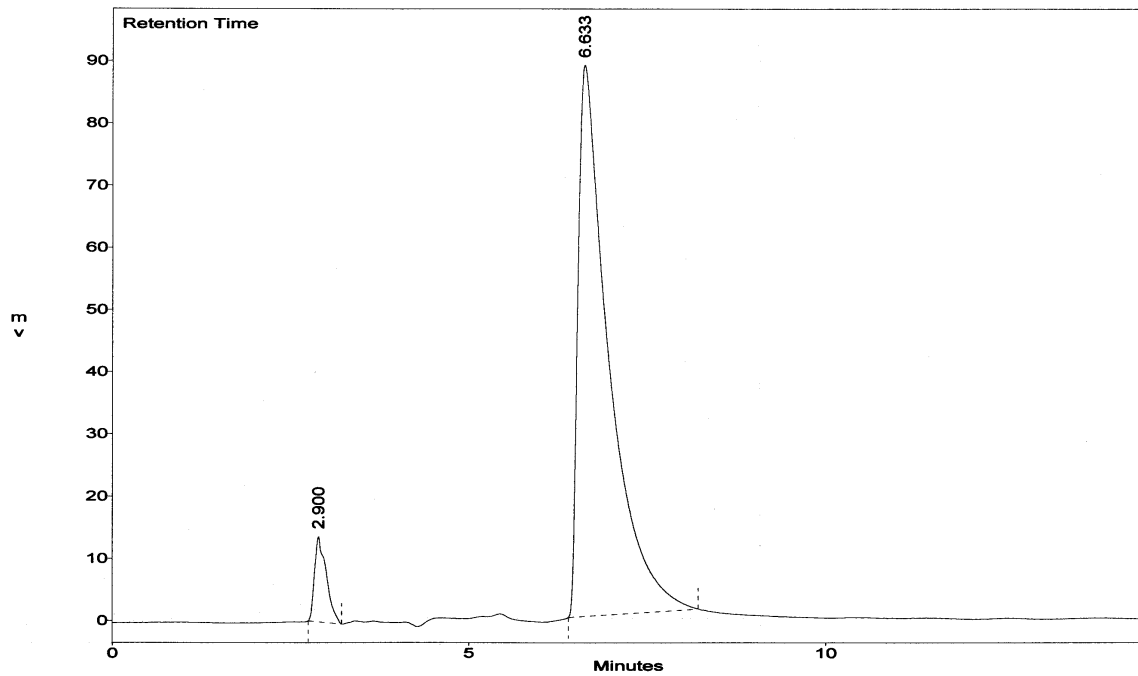
2-(2-(2-(2-(4-((2-(2-(2-(4-Methylbenzenesulfonyl)ethoxy)ethoxy)ethoxy)methyl)-1H-1,2,3-triazol-1-yl)ethoxy)ethoxy)ethyl)isoindoline-1,3-dione



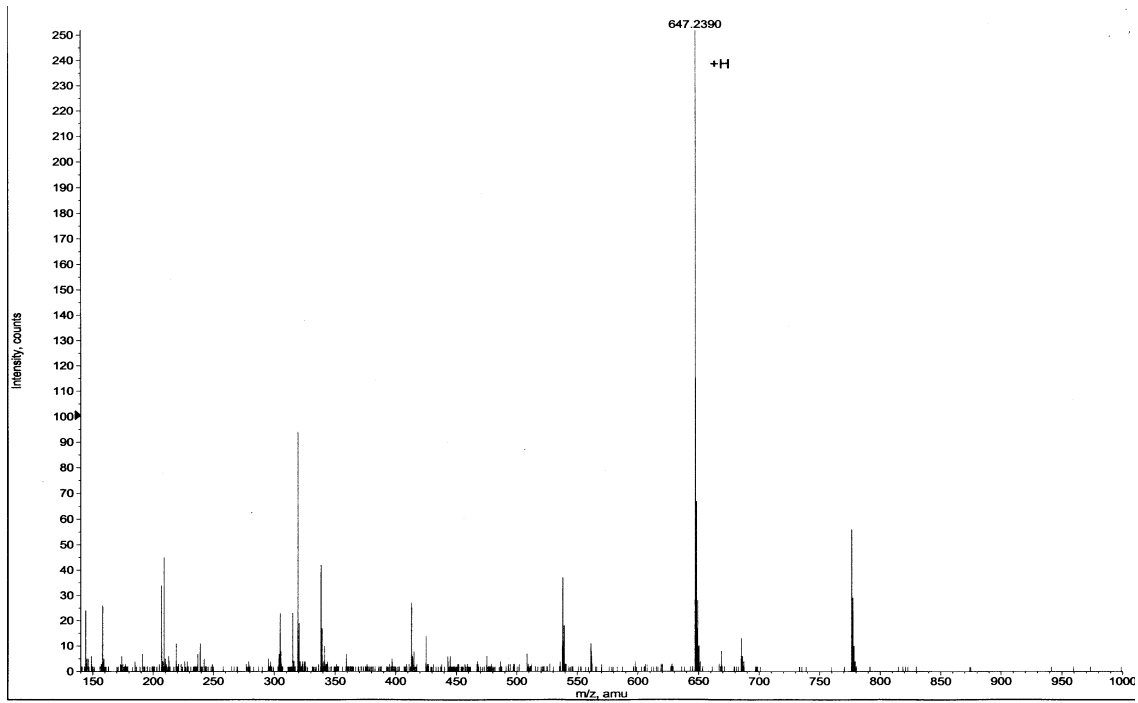
Procedure:

Compound **4** (343 mg, 1.00 mmol) and compound **5** (305 mg, 1.00 mmol) were mixed together in 3.5 mL THF in a scintillation vial at room temperature. An equal amount of DI water (3.5 mL) was then added with vigorous stirring. 10 mol% sodium ascorbate and 5 mol% CuSO₄·5H₂O were added from freshly prepared 1 M aqueous solutions. The vial was capped and stirred for 20 h at room temperature. The mixture was then filtered through a pad of silica gel and washed with 600 mL EtOAc. The organic wash was evaporated *in vacuo* and purified by flash chromatography eluting first with 3:1 EtOAc/hexane then with MeOH, yielding **6** as a pale-yellow oil (446 mg, 69%). $R_f = 0.28$ (EtOAc); ¹H NMR (CDCl₃, 500 MHz): δ (ppm) 2.45 (s, 3H), 3.56-3.58 (m, 4H), 3.60 (s, 4H), 3.61-3.64 (m, 2H), 3.67-3.70 (m, 4H), 3.72 (t, $J = 5.8$ Hz, 2H), 3.80 (t, $J = 5.0$ Hz, 2H), 3.90 (t, $J = 5.8$ Hz, 2H), 4.15 (t, $J = 5.0$ Hz, 2H), 4.46 (t, $J = 5.3$ Hz, 2H), 4.68 (s, 2H), 7.34 (d, $J = 8.5$ Hz, 2H), 7.73 (dd, $J = 6.0$ Hz, 3.0 Hz, 2H), 7.75 (s, 1H), 7.79 (d, $J = 8.5$ Hz, 2H), 7.85 (dd, $J = 6.0$ Hz, 3.0 Hz, 2H); ¹³C NMR (CDCl₃, 125 MHz): δ (ppm) 21.6, 37.2, 50.2, 50.8, 64.4, 68.0, 68.6, 69.2, 69.4, 69.6, 69.9, 70.47, 70.49, 70.5, 70.7, 123.2, 123.9, 127.9, 129.8, 132.0, 132.9, 134.0, 144.8, 168.2; MS (ESI, m/z) 647.2 for [M+H]⁺.

 ^1H NMR ^{13}C NMR



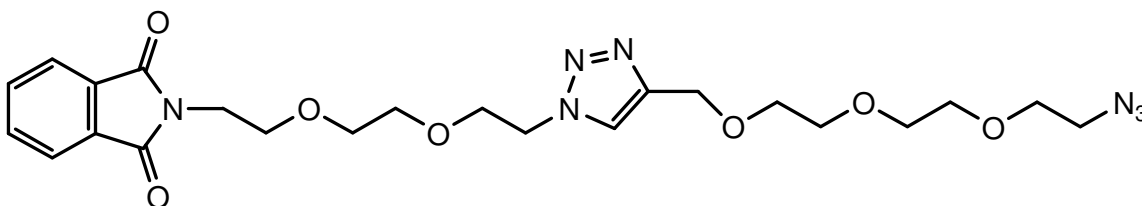
HPLC



MS

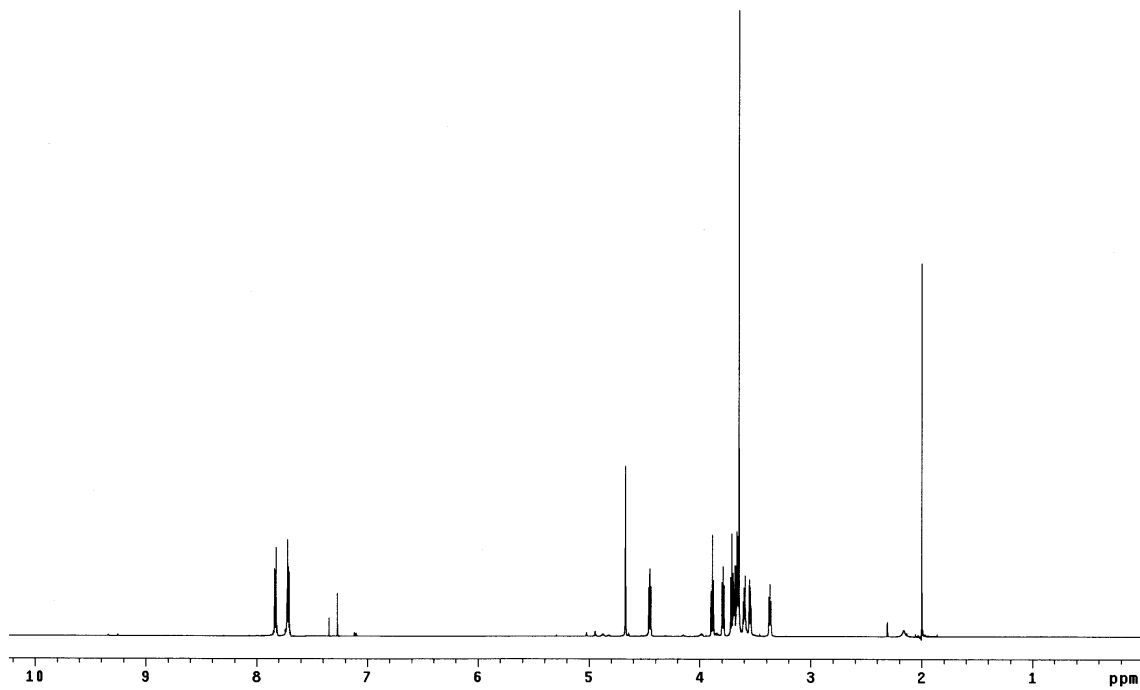
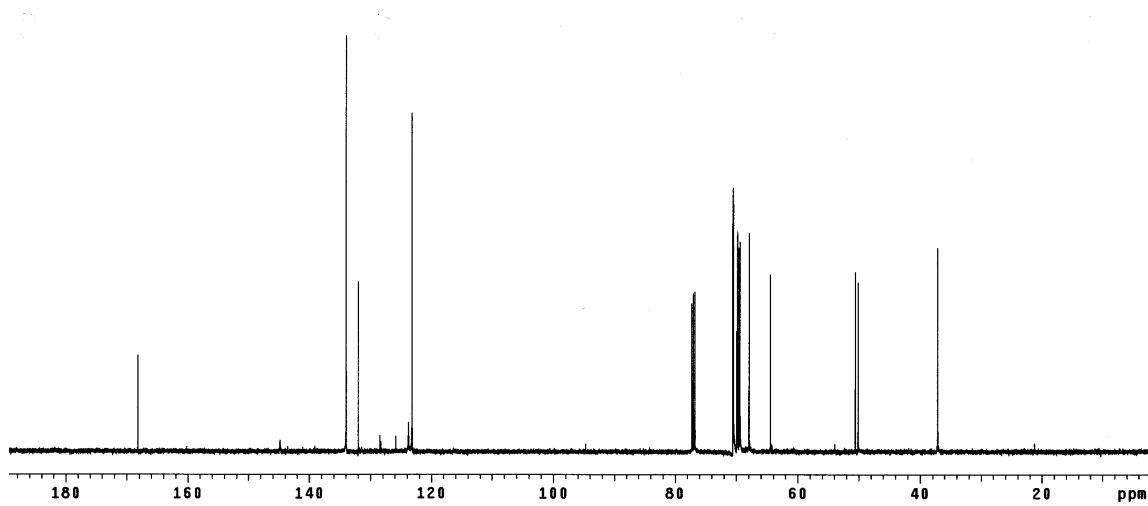
Compound 7

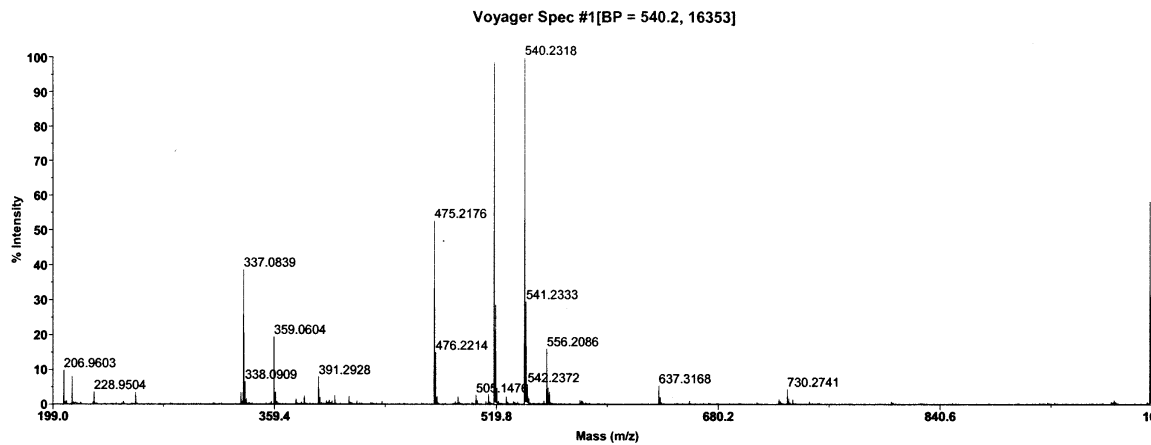
2-(2-(2-(2-(4-((2-(2-(2-Azidoethoxy)ethoxy)ethoxy)methyl)-1H-1,2,3-triazol-1-yl)ethoxy)ethoxy)ethyl)isoindoline-1,3-dione



Procedure:

Compound **6** (1.10 g, 1.70 mmol) and sodium azide (0.222 g, 3.41 mmol) were refluxed in 12 mL MeCN for 40 h. DI water (40 mL) was added and extracted with CH₂Cl₂ (4 x 40 mL). The organic extracts were pooled, dried over Na₂SO₄, filtered, and evaporated *in vacuo*, yielding **7** as a yellow oil (814 mg, 93%). ¹H NMR (CDCl₃, 500 MHz): δ (ppm) 3.37 (t, *J* = 5.3 Hz, 2H), 3.55 (t, *J* = 2.5 Hz, 2H), 3.60 (t, *J* = 4.3 Hz, 2H), 3.65-3.72 (m, 12H), 3.79 (t, *J* = 5.0 Hz, 2H), 3.89 (t, *J* = 5.8 Hz, 2H), 4.45 (t, *J* = 5.0 Hz, 2H), 4.67 (s, 2H), 7.71 (dd, *J* = 6.0 Hz, 3.0 Hz, 2H), 7.73 (s, 1H), 7.83 (dd, *J* = 6.0 Hz, 3.0 Hz, 2H); ¹³C NMR (CDCl₃, 125 MHz): δ (ppm) 37.1, 50.1, 50.6, 64.4, 67.9, 69.4, 69.6, 69.8, 69.9, 70.4, 70.52, 70.53, 70.6, 123.2, 123.8, 132.0, 134.0, 144.8, 168.2; MS (MALDI, *m/z*) 540.2 for [M+Na]⁺.

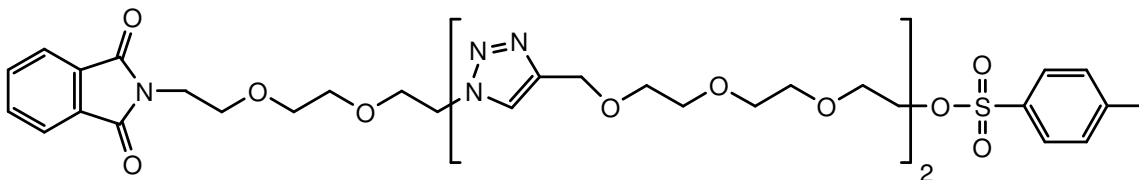
 ^1H NMR ^{13}C NMR



MS

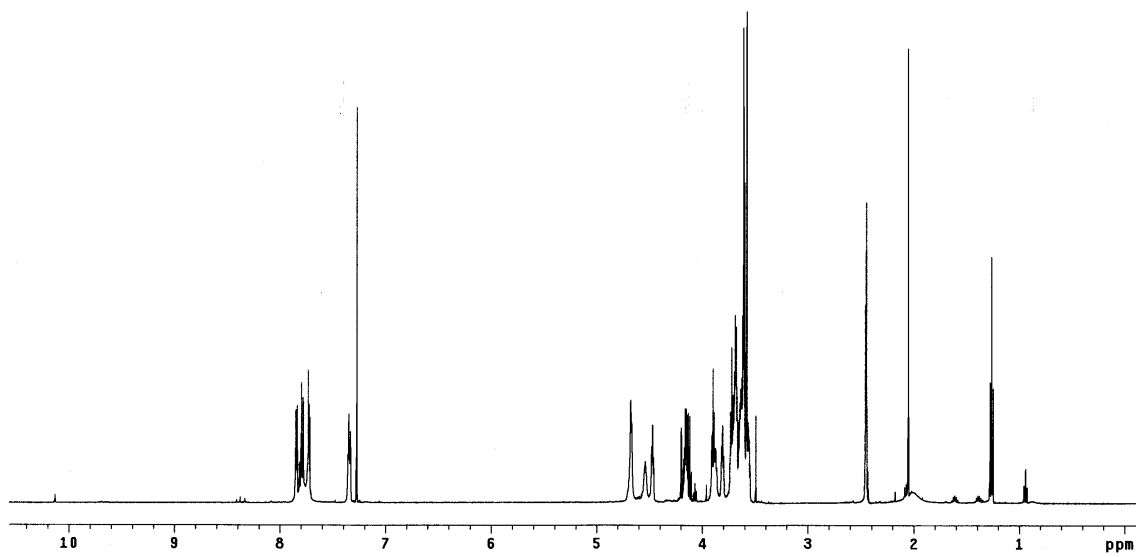
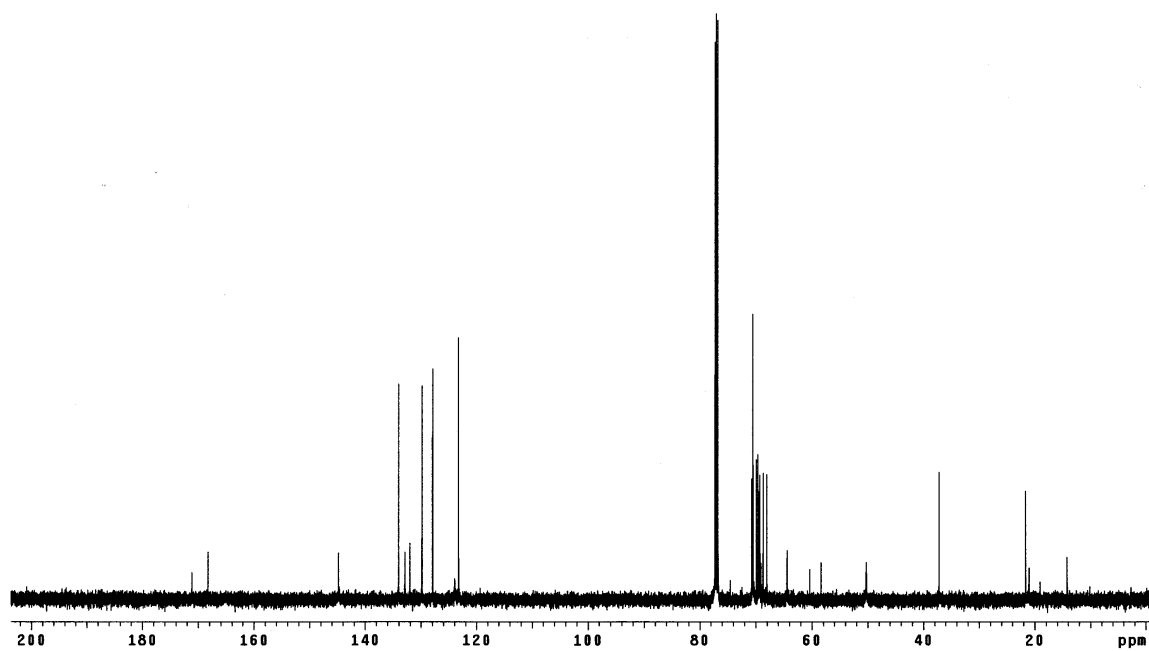
Compound 8

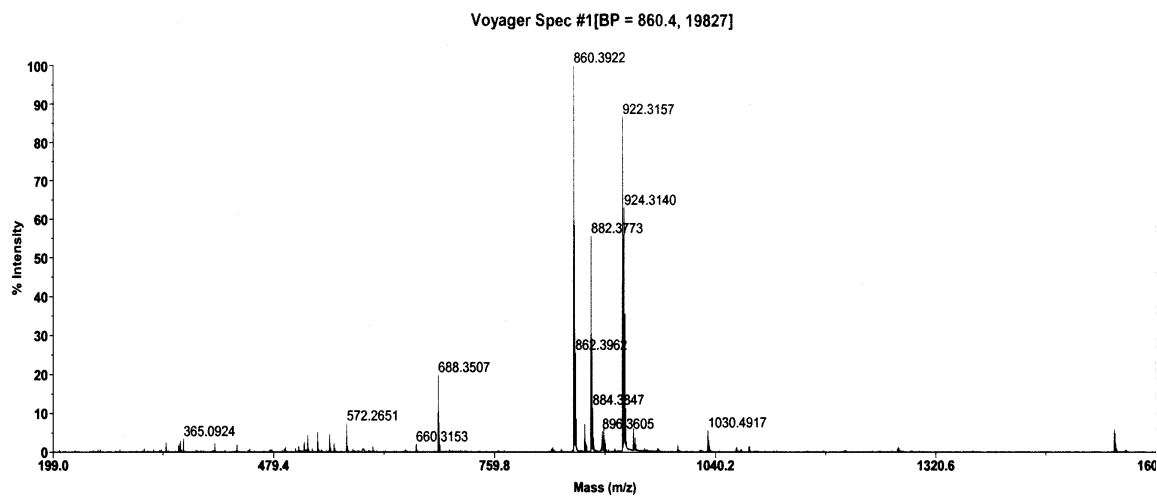
2-(2-(2-(2-(4-((2-(2-(2-(4-((2-(2-(2-(4-Methylbenzenesulfonyl)ethoxy)ethoxy)ethoxy)methyl)-1H-1,2,3-triazol-1-yl)ethoxy)ethoxy)ethoxy)methyl)-1H-1,2,3-triazol-1-yl)ethoxy)ethoxy)ethyl)isoindoline-1,3-dione



Procedure:

Compound **7** (777 mg, 1.50 mmol), compound **4** (514 mg, 1.50 mmol), copper powder (191 mg, 3.00 mmol), and 600 μ L of an aqueous 1M $\text{CuSO}_4 \cdot 5\text{H}_2\text{O}$ solution (40 mol%) were suspended in 5 mL t BuOH/ H_2O (1:1) mixture in a scintillation vial. The vial was capped and the reaction solution stirred vigorously for 12 h at room temperature. It was diluted with 25 mL EtOAc and filtered through a pad of silica gel. The silica was washed with 5% MeOH/EtOAc (500 mL). The organic washings were combined and evaporated under reduced pressure, yielding **8** as a viscous, yellow oil (368 mg, 29%). TLC shows one spot, but NMR indicates presence of impurities. $R_f = 0.33$ (10% MeOH/EtOAc); ^1H NMR (CDCl_3 , 500 MHz): δ (ppm) 2.43 (s, 3H), 3.55-3.74 (m, 22H), 3.80 (t, $J = 5.0$ Hz, 2H), 3.87 (t, $J = 5.0$ Hz, 2H), 3.89 (t, $J = 5.8$ Hz, 2H), 4.12-4.20 (m, 4H), 4.47 (t, $J = 5.0$ Hz, 2H), 4.54 (br, 2H), 4.67 (s, 2H), 4.68 (s, 2H), 7.33 (d, $J = 8.5$ Hz, 2H), 7.72 (dd, $J = 6.0$ Hz, 3.5 Hz, 2H), 7.74 (s, 1H), 7.79 (d, $J = 9.0$ Hz, 2H), 7.78 (s, 1H), 7.84 (dd, $J = 6.0$ Hz, 3.0 Hz, 2H); ^{13}C NMR (CDCl_3 , 125 MHz): δ (ppm) 21.6, 37.2, 50.2, 58.4, 64.4, 68.0, 68.6, 69.0, 69.20, 69.24, 69.4, 69.6, 69.9, 70.43, 70.47, 70.50, 70.51, 70.7, 123.2, 127.9, 129.8, 132.0, 132.9, 134.0, 144.8, 168.2, some signals account for more than one carbon; MS (MALDI, m/z) 860.4 for $[\text{M}+\text{H}]^+$.

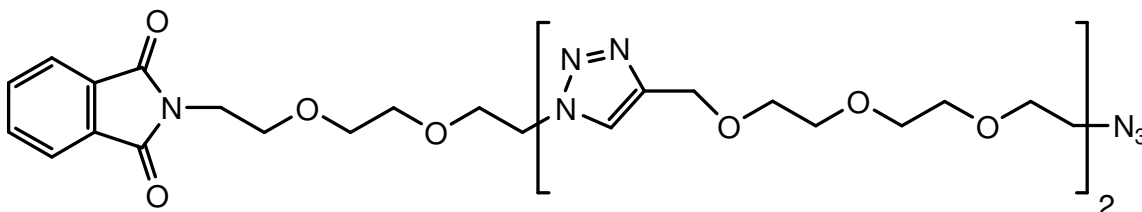
 ^1H NMR ^{13}C NMR



MS

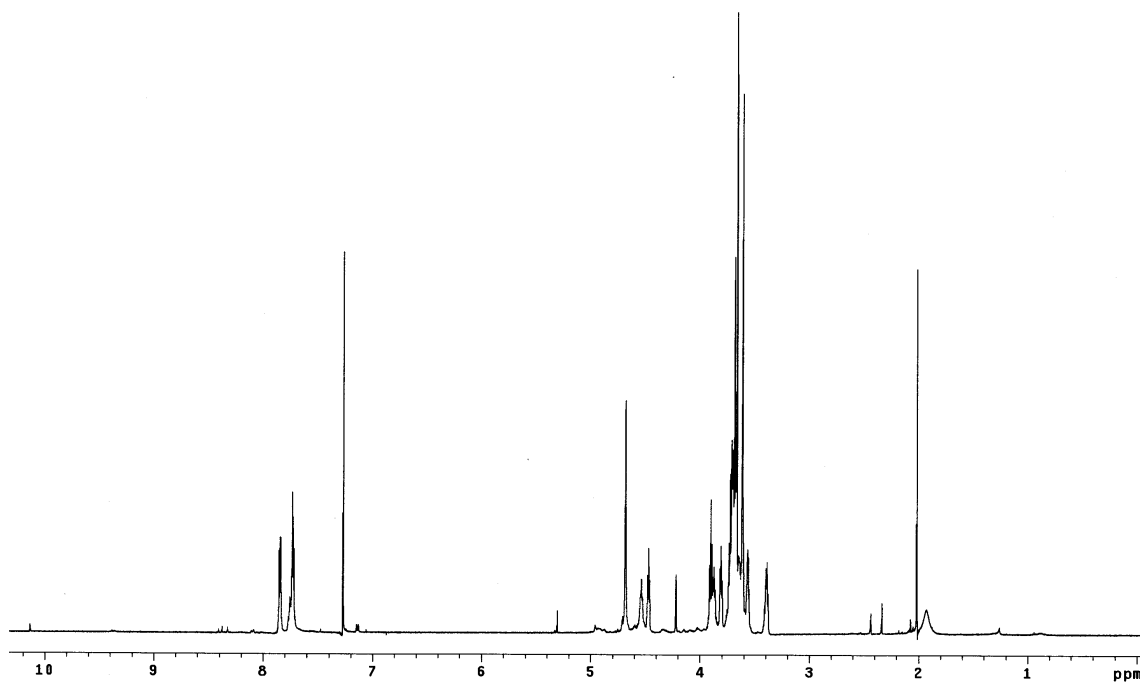
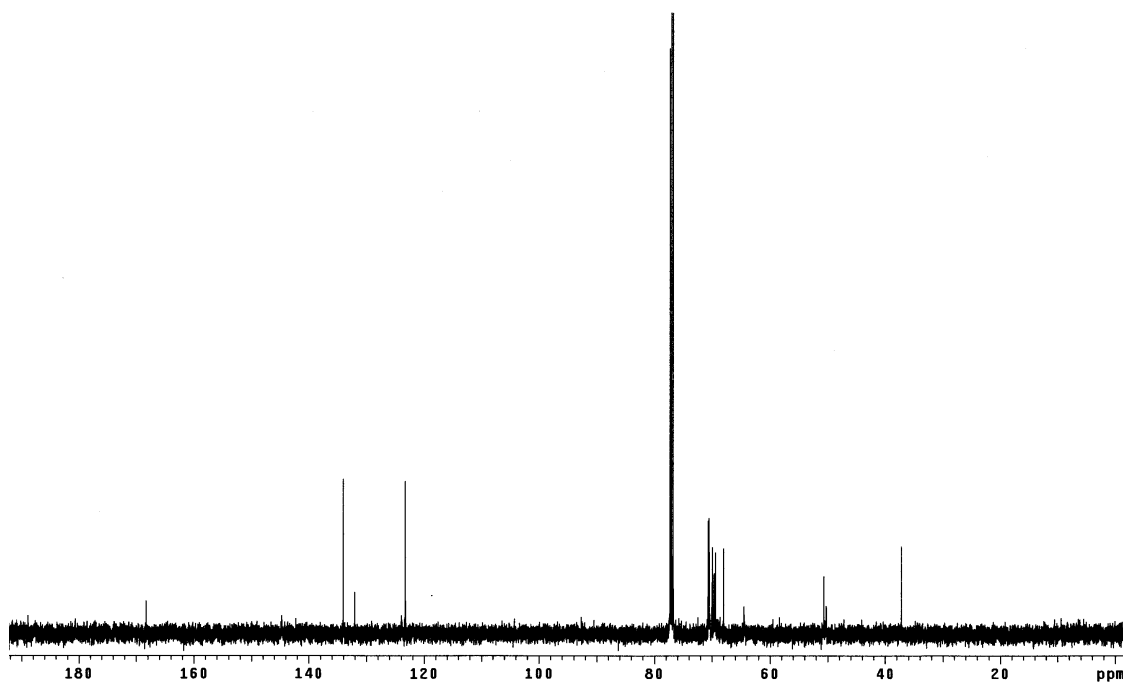
Compound 9

2-(2-(2-(2-(4-((2-(2-(2-(4-((2-(2-(2-Azidoethoxy)ethoxy)ethoxy)methyl)-1*H*-1,2,3-triazol-1-yl)ethoxy)ethoxy)ethoxy)methyl)-1*H*-1,2,3-triazol-1-yl)ethoxy)ethoxy)ethyl)isoindoline-1,3-dione

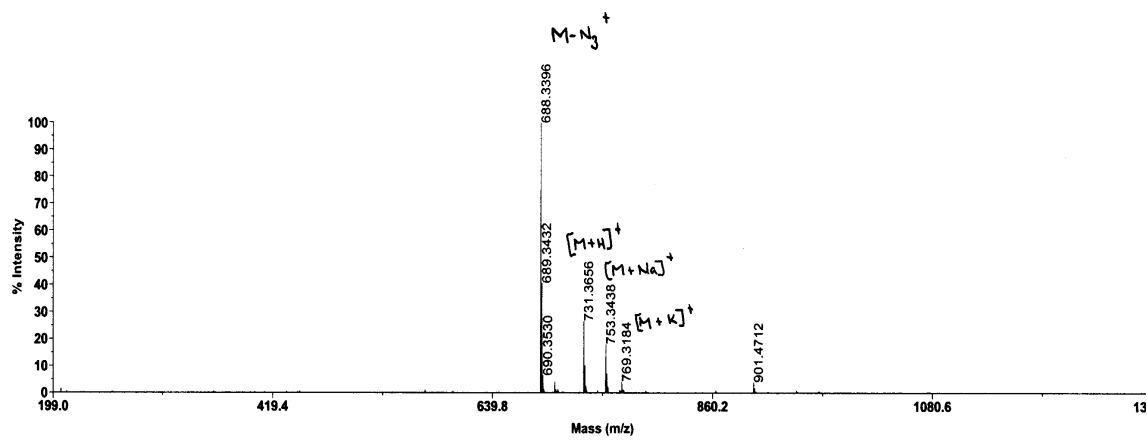


Procedure:

Compound **8** (356 mg, 0.410 mmol) and sodium azide (87.0 mg, 1.34 mmol) were refluxed in 5 mL MeCN for 40 h. DI water (20 mL) was added and extracted with CH₂Cl₂ (5 x 20 mL). The organic extracts were pooled, dried over Na₂SO₄, filtered, and evaporated *in vacuo*, yielding **9** as a yellow oil (265 mg, 88%). ¹H NMR (CDCl₃, 500 MHz): δ (ppm) 3.38 (t, *J* = 5.3 Hz, 2H), 3.56 (t, *J* = 4.8 Hz, 2H), 3.61-3.74 (m, 22H), 3.80 (t, *J* = 5.3 Hz, 2H), 3.87 (t, *J* = 4.8 Hz, 2H), 3.90 (t, *J* = 5.8 Hz, 2H), 4.46 (t, *J* = 5.0 Hz, 2H), 4.53 (t, *J* = 4.8 Hz, 2H), 4.68 (s, 4H), 7.20 (dd, *J* = 6.5 Hz, 3.5 Hz, 2H), 7.76 (s, 1H), 7.77 (s, 1H), 7.84 (dd, *J* = 5.5 Hz, 3.0 Hz, 2H); ¹³C NMR (CDCl₃, 125 MHz): δ (ppm) 37.2, 50.3, 50.6, 64.5, 68.0, 69.4, 69.6, 69.65, 69.9, 70.0, 70.45, 70.48, 70.51, 70.52, 70.58, 70.6, 70.7, 123.2, 132.0, 134.0, 168.2, some signals account for more than one carbon; MS (MALDI, *m/z*) 731.4 for [M+H]⁺.

 ^1H NMR ^{13}C NMR

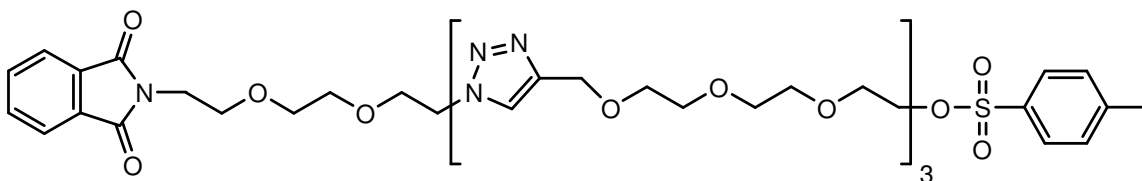
Voyager Spec #1[BP = 688.3, 13184]



MS

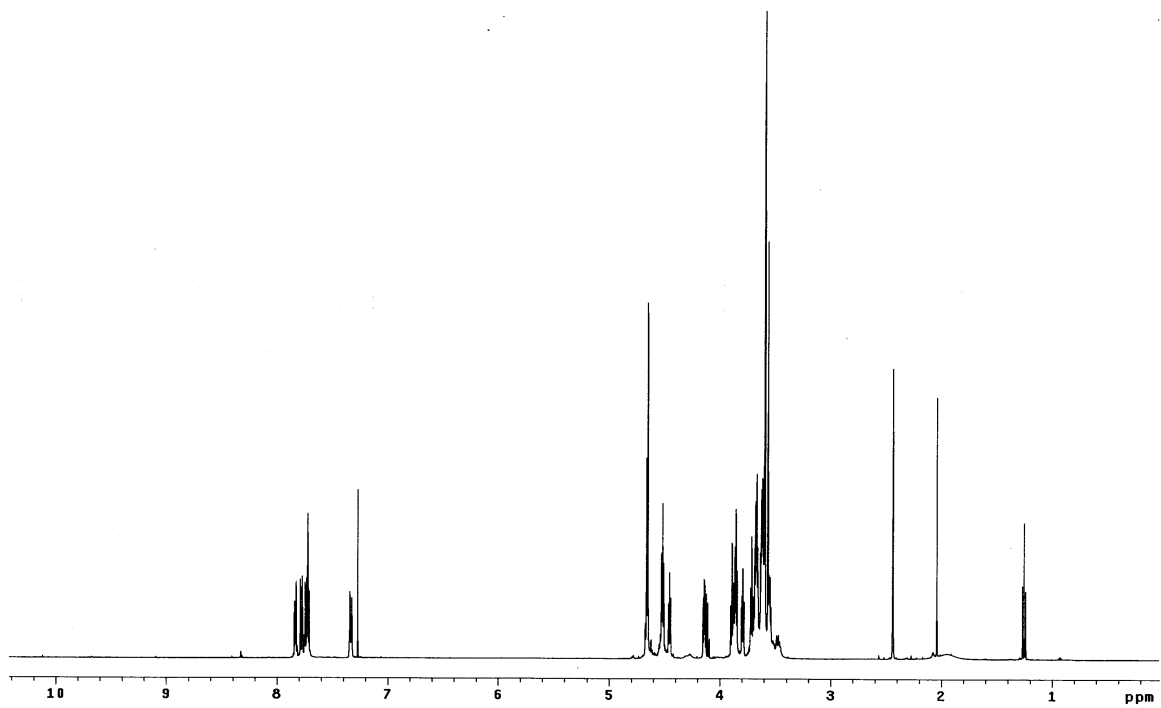
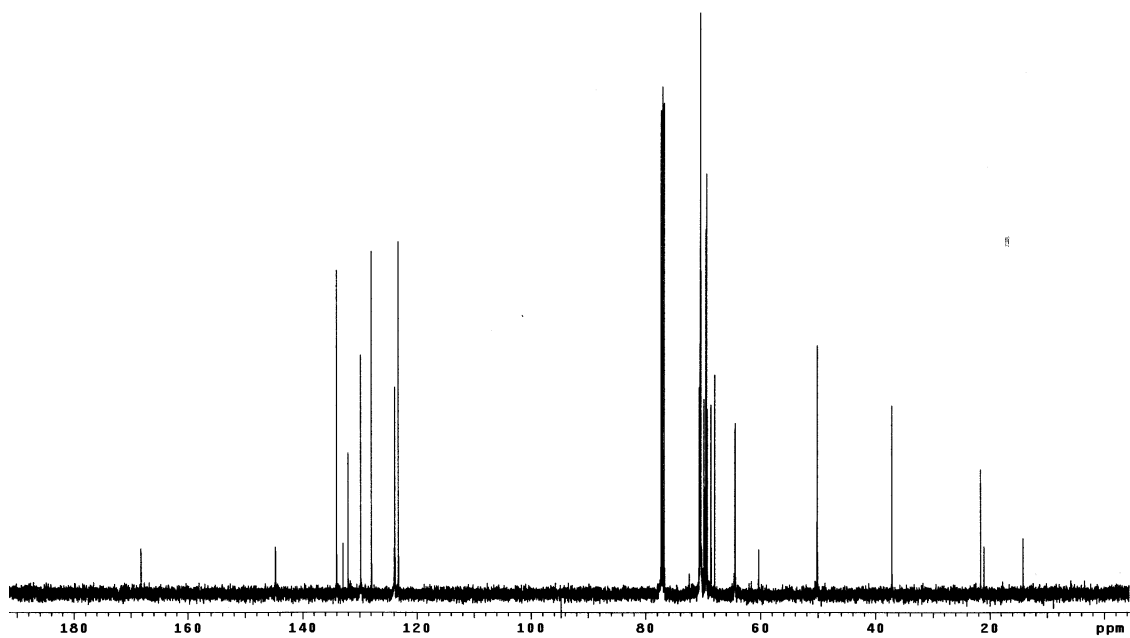
Compound 10

2-(2-(2-(2-(4-((2-(2-(2-(4-((2-(2-(2-(4-((2-(2-(2-(4-Methylbenzenesulfonyl)ethoxy)ethoxy)ethoxy)methyl)-1*H*-1,2,3-triazol-1-yl)ethoxy)ethoxy)ethoxy)methyl)-1*H*-1,2,3-triazol-1-yl)ethoxy)ethoxy)ethoxy)methyl)-1*H*-1,2,3-triazol-1-yl)ethoxy)ethoxy)ethyl)isoindoline-1,3-dione

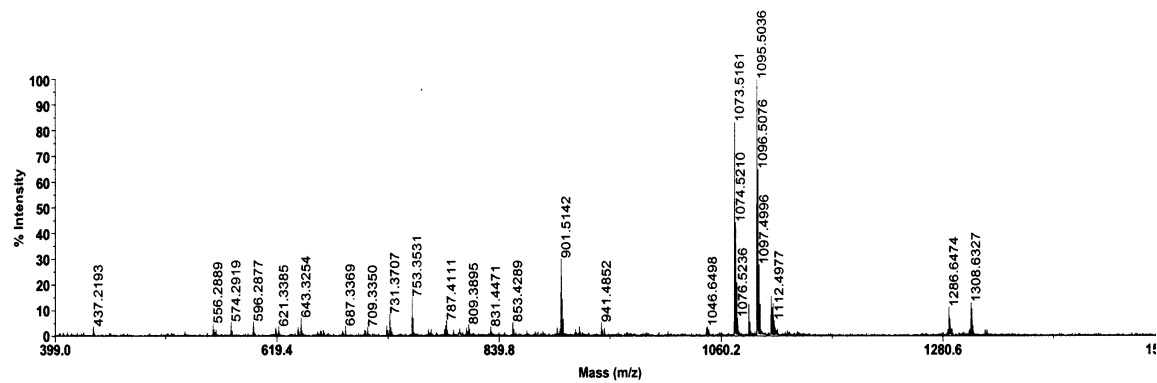


Procedure:

Compound **9** (255 mg, 0.350 mmol), compound **4** (120. mg, 0.350 mmol), copper powder (45 mg, 0.70 mmol), and 140 μ L of an aqueous 1M $\text{CuSO}_4 \cdot 5\text{H}_2\text{O}$ solution (40 mol%) were suspended in 2 mL t BuOH/ H_2O (1:1) mixture in a scintillation vial. The vial was capped and the reaction solution stirred vigorously for 48 h at room temperature. The product was purified by flash chromatography eluting first with 10% MeOH/EtOAc, then with 50% MeOH/EtOAc, yielding **10** as a dull-yellow oil (143 mg, 38%). ^1H NMR (CDCl_3 , 500 MHz): δ (ppm) 2.44 (s, 3H), 3.54-3.72 (m, 34H), 3.79 (t, $J = 5.0$ Hz, 2H), 3.85 (t, $J = 5.3$ Hz, 2H), 3.89 (t, $J = 5.5$ Hz, 2H), 4.13 (t, $J = 6.8$ Hz, 2H), 4.45 (t, $J = 5.3$ Hz, 2H), 4.51 (t, $J = 5.3$ Hz, 4H), 4.65 (s, 4H), 4.66 (s, 2H), 7.33 (d, $J = 8.5$ Hz, 2H), 7.71 (dd, $J = 6.5$ Hz, 3.5 Hz, 2H), 7.72 (s, 2H), 7.74 (s, 1H), 7.78 (d, $J = 8.5$ Hz, 2H), 7.83 (dd, $J = 6.5$ Hz, 3.5 Hz, 2H); ^{13}C NMR (CDCl_3 , 125 MHz): δ (ppm) 21.6, 37.2, 50.1, 64.4, 64.5, 67.9, 68.6, 69.2, 69.4, 69.5, 69.8, 70.3, 70.40, 70.44, 70.45, 70.5, 70.7, 123.2, 123.8, 127.9, 129.8, 132.0, 132.9, 134.0, 144.6, 144.7, 168.2, some signals account for more than one carbon; MS (MALDI, m/z) 1095.5 for $[\text{M}+\text{Na}]^+$.

 ^1H NMR ^{13}C NMR

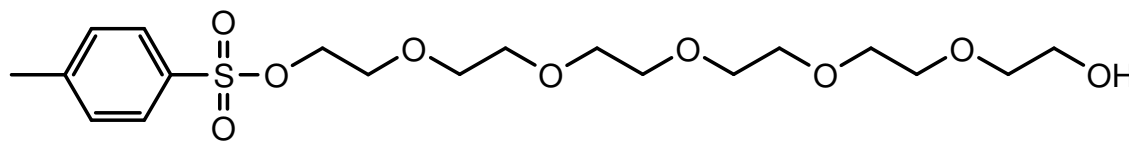
Voyager Spec #1[BP = 1095.5, 12083]



MS

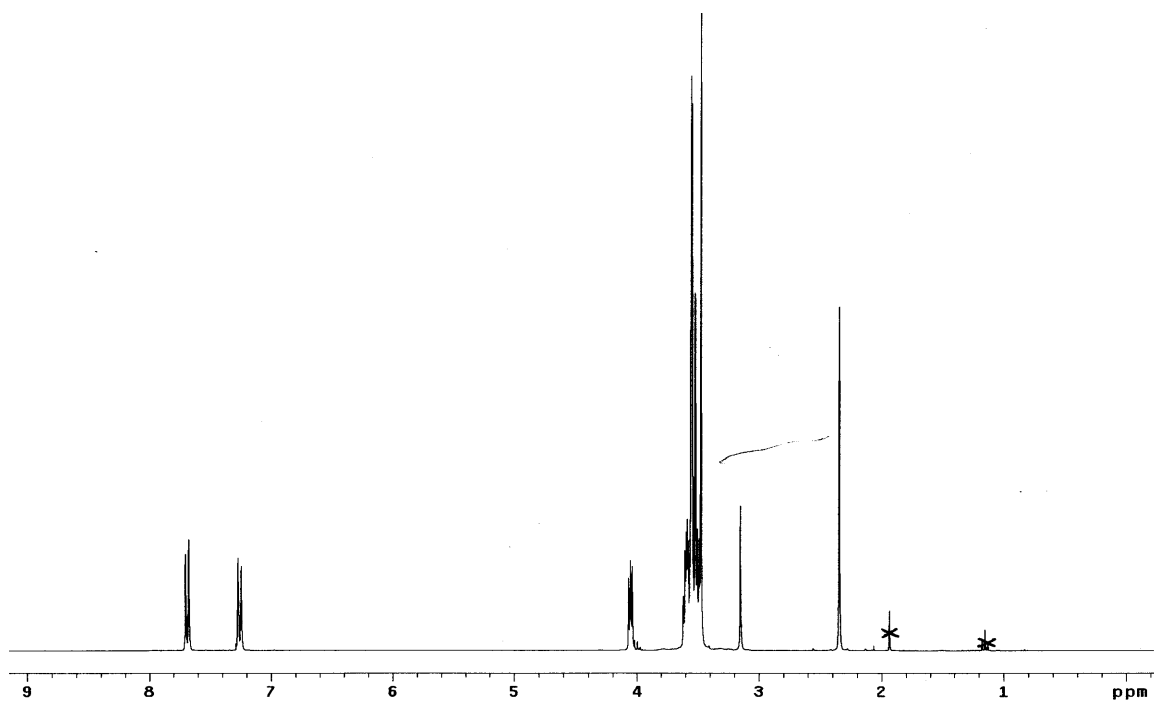
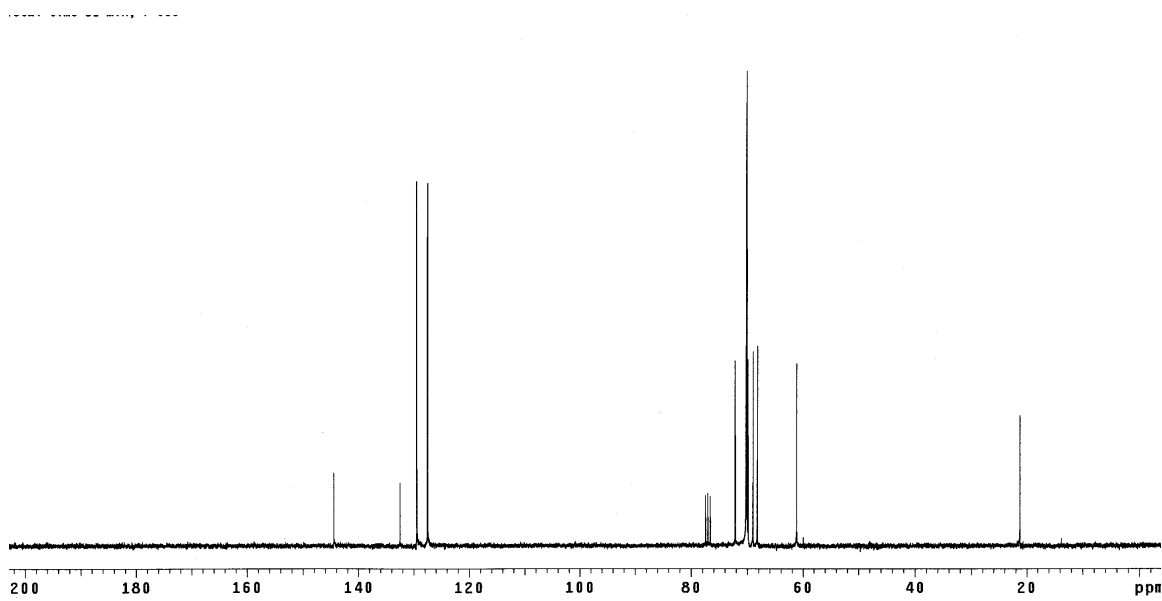
Compound 11

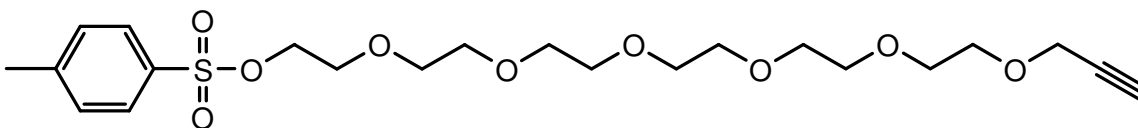
2-(2-(2-(2-(2-(2-Hydroxyethoxy)ethoxy)ethoxy)ethoxy)ethyl 4-methylbenzenesulfonate¹¹¹



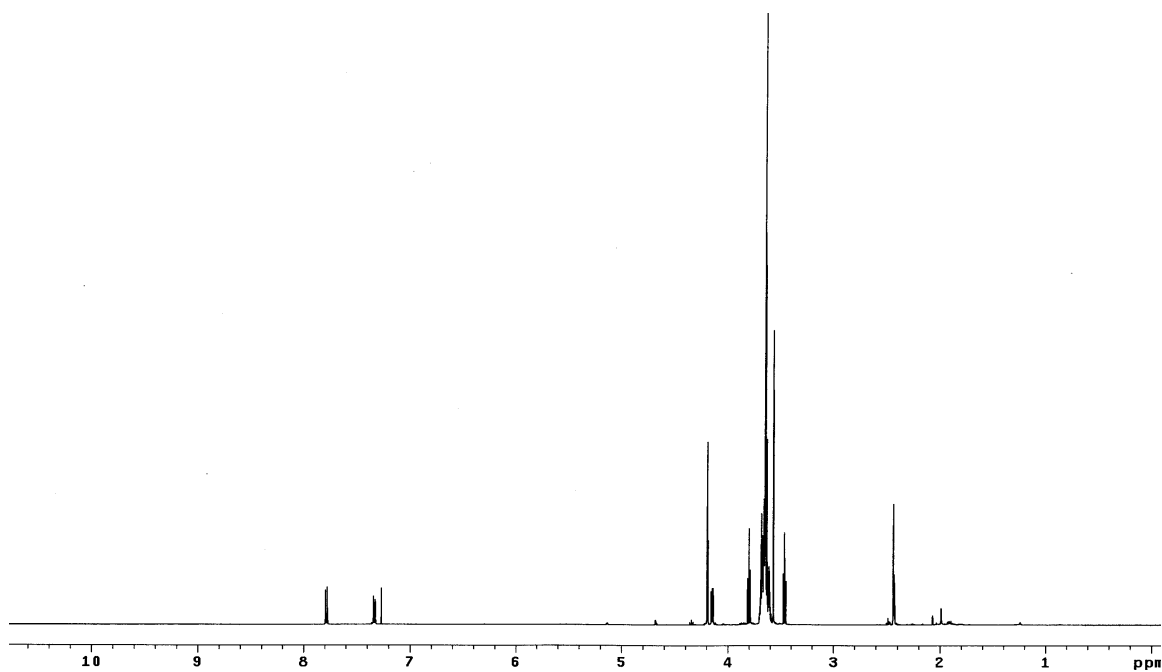
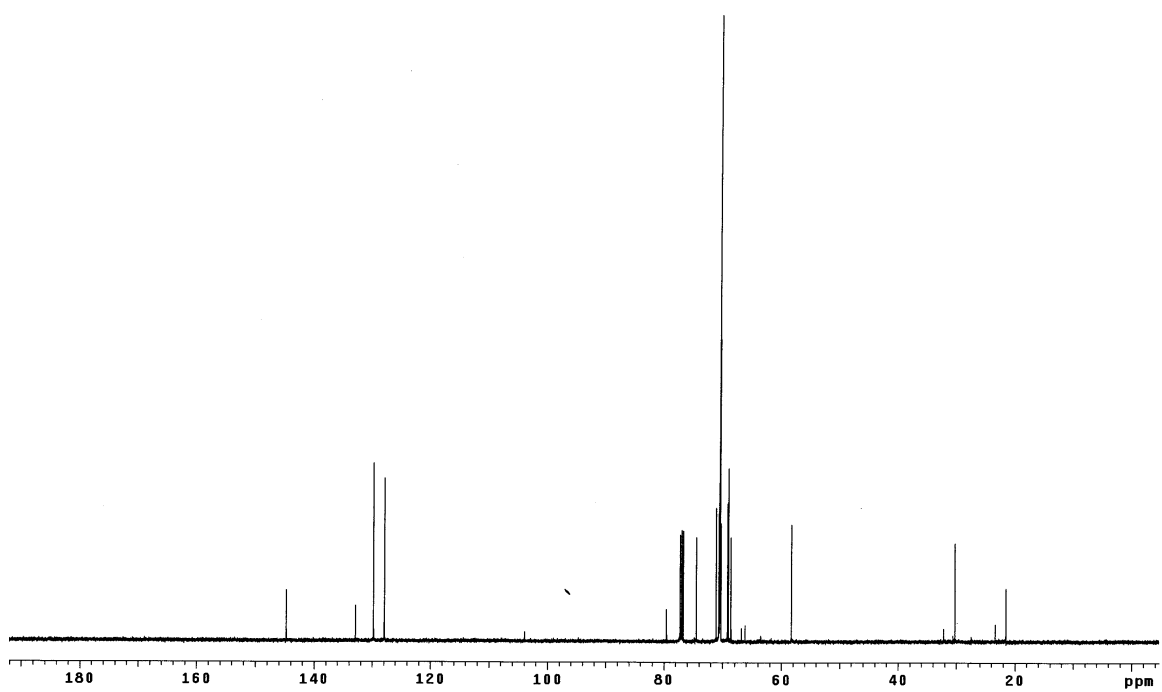
Procedure:

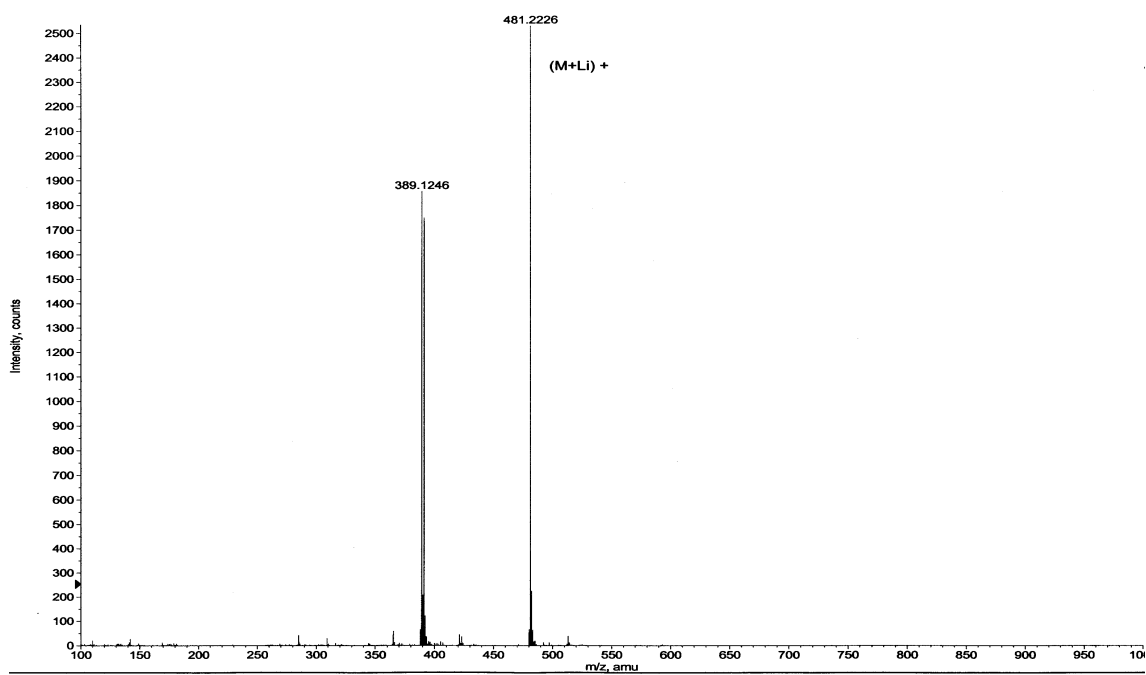
Hexaethylene glycol (5.66 g, 20.0 mmol) was solubilized in 400 mL CH₂Cl₂ and cooled to 0 °C. Silver(I) oxide (6.96 g, 30.0 mmol) was added and the mixture stirred for about 10 minutes followed by sequential additions of *p*-toluenesulfonyl chloride (4.20 g, 22.0 mmol) and potassium iodide (0.660 g, 4.00 mmol). The reaction stirred for 20 minutes and filtered through celite, washing with EtOAc. The organic washings was evaporated *in vacuo* and the resulting residue purified by flash chromatography using 1:1 EtOAc/ acetone to afford **11** as a colorless oil (7.80 g, 89%). ¹H NMR (CDCl₃, 300 MHz): δ (ppm) 2.35 (s, 3H), 3.15 (s, 1H), 3.47-3.62 (m, 22H), 4.05 (t, *J* = 5.7 Hz, 2H), 7.25 (d, *J* = 8.1 Hz, 2H), 7.68 (d, *J* = 8.4 Hz, 2H); ¹³C NMR (CDCl₃, 75 MHz): δ (ppm) 21.2, 61.1, 68.2, 69.0, 69.8, 70.07, 70.1, 70.2, 72.1, 127.5, 129.5, 132.5, 144.4, some signals account for more than one carbon.

 ^1H NMR ^{13}C NMR

Compound 12**2-(2-(2-(2-(2-(2-Prop-2-ynoxy)ethoxy)ethoxy)ethoxy)ethoxy)ethyl 4-methylbenzenesulfonate****Procedure:**

Compound **11** (4.56 g, 10.5 mmol) and propargyl bromide (3.11 g, 20.9 mmol) was mixed in 50 mL distilled THF at -5 °C. After the scoop-wise addition of sodium hydride (0.275 g, 11.5 mmol), the reaction flask was capped and stirred under N₂ allowing the yellowish-orange solution to warm gradually to room temperature. The reaction mixture was then gently heated to 40 °C, stirring for 22 h. DI water (150 mL) was added and extracted with CH₂Cl₂ (3 x 100 mL). The combined organic extracts were dried over Na₂SO₄ and evaporated under reduced pressure. The crude product was purified by column chromatography eluting with 1:1 EtOAc/acetone to yield **12** as a yellow oil (2.26 g, 46%). HPLC (1:1 MeCN/H₂O with 0.1% TFA): retention time 18.8 minutes, purity 86%; ¹H NMR (CDCl₃, 500 MHz): δ (ppm) 2.42 (t, *J* = 2.0 Hz, 1H), 2.43 (s, 3H), 3.45 (t, *J* = 6.5 Hz, 2H), 3.48-3.70 (m, 20H), 3.80 (t, *J* = 6.5 Hz, 2H), 4.19 (d, *J* = 2.5 Hz, 2H), 7.33 (d, *J* = 8.0 Hz, 2H), 7.78 (d, *J* = 8.0 Hz, 2H); ¹³C NMR (CDCl₃, 125 MHz): δ (ppm) 21.6, 30.3, 58.3, 68.6, 69.0, 69.2, 70.3, 70.43, 70.46, 70.48, 70.51, 70.53, 70.6, 70.7, 71.1, 79.6, 127.9, 129.7, 132.9, 144.7; MS (ESI, *m/z*) 481.2 for [M+Li]⁺.

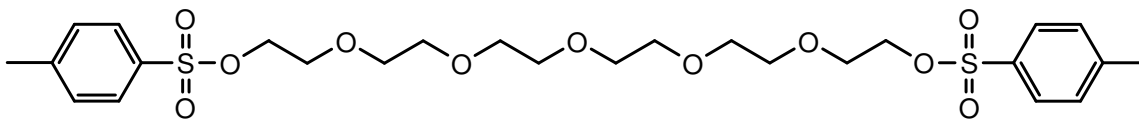
 ^1H NMR ^{13}C NMR



MS

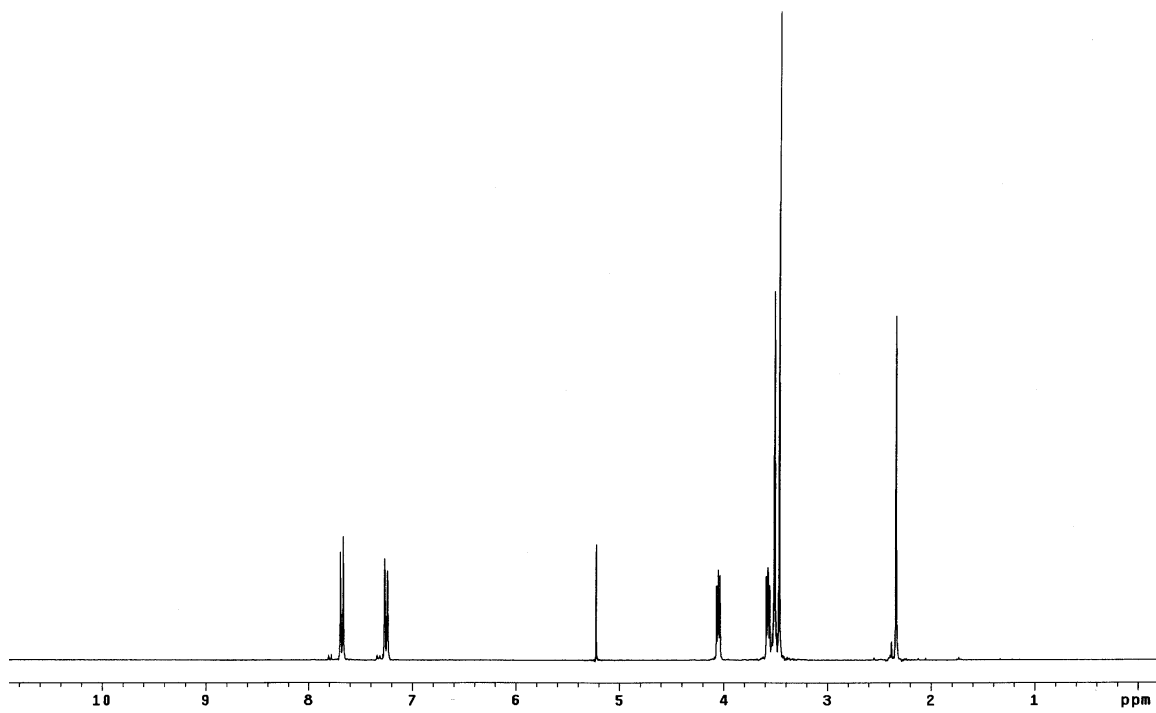
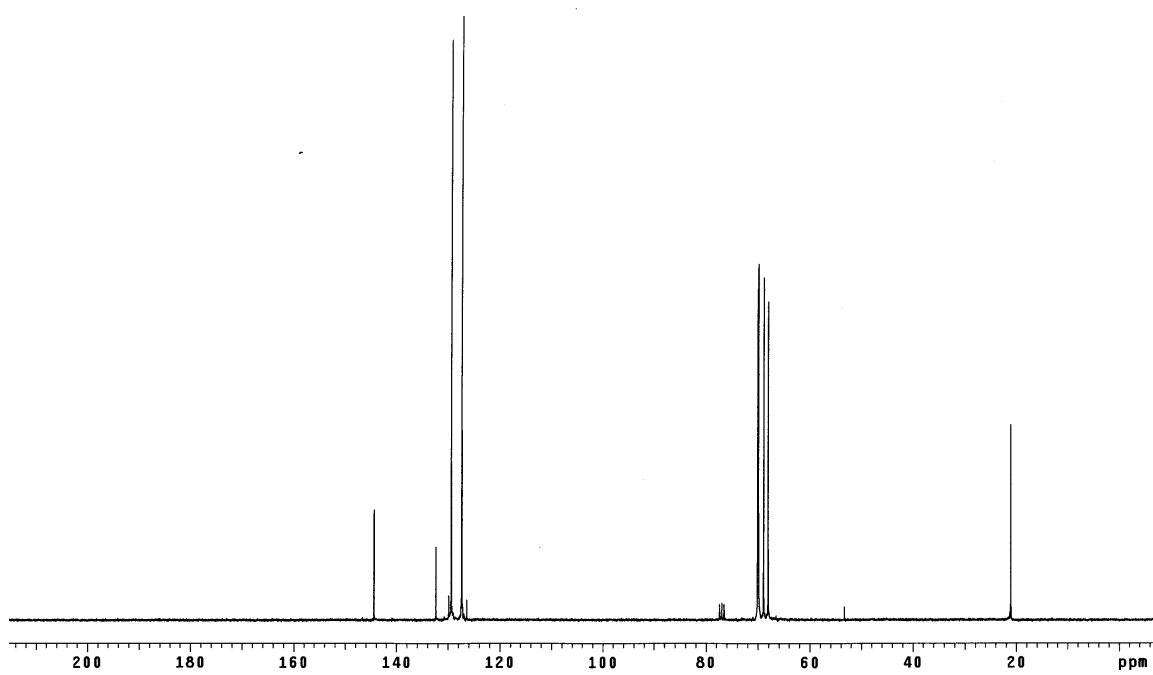
Compound 13

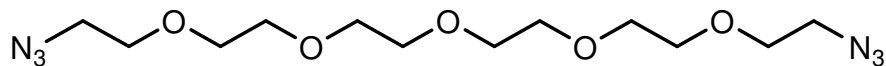
1-(2-(2-(2-(2-(2-(4-Methylbenzenesulfonyloxy)ethoxy)ethoxy)ethoxy)ethoxy)ethoxy)ethyl 4-methylbenzenesulfonate¹¹⁸



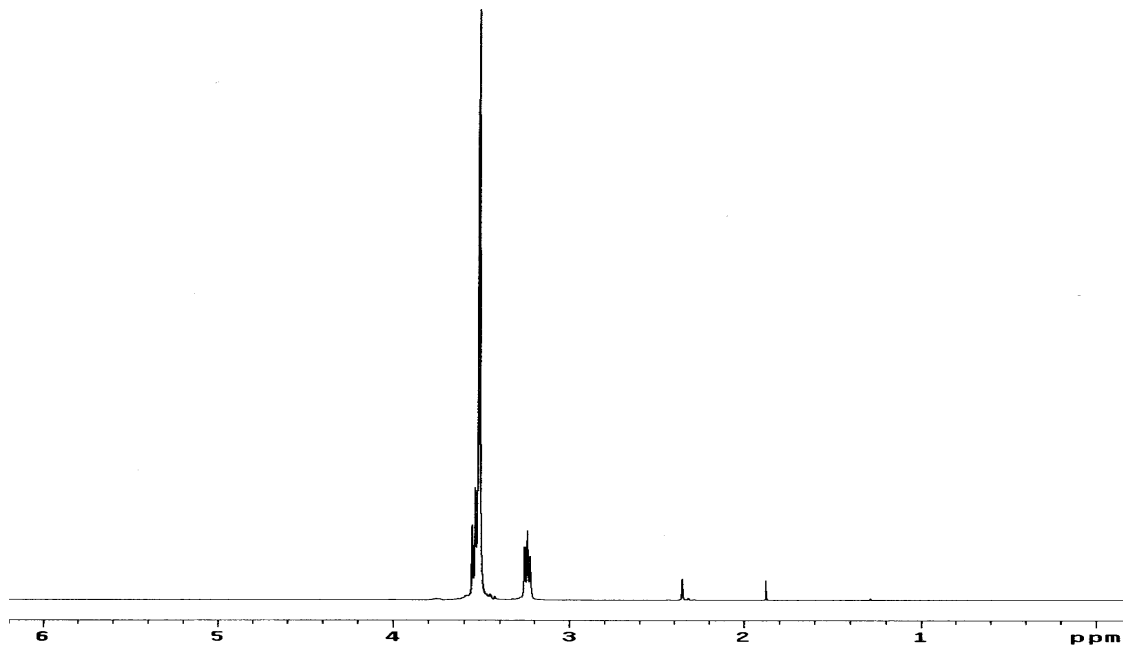
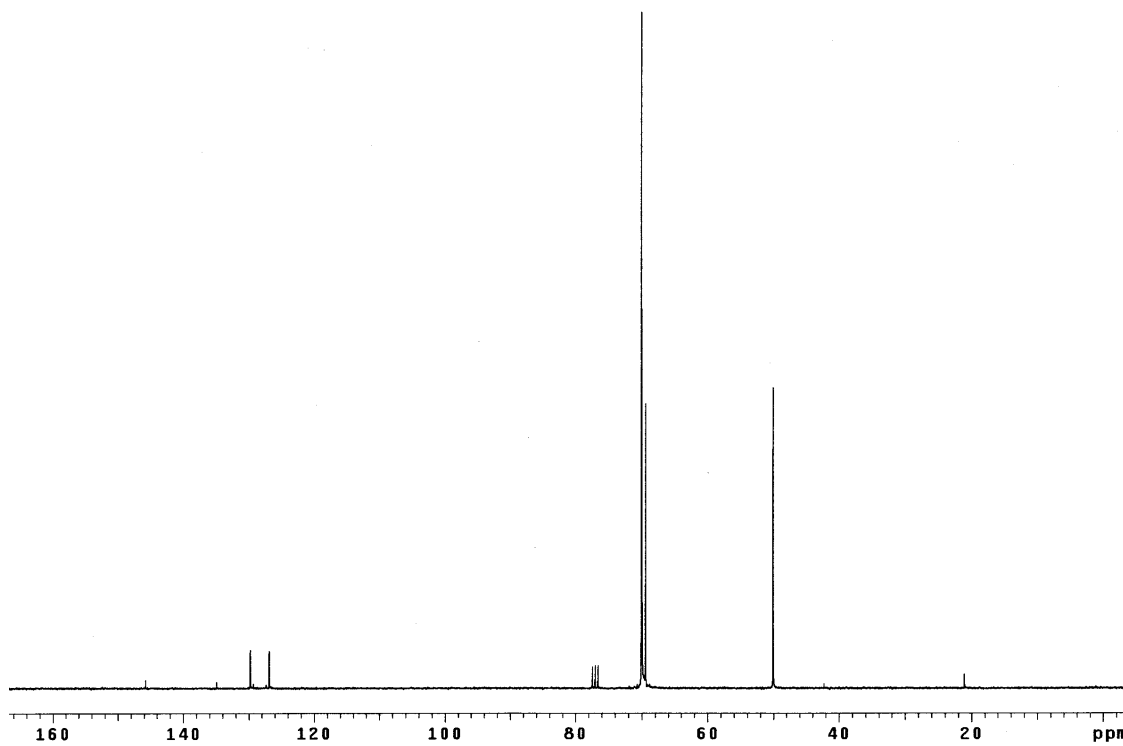
Procedure:

Hexaethylene glycol (27.9 g, 98.9 mmol) and *p*-toluenesulfonyl chloride (56.6 g, 296 mmol) were dissolved in 150 mL THF. The mixture was cooled to 0 °C and potassium hydroxide (42 mL of a 16 M solution) was added very slowly. The reaction solution was allowed to warm to room temperature and stirred for 8 h after which it was poured into 300 mL of a 2:1 CH₂Cl₂/ice-water mixture and extracted with CH₂Cl₂ (3 x 200 mL). The pooled organic extracts were washed with 2M KOH (2 x 200 mL), brine (2 x 200 mL), and water (6 x 200 mL). The extracts were dried over MgSO₄, filtered, and evaporated *in vacuo*, yielding **13** as a yellow oil (49.2 g, 84%). ¹H NMR (CDCl₃, 300 MHz): δ (ppm) 2.34 (s, 6H), 3.47 (s, 8H), 3.51 (s, 8H), 3.57 (t, *J* = 4.8 Hz, 4H), 4.05 (t, *J* = 4.7 Hz, 4H), 7.25 (d, *J* = 8.4 Hz, 4H), 7.68 (d, *J* = 8.1 Hz, 4H); ¹³C NMR (CDCl₃, 75 MHz): δ (ppm) 21.1, 68.1, 69.0, 69.9, 70.0, 70.1, 127.4, 129.4, 132.4, 144.4, some signals account for more than one carbon.

 ^1H NMR ^{13}C NMR

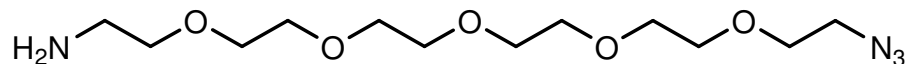
Compound 14**1-(2-(2-(2-(2-(2-Azidoethoxy)ethoxy)ethoxy)ethoxy)ethoxy)-2-azidoethane¹¹³****Procedure:**

Compound **13** (36.2 g, 61.3 mmol) and sodium azide (15.9 g, 245 mmol) were refluxed in 600 mL MeCN for 43 h. DI water (600 mL) was added and extracted with CH₂Cl₂ (3 x 200 mL). The combined organic extracts were dried over Na₂SO₄, decanted, and evaporated under reduced pressure, yielding **14** as a pale-orange oil (18.6 g, 91%). ¹H NMR (CDCl₃, 300 MHz): δ (ppm) 3.23 (t, *J* = 5.1 Hz, 4H), 3.51-3.55 (m, 20H); ¹³C NMR (CDCl₃, 75 MHz): δ (ppm) 50.0, 69.4, 69.9, 69.99, 70.02, some signals account for more than one carbon.

 $^1\text{H NMR}$  $^{13}\text{C NMR}$

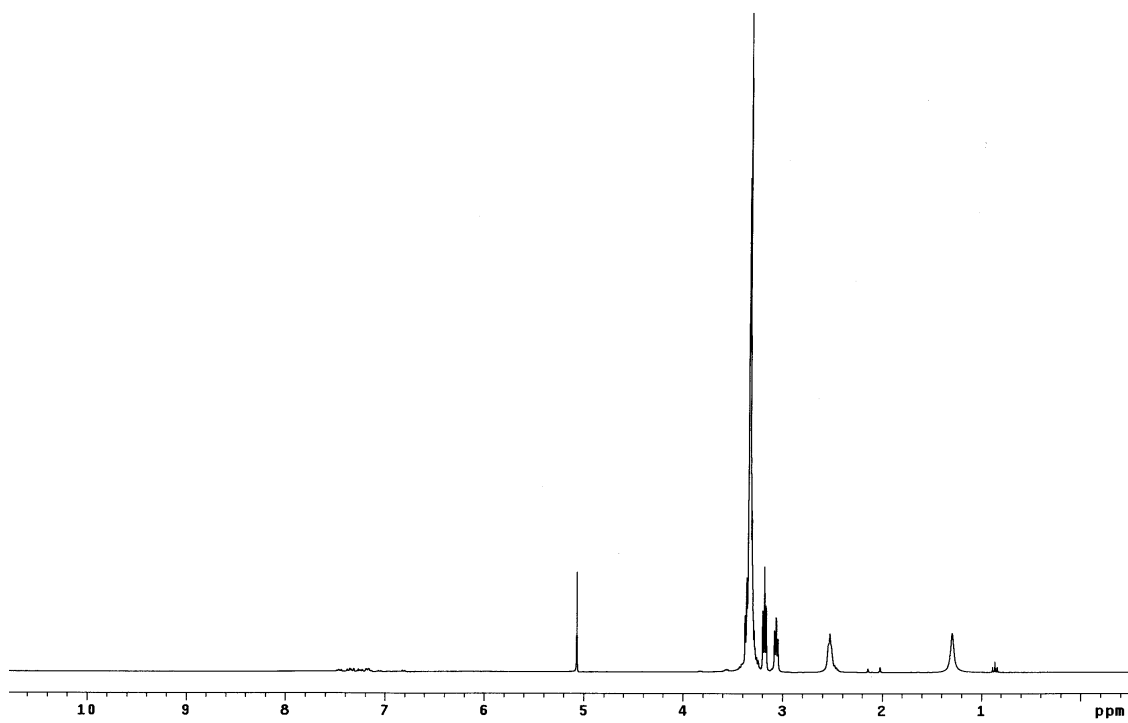
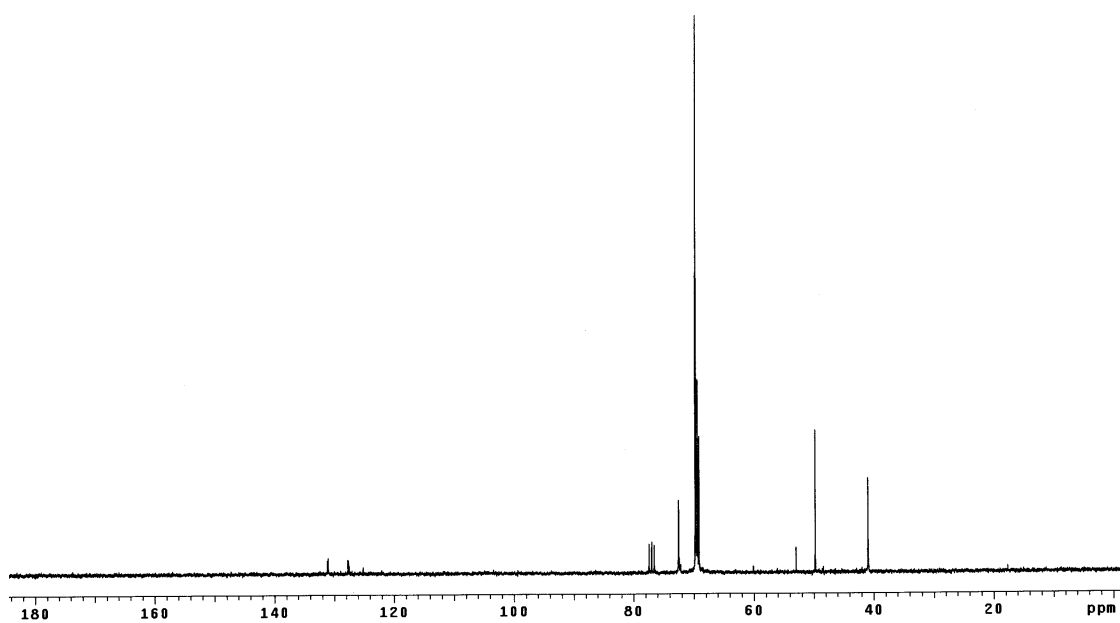
Compound 15

2-(2-(2-(2-(2-(2-Azidoethoxy)ethoxy)ethoxy)ethoxy)ethoxy)ethanamine¹²⁰



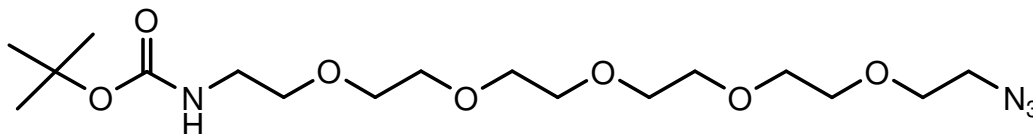
Procedure:

Compound **14** (18.6 g, 56.0 mmol) was solubilized in 150 mL 0.65M H₃PO₄. Triphenylphosphine (12.2 g, 46.7 mmol) in 50 mL anhydrous ether was added drop-wise using an addition funnel over a period of 20 minutes. The funnel was rinsed with 20 mL ether and the washing added to the reaction mixture. The reaction flask was capped and stirred at room temperature for 24 h under N₂. The reaction solution was then washed with ether (3 x 50 mL) to get rid of triphenylphosphine oxide. Potassium hydroxide powder (16 g) was added slowly with gentle swirling (caution: *exothermic reaction!*). More triphenylphosphine oxide was observed crystallizing out. The ether was allowed to slowly evaporate at room temperature, further inducing more triphenylphosphine oxide to crystallize out into the aqueous layer. The flask was then capped tightly and stored at -5 °C to -10 °C for 12 h to induce even more triphenylphosphine oxide crystallizations. The white solid was then filtered and potassium hydroxide powder (30 g) was added and extracted with CH₂Cl₂ (12 x 50 mL). The combined organic extracts were dried over Na₂SO₄, filtered, and evaporated *in vacuo*, yielding **15** as a yellow liquid (11.5 g, 67%).
¹H NMR (CDCl₃, 300 MHz): δ (ppm) 2.53 (br, 2H), 3.06 (t, *J* = 5.1 Hz, 2H), 3.18 (t, *J* = 5.3 Hz, 2H), 3.29-3.38 (m, 20H); ¹³C NMR (CDCl₃, 75 MHz): δ (ppm) 40.9, 49.8, 69.1, 69.4, 69.65, 69.68, 69.72, 69.75, 72.5, some signals account for more than one carbon.

 ^1H NMR ^{13}C NMR

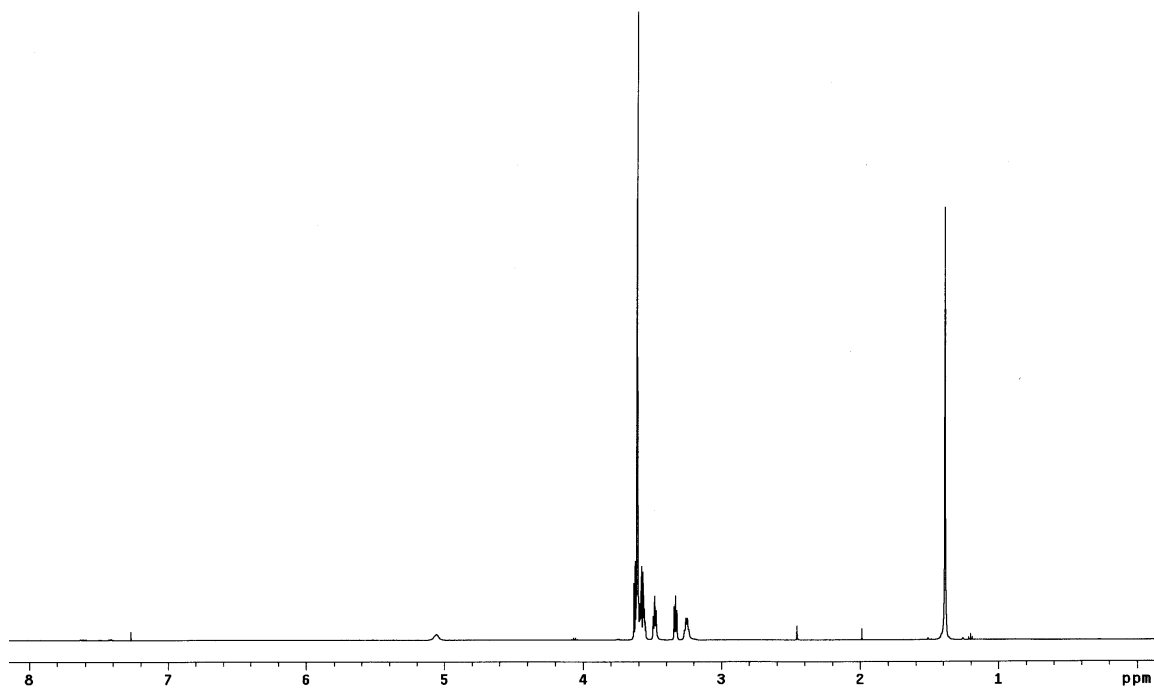
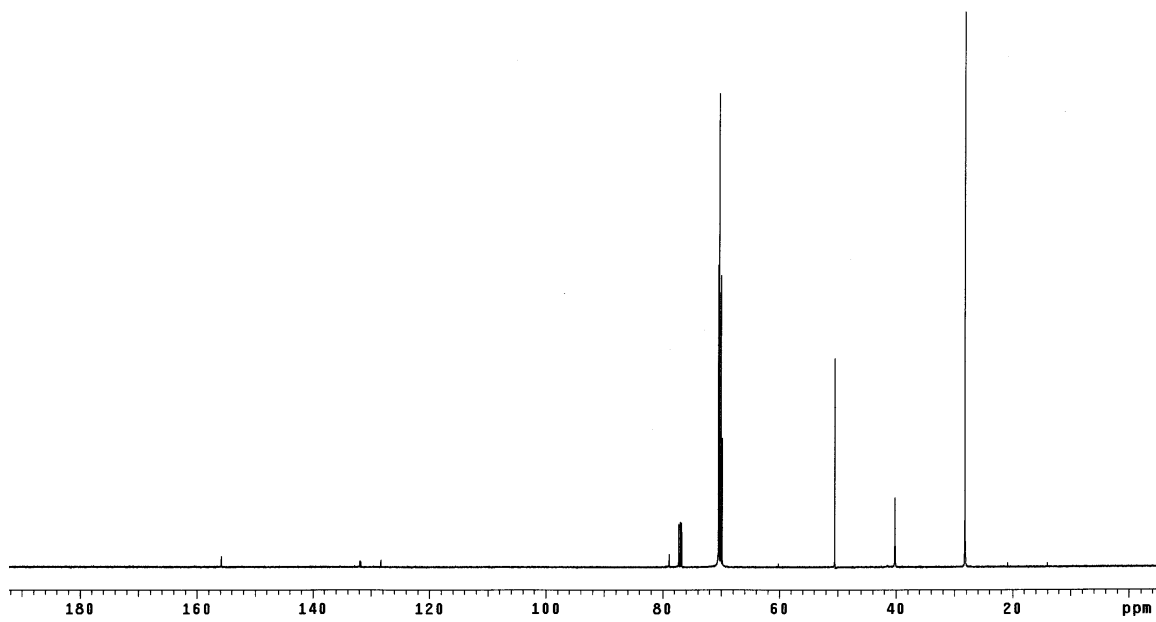
Compound 16

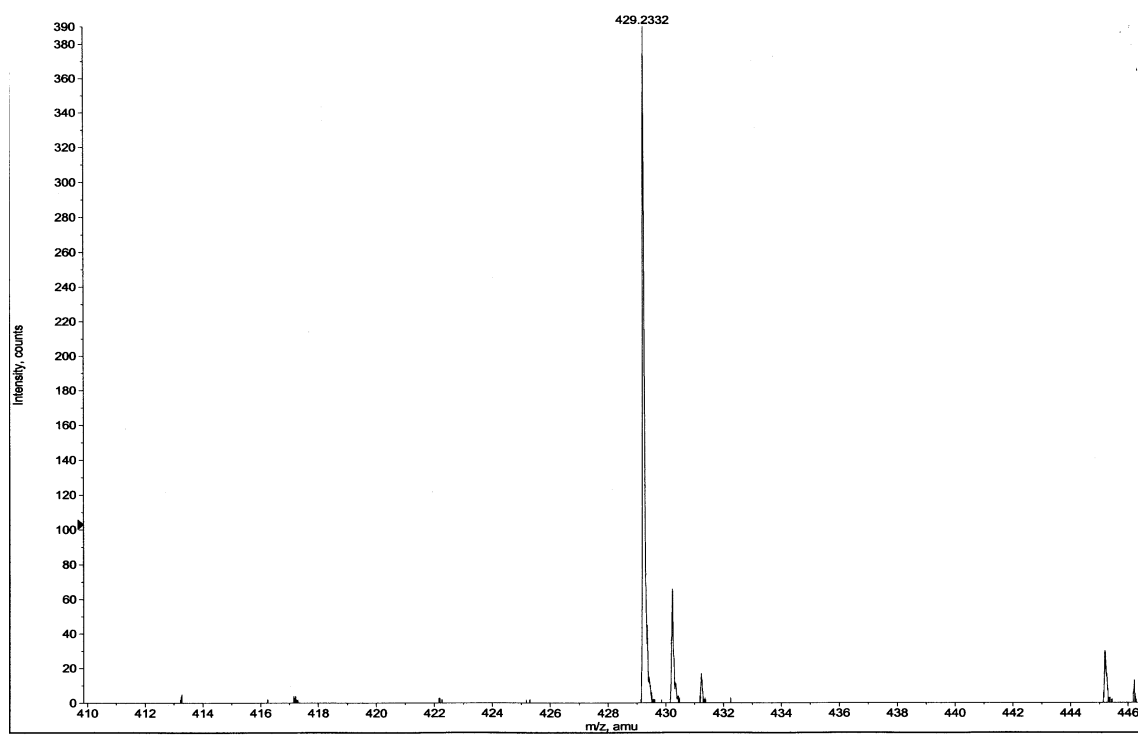
2-(2-(2-(2-(2-(2-Azidoethoxy)ethoxy)ethoxy)ethoxy)ethoxy)ethyl *tert*-butylcarbamate



Procedure:

Compound **15** (13.2 g, 43.2 mmol) and di-*tert*-butylcarbonate (9.42 g, 43.2 mmol) were dissolved in 100 mL CH₂Cl₂ at room temperature. NaOH (1.40 g, 35.0 mmol) was added and the reaction mixture stirred for 4 h. The cloudy solution was filtered through celite and evaporated *in vacuo*. The product residue was purified by column chromatography using EtOAc, yielding **16** as a yellow oil (6.36 g, 50%). HPLC (1:1 MeCN/H₂O with 0.1% TFA): retention time 17.1 minutes, purity 82%; $R_f = 0.68$ (EtOAc); ¹H NMR (CDCl₃, 500 MHz): δ (ppm) 1.39 (s, 9H), 3.25 (br, 2H), 3.33 (t, $J = 5.0$ Hz, 2H), 3.48 (t, $J = 5.3$ Hz, 2H), 3.55-3.63 (m, 18H), 5.10 (br, 1H); ¹³C NMR (CDCl₃, 125 MHz): δ (ppm) 28.2, 40.2, 50.5, 69.9, 70.02, 70.05, 70.3, 70.39, 70.4, 70.43, 70.48, 70.5, 78.9, 155.8, some signals account for more than one carbon; MS (ESI, m/z) 429.2 for [M+Na]⁺.

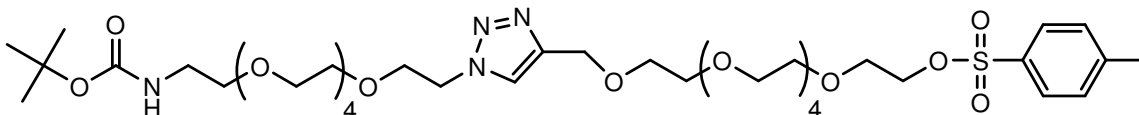
 ^1H NMR ^{13}C NMR



MS

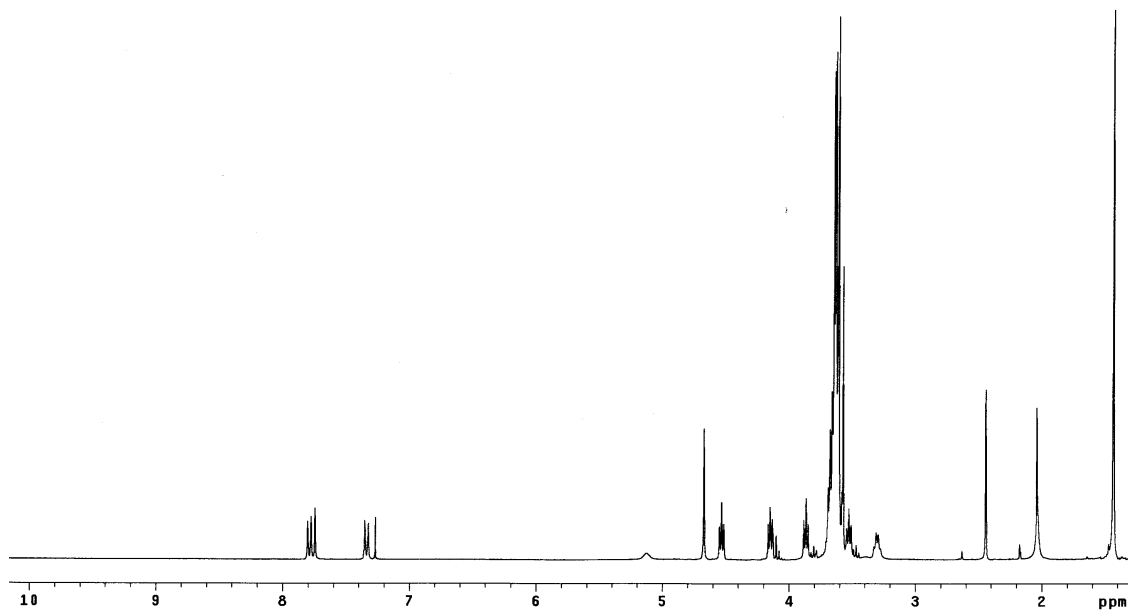
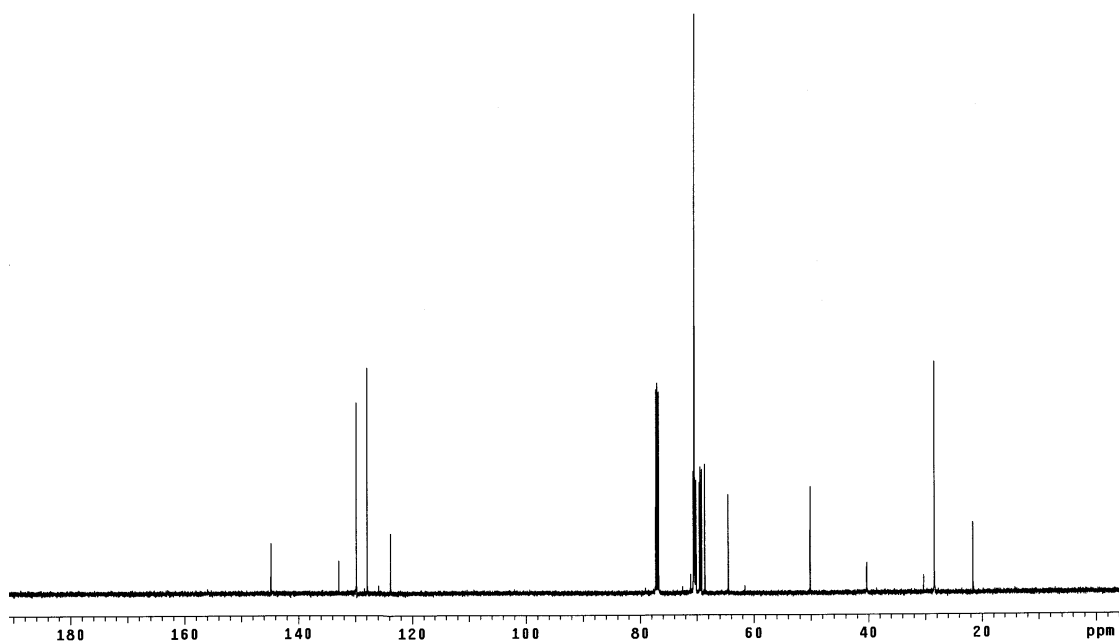
Compound 17

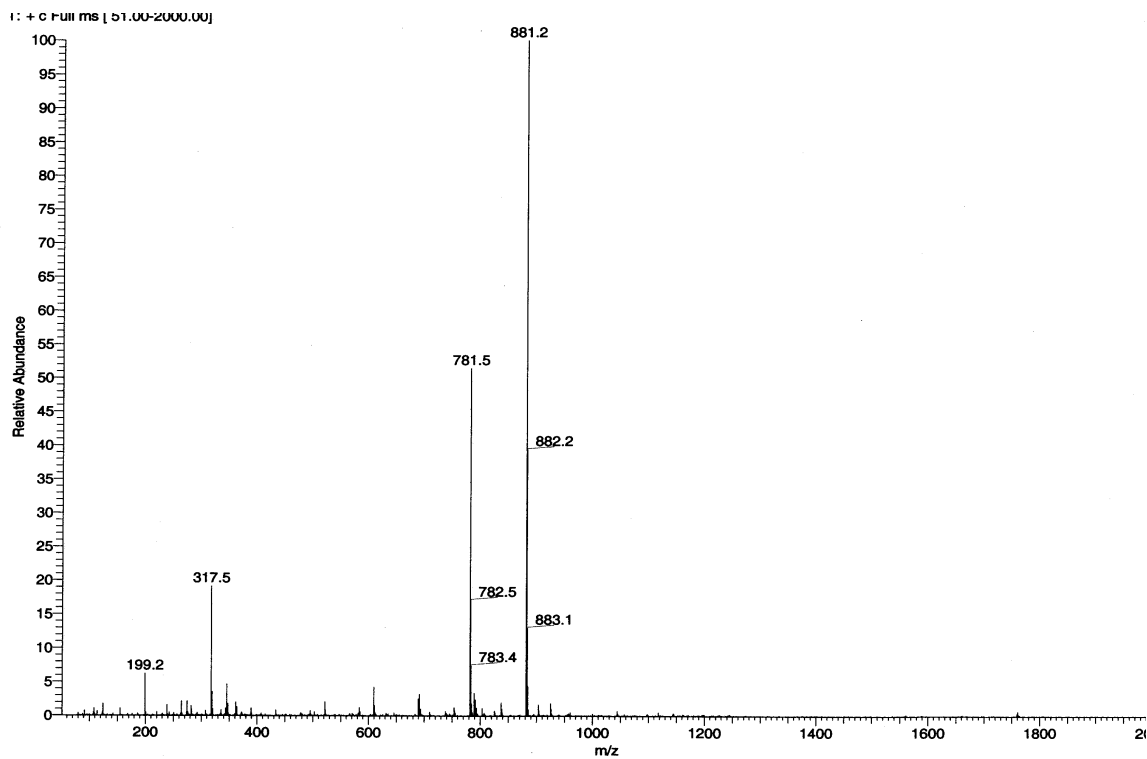
2-(2-(2-(2-(2-(2-4-((2-(2-(2-(2-(2-(4-Methylbenzenesulfonyloxy)ethoxy)ethoxy)ethoxy)ethoxy)ethoxy)methyl)-1*H*-1,2,3-triazol-1-yl)ethoxy)ethoxy)ethoxy)ethoxy)ethyl *tert*-butylcarbamate



Procedure:

Compound **12** (237 mg, 0.50 mmol) and compound **16** (203 mg, 0.50 mmol) were mixed together in 1.5 mL THF/H₂O mixture in a scintillation vial at room temperature. 10 mol% sodium ascorbate and 5 mol% CuSO₄·5H₂O were added from freshly prepared 1 M aqueous solutions. The vial was capped and stirred vigorously for 24 h at room temperature. Column chromatography using 1:1 EtOAc/ acetone afforded a clear, yellow oil (270 mg, 61%). ¹H NMR (CDCl₃, 300 MHz): δ (ppm) 1.43 (s, 9H), 2.44 (s, 3H), 3.31 (t, *J* = 5.3 Hz, 2H), 3.53 (t, *J* = 5.3 Hz, 2H), 3.57-3.69 (m, 38H), 3.86 (t, *J* = 5.1 Hz, 2H), 4.15 (t, *J* = 5.6 Hz, 2H), 4.53 (t, *J* = 5.1 Hz, 2H), 4.67 (s, 2H), 5.10 (br, 1H), 7.35 (d, *J* = 8.7 Hz, 2H), 7.75 (s, 1H), 7.79 (d, *J* = 8.4 Hz, 2H); ¹³C NMR (CDCl₃, 75 MHz): δ (ppm) 21.6, 28.4, 40.3, 50.2, 64.5, 68.6, 69.2, 69.4, 69.5, 70.1, 70.2, 70.4, 70.5, 70.7, 71.2, 123.8, 125.9, 127.9, 129.8, 132.9, 144.76, 144.8, some signals account for more than one carbon; MS (APCI, *m/z*) 881.2 for [M+H]⁺.

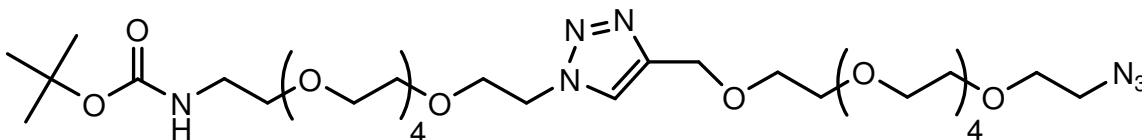
 ^1H NMR ^{13}C NMR



MS

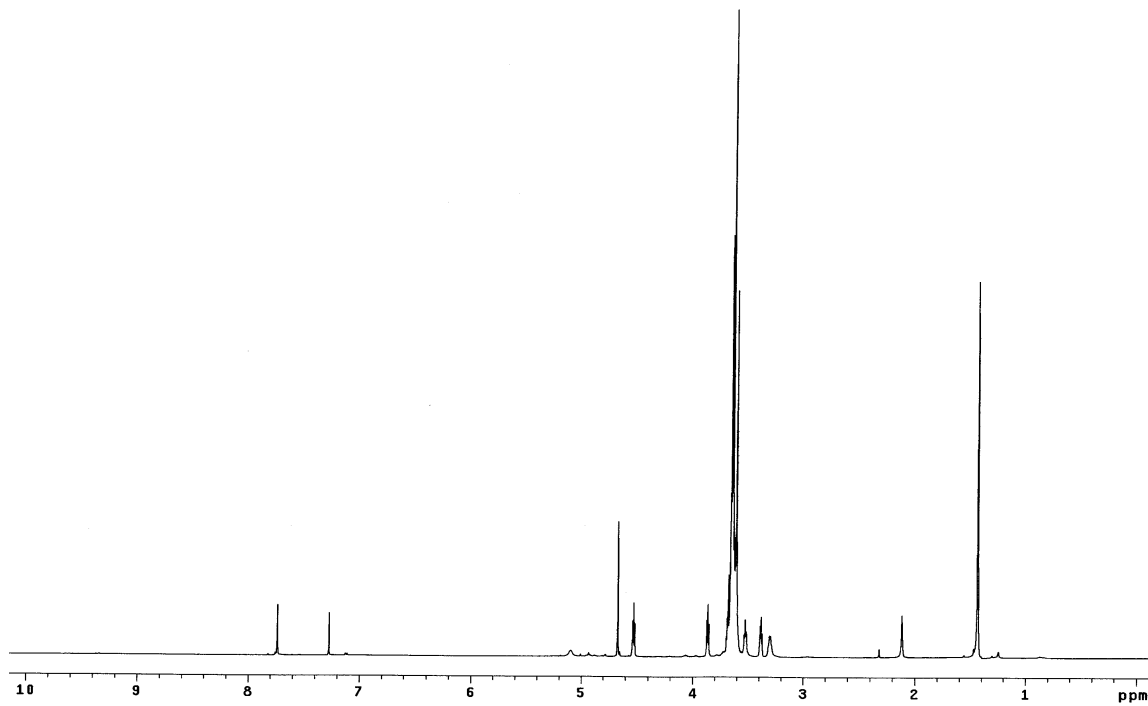
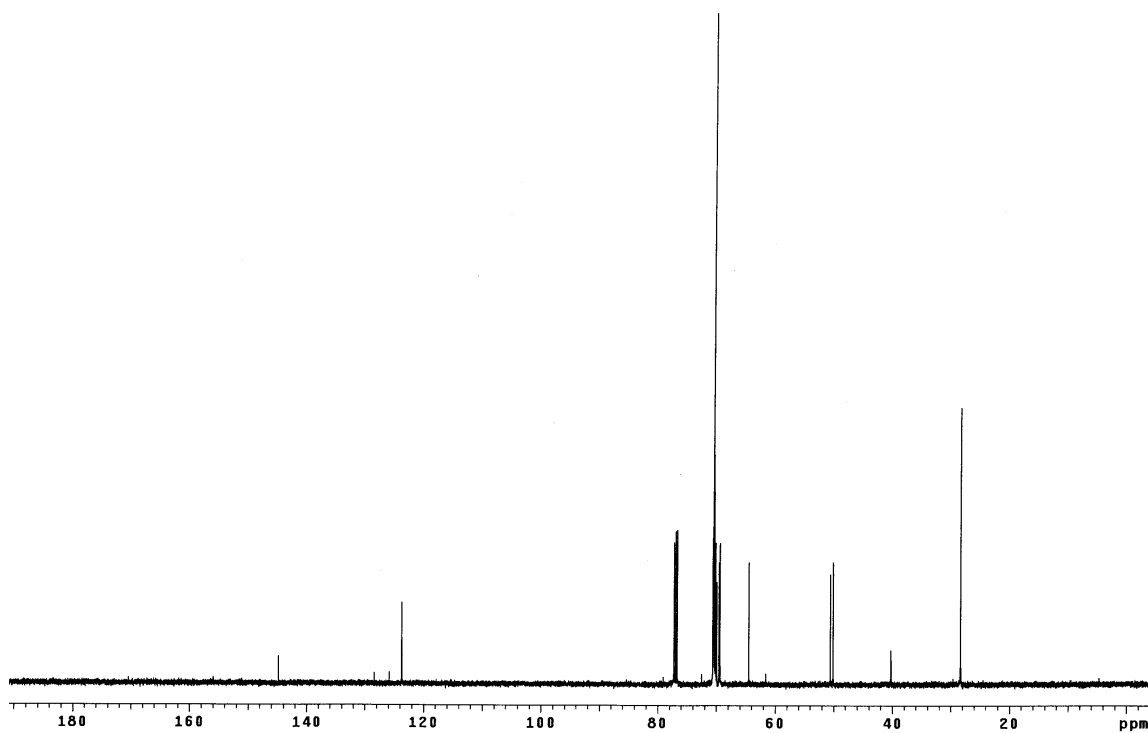
Compound 18

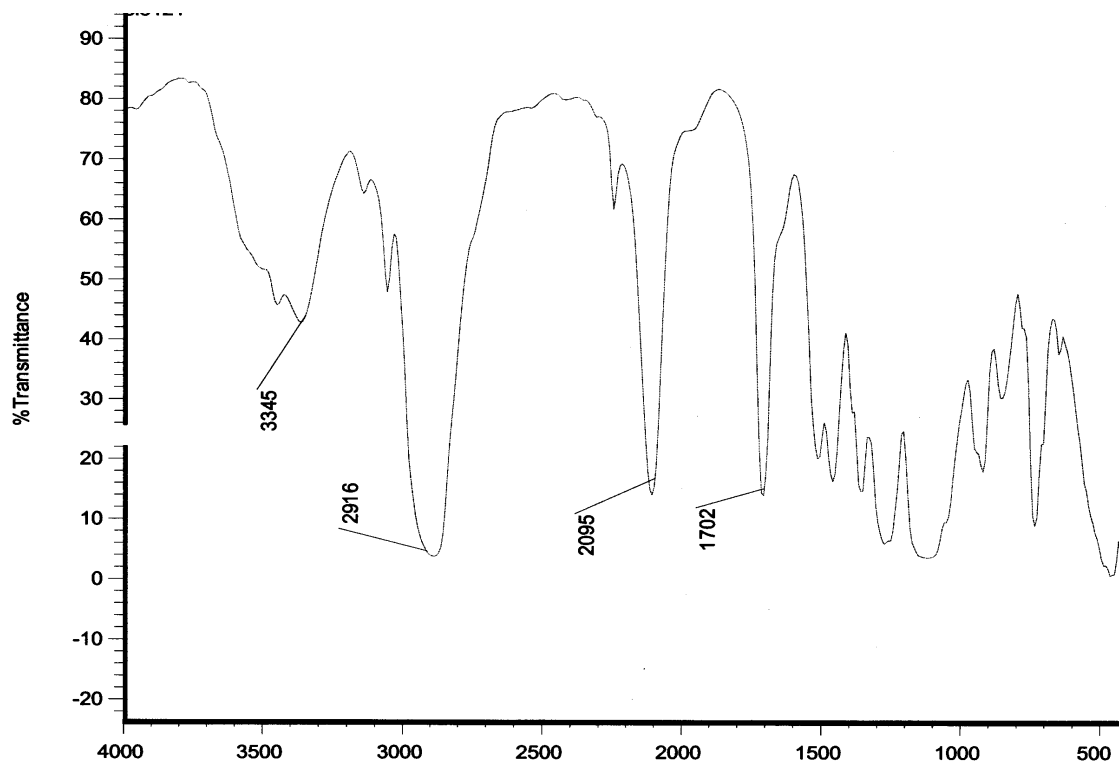
2-(2-(2-(2-(2-(2-4-((2-(2-(2-(2-(2-(2-Azidoethoxy)ethoxy)ethoxy)ethoxy)ethoxy)ethoxy)methyl)-1*H*-1,2,3-triazol-1-yl)ethoxy)ethoxy)ethoxy) ethoxy)ethoxy)ethyl *tert*-butylcarbamate



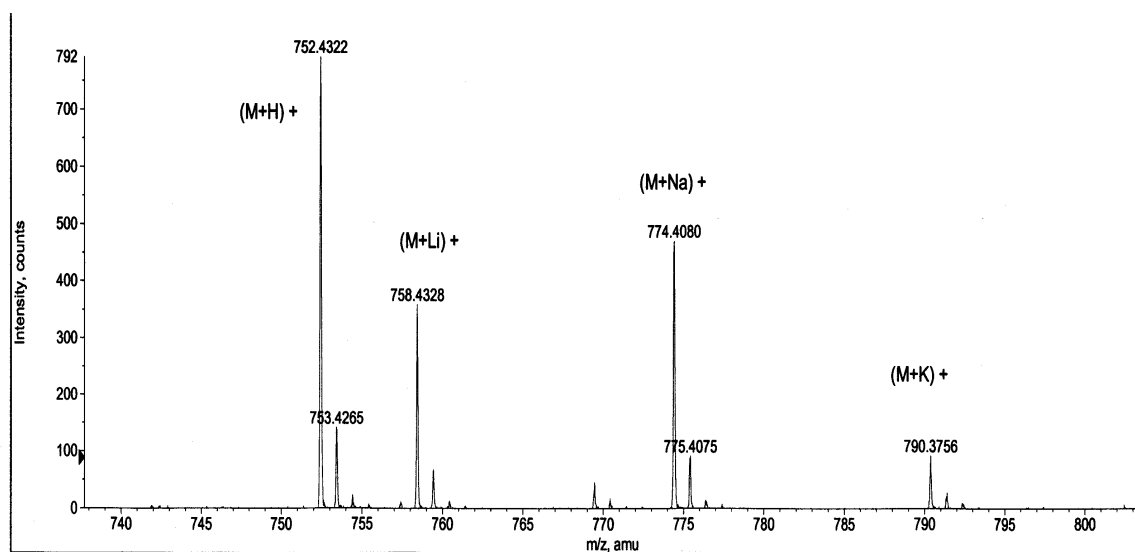
Procedure:

Compound **17** (52.7 mg, 60 μ mol) and sodium azide (10.0 mg, 0.15 mmol) were refluxed in 4 mL MeCN for 32 h. DI water (6 mL) was added and extracted with CH₂Cl₂ (5 x 10 mL). The organic extracts were pooled, dried over Na₂SO₄, filtered, and evaporated under reduced pressure, yielding **18** as a yellow oil (34.7 mg, 77%). ¹H NMR (CDCl₃, 500 MHz): δ (ppm) 1.43 (s, 9H), 3.30 (t, *J* = 5.0 Hz, 2H), 3.38 (t, *J* = 5.0 Hz, 2H), 3.52 (t, *J* = 5.0 Hz, 2H), 3.60 (m, 38H), 3.86 (t, *J* = 5.0 Hz, 2H), 4.52 (t, *J* = 5.0 Hz, 2H), 4.67 (s, 2H), 5.09 (br, 1H), 7.74 (s, 1H); ¹³C NMR (CDCl₃, 125 MHz): δ (ppm) 28.4, 40.3, 50.1, 50.6, 64.5, 69.4, 69.6, 69.96, 70.15, 70.18, 70.41, 70.44, 70.50, 70.51, 70.56, 70.59, 70.62, 123.7, 144.8, some signals account for more than one carbon; IR (film): ν (cm⁻¹) 1702, 2095, 2916, 3345; MS (ESI, *m/z*) 752.4 for [M+H]⁺.

 ^1H NMR ^{13}C NMR



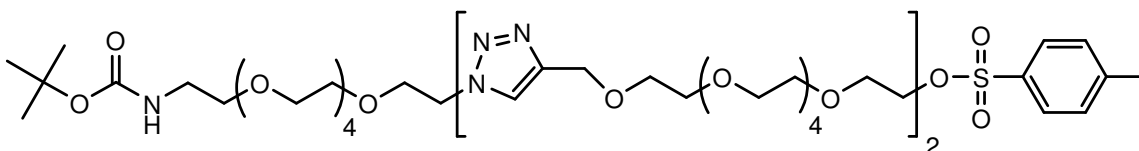
IR



MS

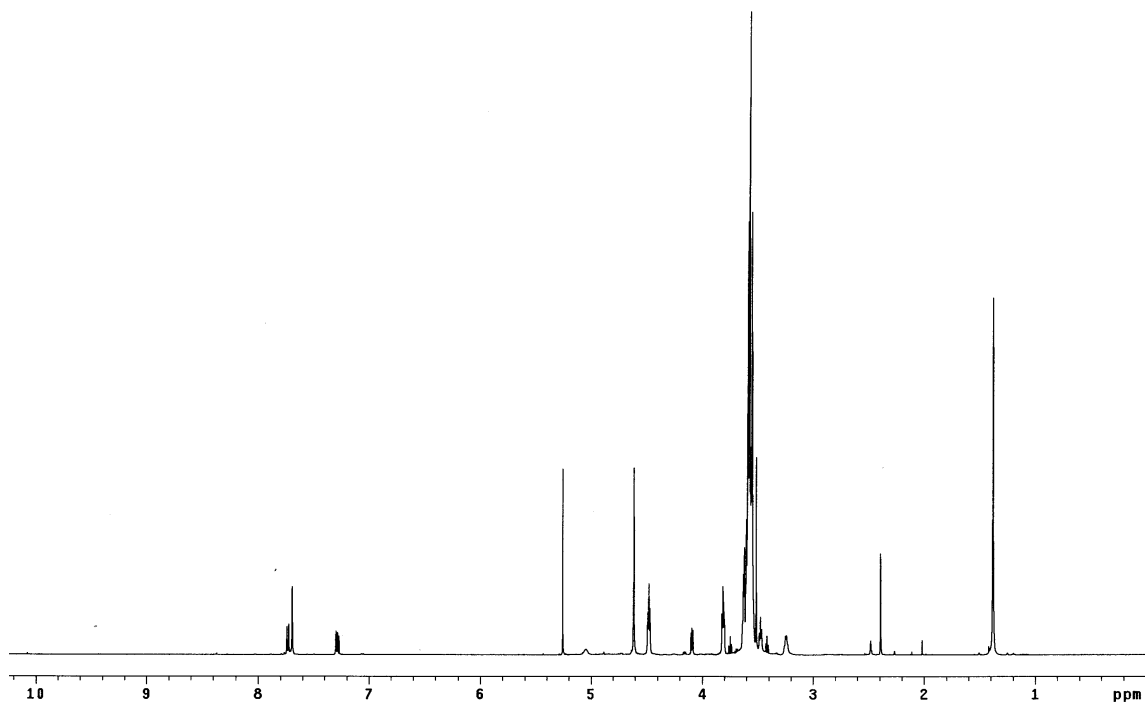
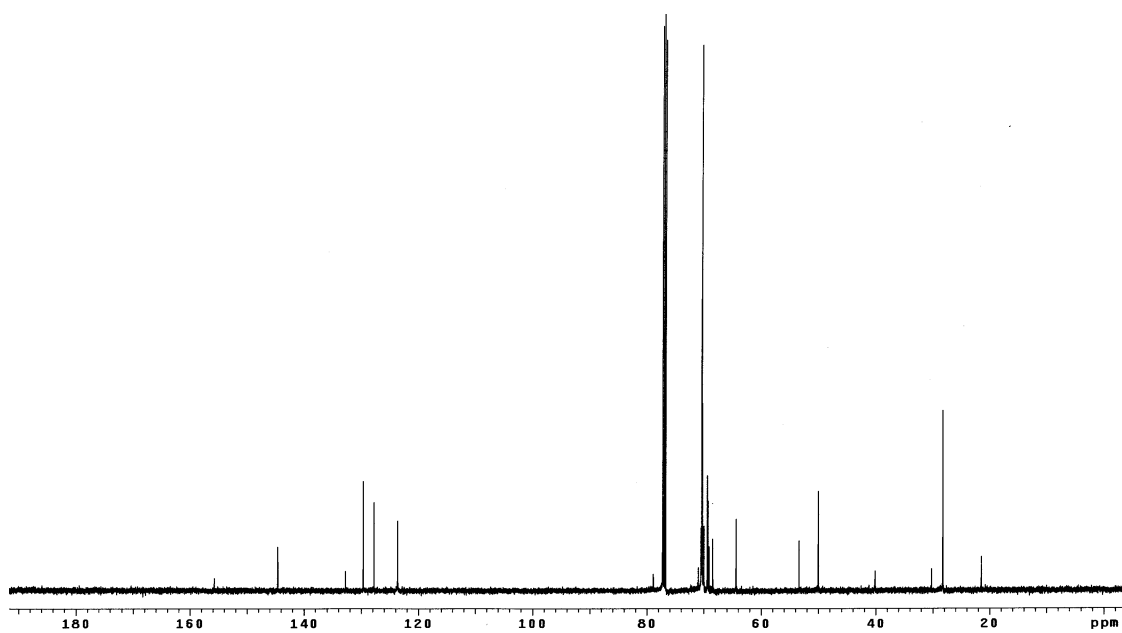
Compound 19

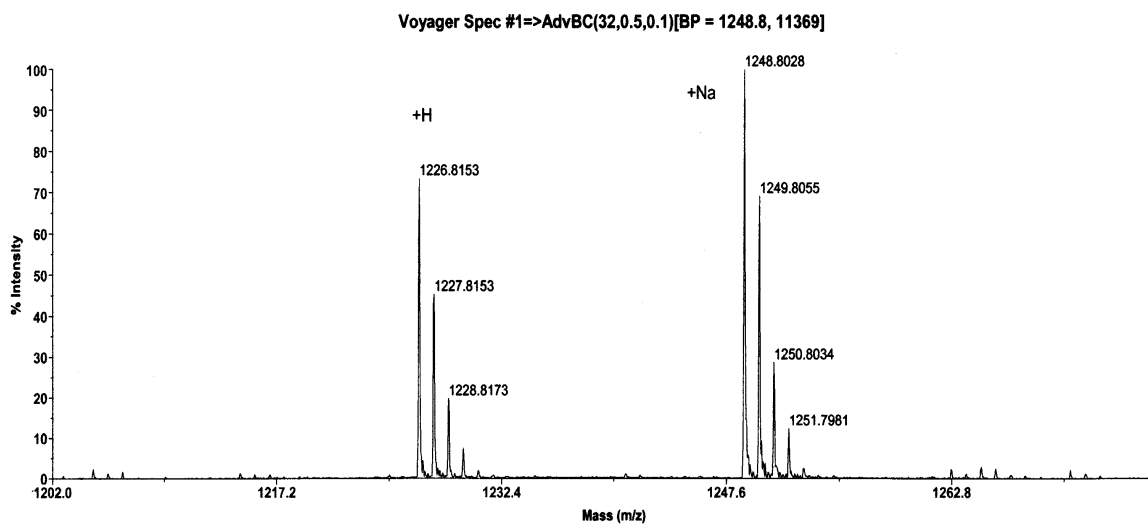
2-(2-(2-(2-(2-(2-(4-((2-(2-(2-(2-(2-(2-(4-((2-(2-(2-(2-(2-(4-Methylbenzenesulfonyl
oxy)ethoxy)ethoxy)ethoxy)ethoxy) ethoxy)methyl)-1*H*-1,2,3-triazol-1-yl)
ethoxy)ethoxy)ethoxy) ethoxy)ethoxy)ethoxy)methyl)- 1*H*-1,2,3-triazol-1-yl) ethoxy)
ethoxy)ethoxy)ethoxy)ethyl *tert*-butylcarbamate



Procedure:

Compound **18** (328 mg, 0.440 mmol), compound **12** (207 mg, 0.440 mmol), copper powder (140. mg, 2.20 mmol), and 800 μ L of an aqueous 1M $\text{CuSO}_4 \cdot 5\text{H}_2\text{O}$ solution (40 mol%) were suspended in 10 mL t BuOH/ H_2O (1:1) mixture in a scintillation vial. The vial was capped and the reaction solution stirred vigorously for 64 h at room temperature. The mixture was filtered through celite and washed with MeOH and evaporated under reduced pressure. The residue was diluted with CH_2Cl_2 and washed with brine/EDTA solution (1 x 60 mL) and evaporated under reduced pressure. The crude product was purified by flash chromatography eluting first with EtOAc/acetone (1:1) then with MeOH, yielding **19** as a yellow oil (296 mg, 55%). ^1H NMR (CDCl_3 , 500 MHz): δ (ppm) 1.38 (s, 9H), 2.39 (s, 3H), 3.25 (t, $J = 5.0$ Hz, 2H), 3.47 (t, $J = 5.0$ Hz, 2H), 3.52-3.64 (m, 58H), 3.81 (t, $J = 5.0$ Hz, 4H), 4.09 (t, $J = 4.8$ Hz, 2H), 4.47 (t, $J = 5.3$ Hz, 4H), 4.61 (s, 4H), 5.05 (br, 1H), 7.29 (d, $J = 8.5$ Hz, 2H), 7.69 (s, 2H), 7.73 (d, $J = 8.5$ Hz, 2H); ^{13}C NMR (CDCl_3 , 125 MHz): δ (ppm) 21.4, 28.2, 30.2, 40.1, 50.0, 53.3, 64.3, 68.4, 69.1, 69.3, 69.4, 69.99, 70.26, 70.28, 70.3, 70.34, 70.5, 70.97, 78.9, 123.6, 127.8, 129.6, 132.7, 144.6, 144.64, 155.8, some signals account for more than one carbon; MS (MALDI, m/z) 1248.8 for $[\text{M}+\text{Na}]^+$.

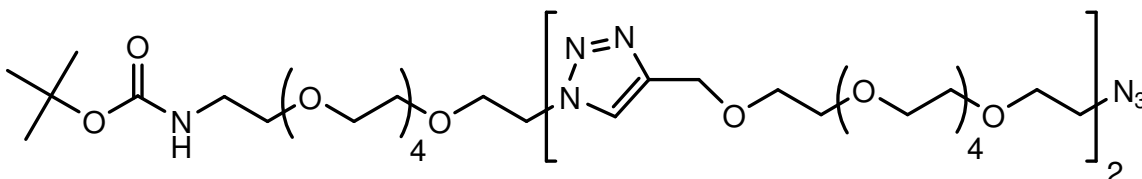
 ^1H NMR ^{13}C NMR



MS

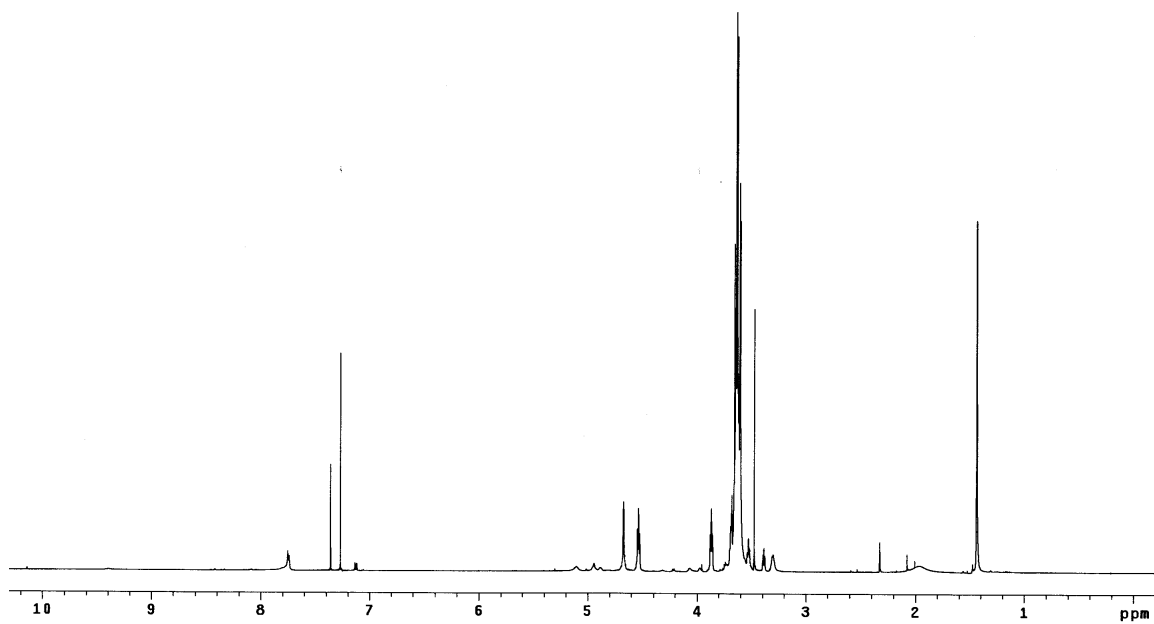
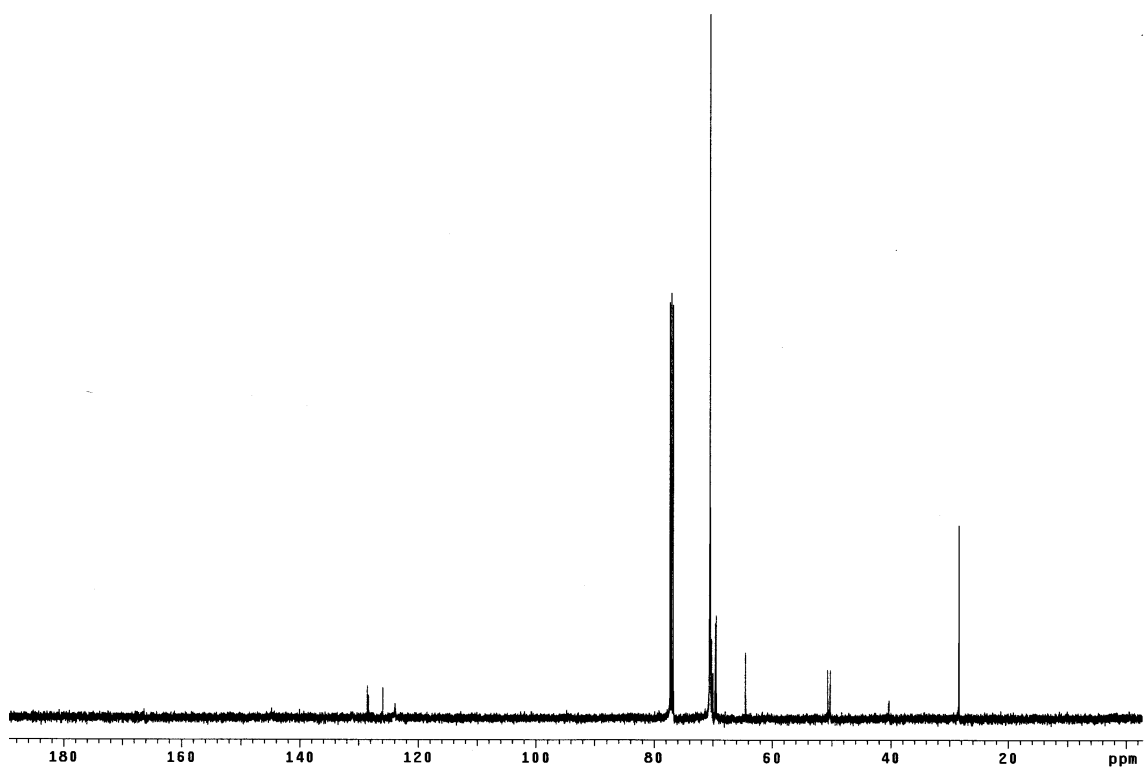
Compound 20

2-(2-(2-(2-(2-(2-(4-((2-(2-(2-(2-(2-(2-(4-((2-(2-(2-(2-(2-Azidoethoxy)ethoxy)ethoxy)ethoxy)ethoxy)ethoxy)methyl)-1*H*-1,2,3-triazol-1-yl) ethoxy)ethoxy)ethoxy)ethoxy)ethoxy)ethoxy)methyl)- 1*H*-1,2,3-triazol-1-yl) ethoxy)ethoxy)ethoxy)ethoxy)ethoxy) ethyl *tert*-butylcarbamate

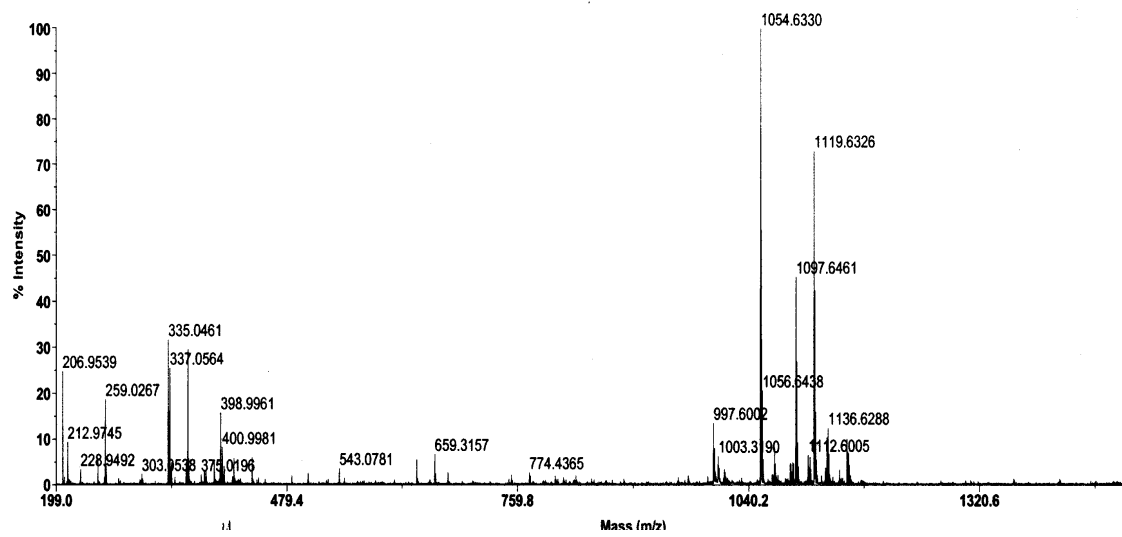


Procedure:

Compound **19** (296 mg, 0.24 mmol) and sodium azide (50.0 mg, 0.77 mmol) were refluxed in 5 mL MeCN for 41 h. DI water (15 mL) was added and extracted with CH₂Cl₂ (4 x 20 mL). The organic extracts were pooled, dried over Na₂SO₄, filtered, and evaporated under reduced pressure, yielding **20** as a yellow oil (216 mg, 82%). ¹H NMR (CDCl₃, 500 MHz): δ (ppm) 1.44 (s, 9H), 3.30 (t, *J* = 5.0 Hz, 2H), 3.38 (t, *J* = 5.0 Hz, 2H), 3.48 (s, 2H), 3.53 (t, *J* = 5.0 Hz, 2H), 3.60-3.70 (m, 56H), 3.87 (t, *J* = 5.0 Hz, 4H), 4.53 (t, *J* = 5.3 Hz, 4H), 4.67 (s, 4H), 5.10 (br, 1H), 7.74 (s, 1H), 7.75 (s, 1H); ¹³C NMR (CDCl₃, 125 MHz): δ (ppm) 28.4, 40.3, 50.2, 50.6, 64.5, 69.4, 69.58, 69.59, 69.99, 70.18, 70.2, 70.3, 70.43, 70.47, 70.5, 70.57, 70.61, 70.64, 123.8, 125.9, 128.3, 128.5, 144.7, some signals account for more than one carbon; MS (MALDI, *m/z*) 1119.6 for [M+Na]⁺.

 $^1\text{H NMR}$  $^{13}\text{C NMR}$

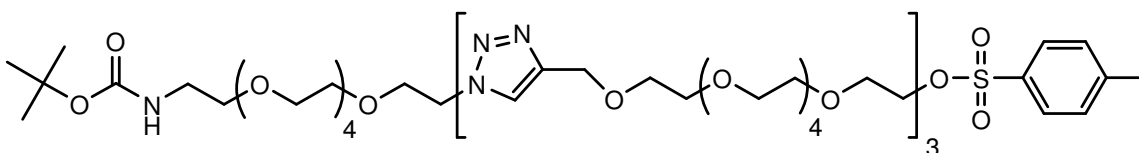
Voyager Spec #1[BP = 1054.6, 12006]



MS

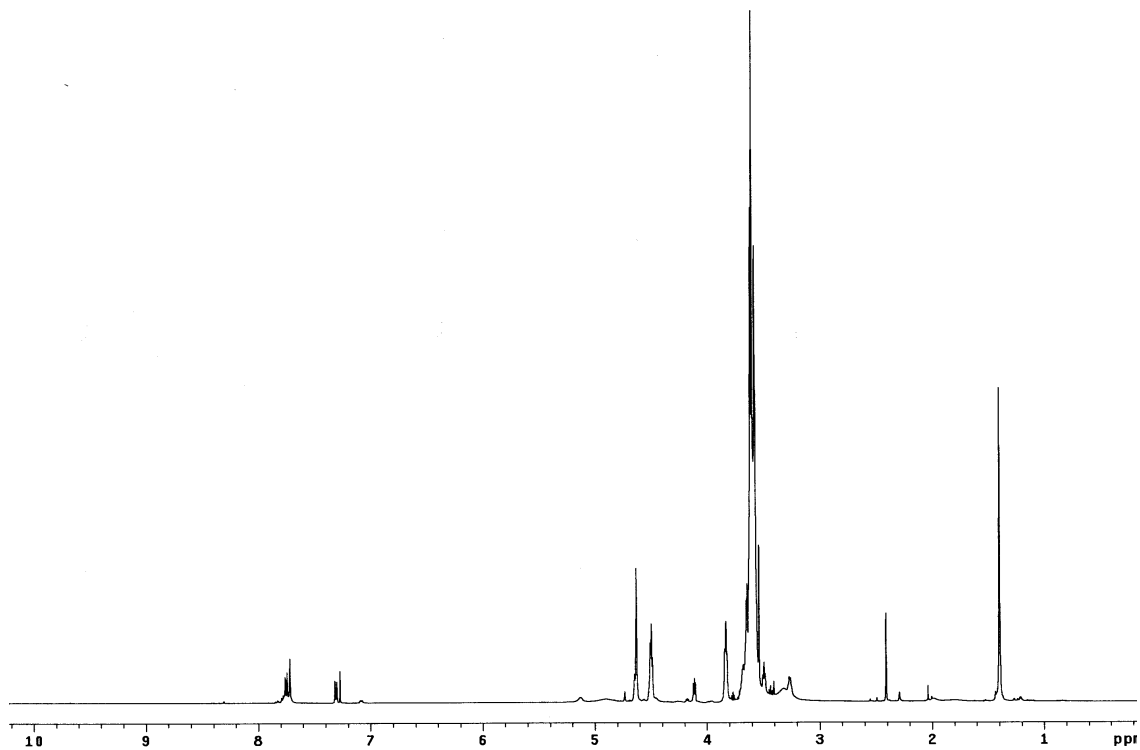
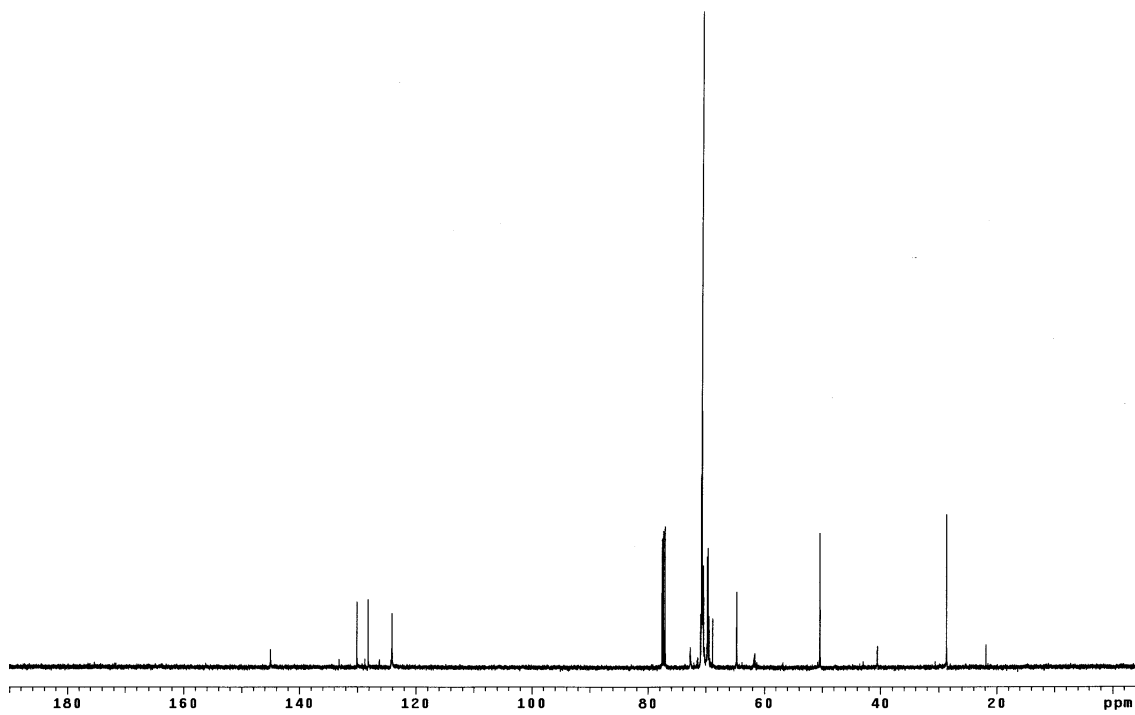
Compound 21

2-(2-(2-(2-(2-(2-(4-((2-(2-(2-(2-(2-(2-(4-((2-(2-(2-(2-(2-(4-Methylbenzenesulfonyloxy)ethoxy)ethoxy)ethoxy)ethoxy) ethoxy)methyl)-1*H*-1,2,3-triazol-1-yl) ethoxy)ethoxy)ethoxy)ethoxy)ethoxy)ethoxy)methyl)-1*H*-1,2,3-triazol-1-yl)ethoxy)ethoxy)ethoxy)ethoxy)ethoxy)ethoxy)methyl)-1*H*-1,2,3-triazol-1-yl)ethoxy)ethoxy)ethoxy)ethoxy)ethyl *tert*-butylcarbamate

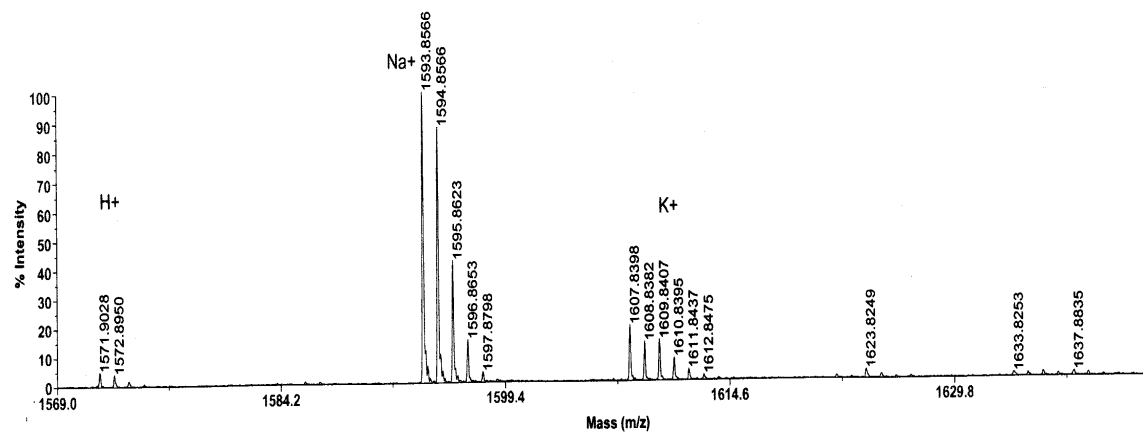


Procedure:

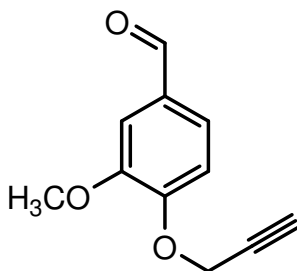
Compound **20** (202 mg, 0.18 mmol), compound **12** (87.0 mg, 0.18 mmol), copper powder (23.0 mg, 0.36 mmol), and 80 μ L of an aqueous 1M $\text{CuSO}_4 \cdot 5\text{H}_2\text{O}$ solution (40 mol%) were suspended in 1.5 mL $t\text{BuOH}/\text{H}_2\text{O}$ (1:1) mixture in a scintillation vial. The vial was capped and the reaction solution stirred vigorously for 48 h at room temperature. The reaction was diluted with EtOAc and filtered through celite. The crude product was purified by column chromatography eluting first with 10% MeOH/EtOAc then with 50% MeOH/EtOAc, yielding **21** as a light-yellow gel (87 mg, 30%). ^1H NMR (CDCl_3 , 500 MHz): δ (ppm) 1.40 (s, 9H), 2.41 (s, 3H), 3.26 (t, $J = 5.0$ Hz, 4H), 3.49 (t, $J = 5.0$ Hz, 4H), 3.53-3.69 (m, 74H), 3.83 (t, $J = 4.8$ Hz, 6H), 4.11 (t, $J = 4.8$ Hz, 2H), 4.49 (t, $J = 4.8$ Hz, 6H), 4.63 (s, 2H), 4.64 (s, 2H), 4.65 (s, 2H), 5.12 (br, 1H), 7.30 (d, $J = 8$ Hz, 2H), 7.72 (s, 3H), 7.75 (d, $J = 7.5$ Hz, 2H); ^{13}C NMR (CDCl_3 , 125 MHz): δ (ppm) 21.9, 28.6, 40.5, 50.3, 50.4, 61.6, 64.7, 68.9, 69.5, 69.55, 69.7, 69.8, 70.3, 70.4, 70.55, 70.6, 70.7, 70.9, 72.7, 72.74, 124.07, 124.1, 128.2, 130.1, 145.0, some signals account for more than one carbon; MS (MALDI, m/z) 1593.8 for $[\text{M}+\text{Na}]^+$.

 ^1H NMR ^{13}C NMR

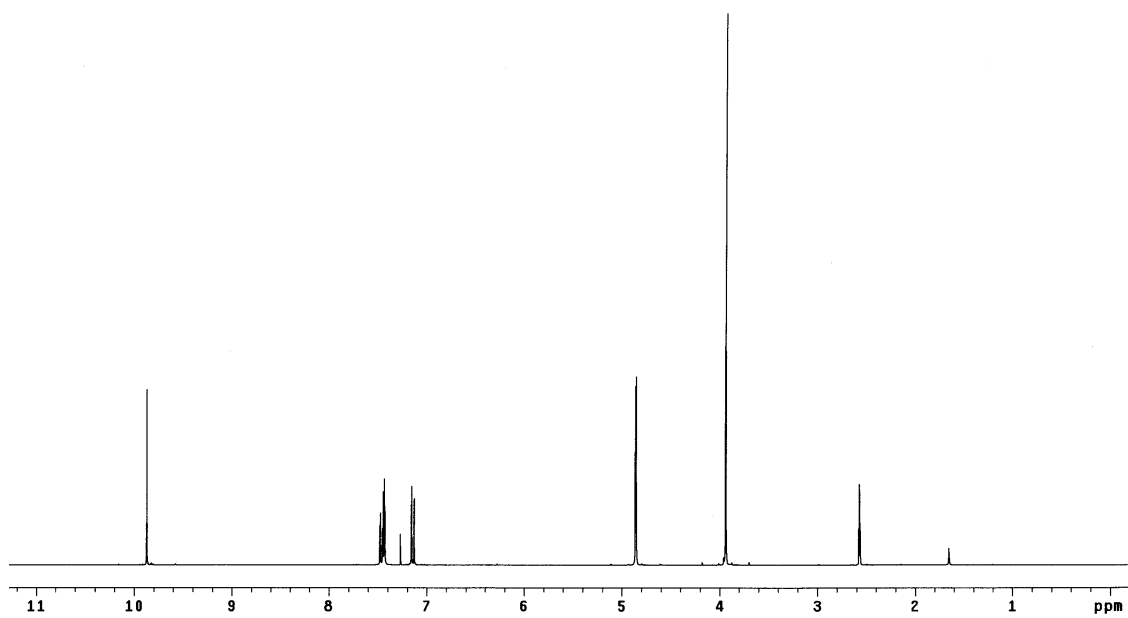
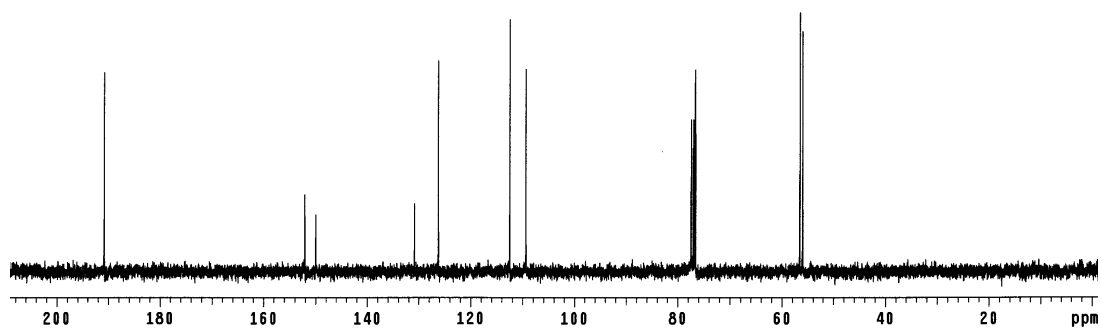
Voyager Spec #1[BP = 1593.8, 14124]



MS

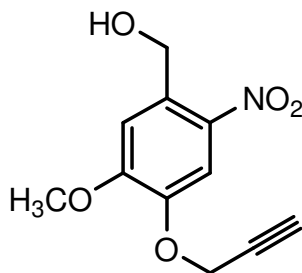
Compound 22**3-methoxy-4-(prop-2-ynyloxy)benzaldehyde¹²³****Procedure:**

Vanillin (15.2 g, 100. mmol) and potassium carbonate (13.8 g, 100. mmol) were dissolved in 300 mL acetone. The mixture was stirred for 0.5 h at room temperature. Propargyl bromide (15.6 g, 105 mmol) mixed with 50 mL acetone was then added gradually to the reaction solution. The mixture was refluxed for 24 h, after which 400 mL DI H₂O was added to precipitate the product **22** as a light-yellow solid (16.8 g, 88%). ¹H NMR (CDCl₃, 300 MHz): δ (ppm) 2.57 (t, *J* = 2.3 Hz, 1H), 3.94 (s, 3H), 4.86 (d, *J* = 2.4 Hz, 2H), 7.14 (d, *J* = 8.4 Hz, 1H), 7.45 (d, *J* = 7.2 Hz, 1H), 7.48 (s, 1H), 9.87 (s, 1H); ¹³C NMR (CDCl₃, 75 MHz): δ (ppm) 55.99, 56.54, 76.64, 77.39, 109.38, 112.50, 126.24, 130.87, 149.97, 152.06, 190.86.

 $^1\text{H NMR}$  $^{13}\text{C NMR}$

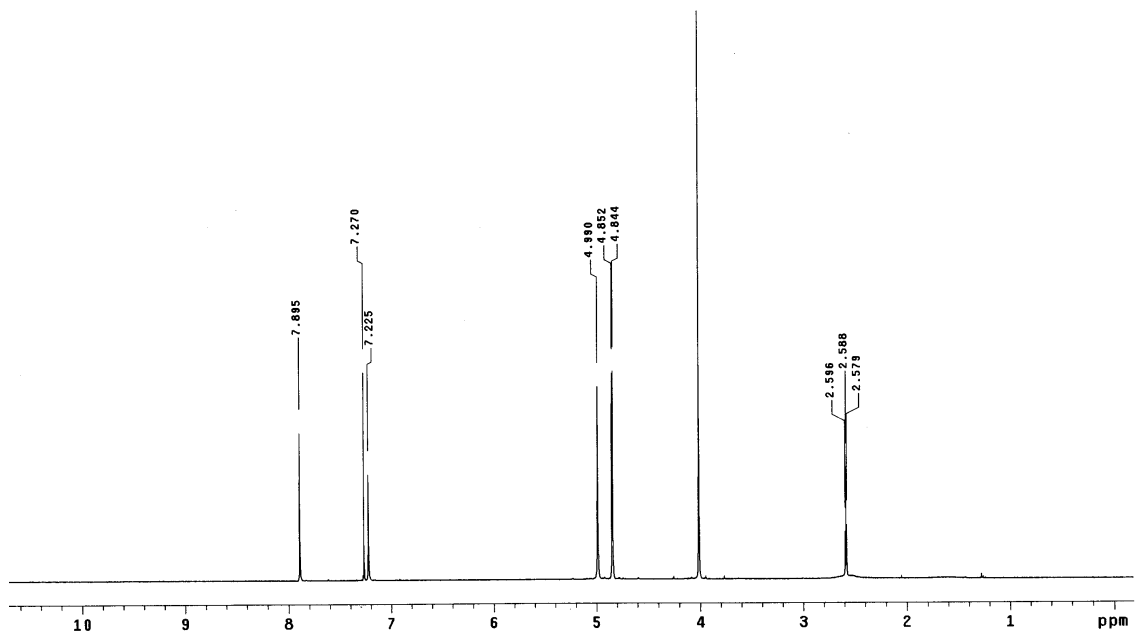
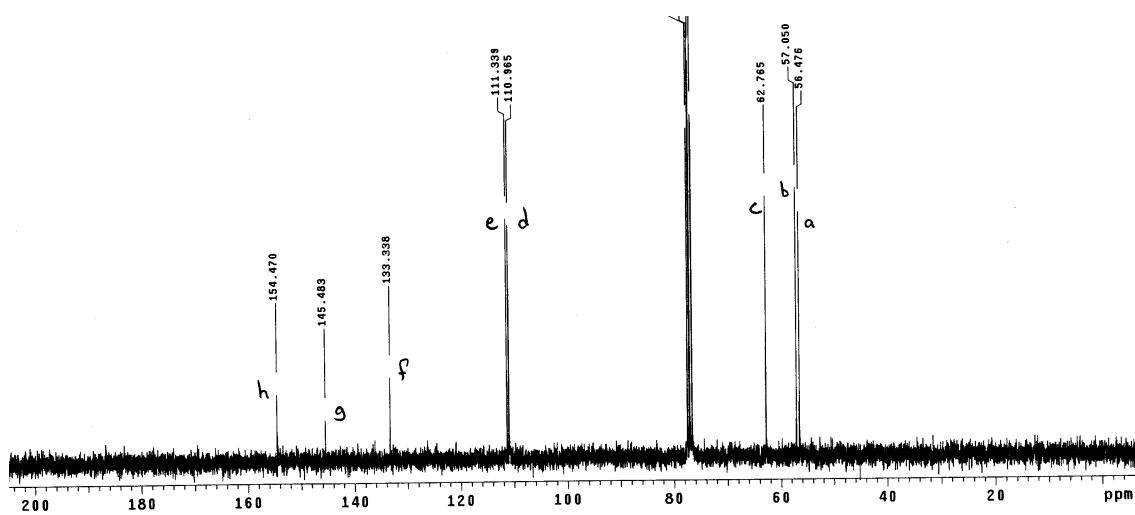
Compound 23

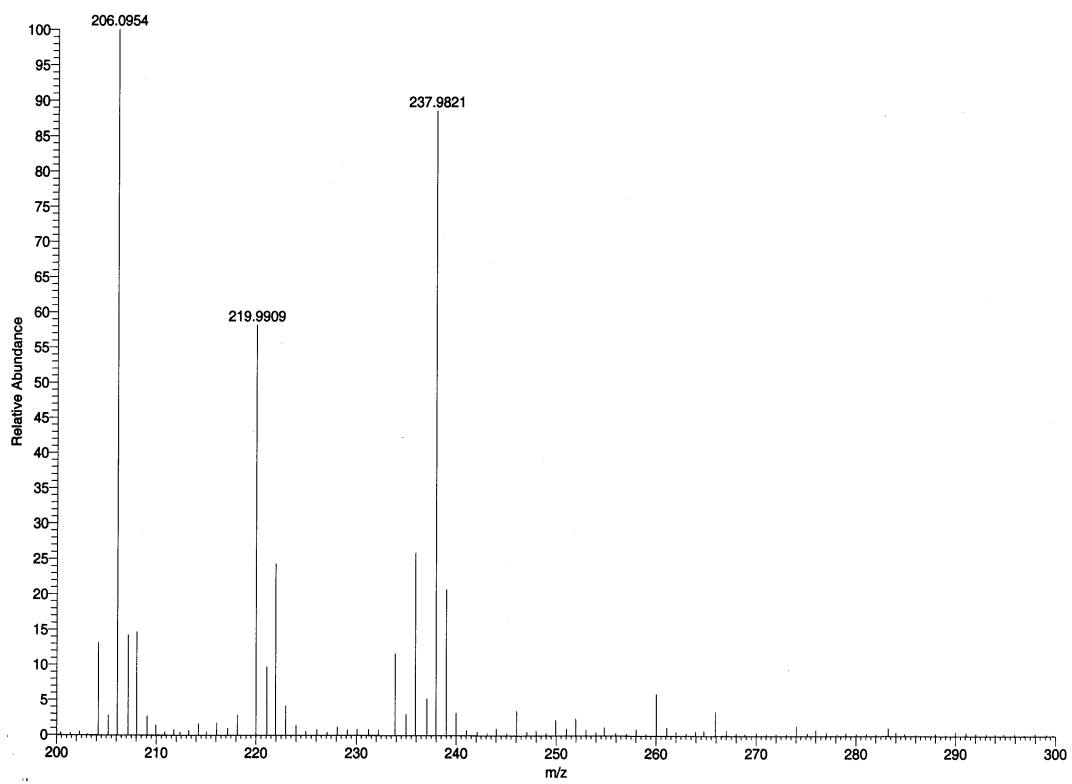
5-methoxy-2-nitro-4-(prop-2-ynoxy)phenyl methanol



Procedure:

Compound **22** (16.8 g, 88.6 mmol) in 75 mL of acetic anhydride was added slowly to a thoroughly chilled solution of concentrated nitric acid (300 mL) and acetic anhydride (125 mL) in an ice-bath. The mixture was stirred for 2 h at 0 °C, then 2 h at room temperature. It was diluted with 1.2 L EtOAc, washed with brine (1 x 1 L), saturated NaHCO₃ solution (3 x 1 L), and brine again (2 x 1 L). The resulting organic layer was dried over Na₂SO₄ and filtered through a pad of silica gel over celite, washing with plenty of EtOAc. Evaporation under reduced pressure afforded the nitrated product as an orange solid, which was dissolved in 675 mL absolute EtOH and chilled to 0 °C. Sodium borohydride (7.56 g, 200. mmol) was added scoop-wise to the chilled mixture. The reaction was allowed to gradually warm to room temperature then quenched with 100 mL saturated NH₄Cl solution. It was diluted with 1 L EtOAc then washed with DI H₂O (1 x 1 L) and brine (1 x 1 L). The organic phase was dried over Na₂SO₄, filtered, and evaporated *in vacuo*. The crude product was purified by flash chromatography using 1:1 EtOAc/hexane to yield **23** as a yellow solid (12.8 g, 61% – 2 steps); m.p. 126-131 °C; ¹H NMR (CDCl₃, 300 MHz): δ (ppm) 2.59 (t, *J* = 2.6 Hz, 1H), 4.01 (s, 3H), 4.84 (d, *J* = 2.4 Hz, 2H), 4.99 (s, 2H), 7.23 (s, 1H), 7.89 (s, 1H); ¹³C NMR (CDCl₃, 75 MHz): δ (ppm) 56.47, 57.05, 62.77, 77.11, 110.97, 111.34, 133.34, 145.48, 154.47; MS (APCI, *m/z*) 238.0 for [M+H]⁺.

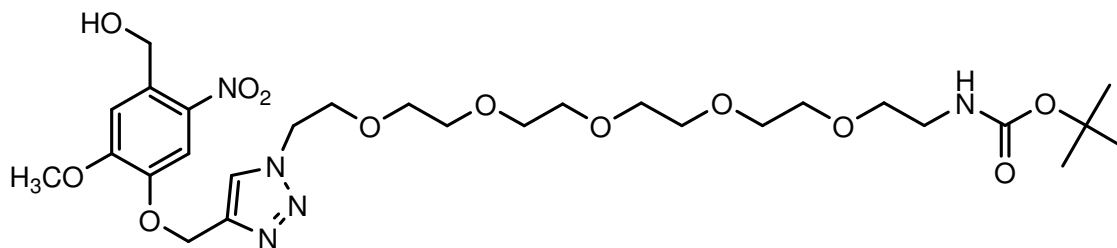
 $^1\text{H NMR}$  $^{13}\text{C NMR}$



MS

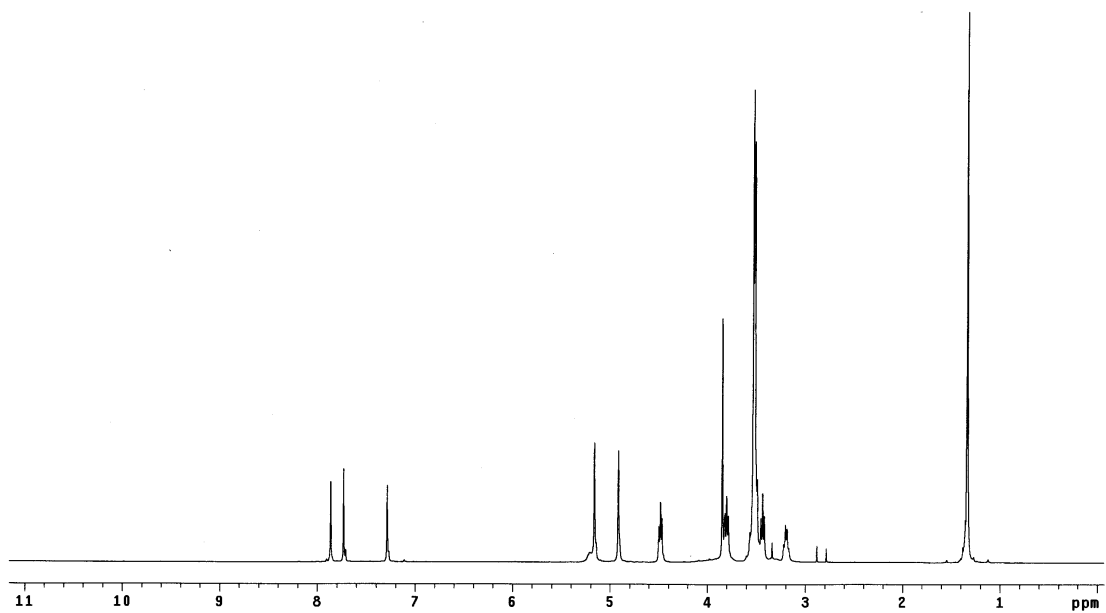
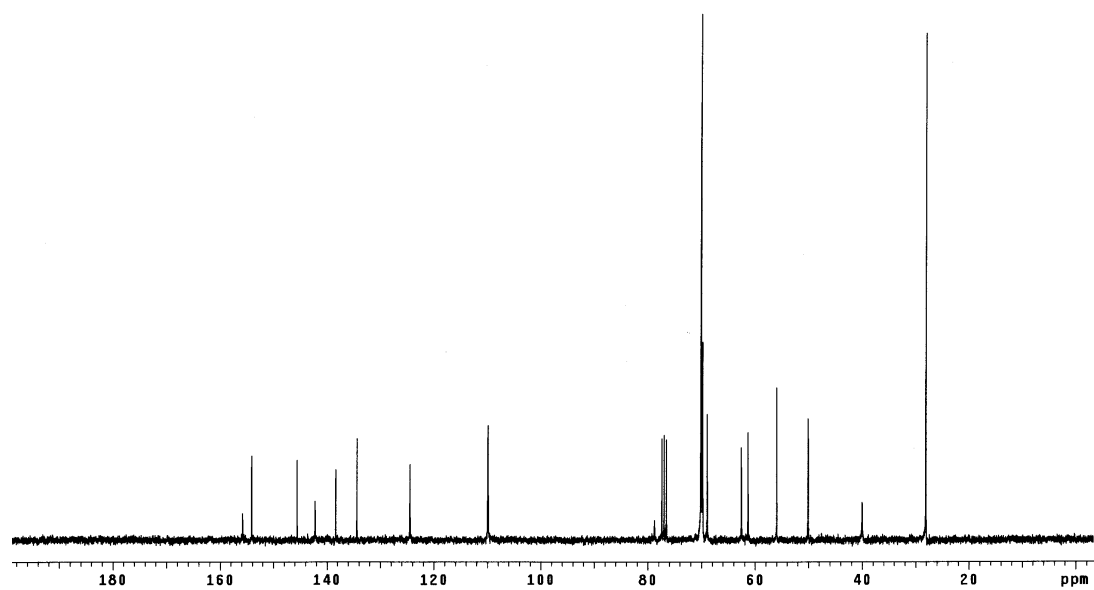
Compound 24

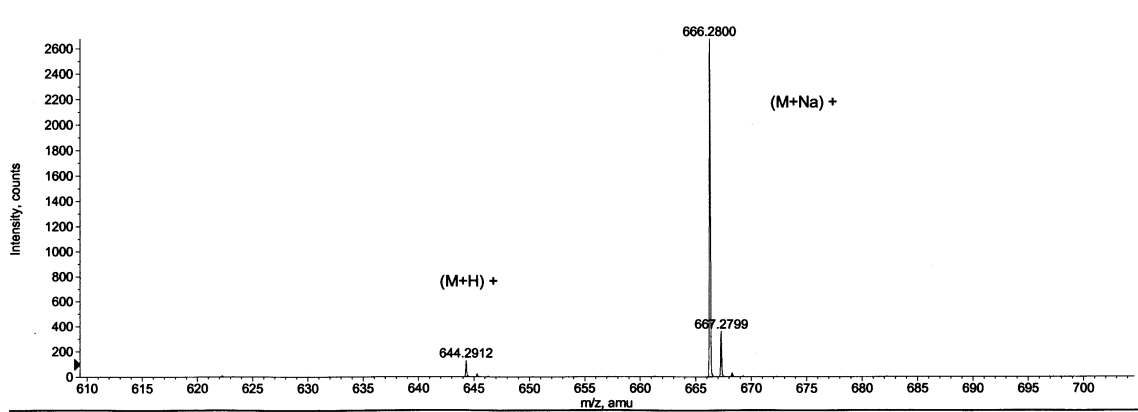
2-(2-(2-(2-(2-(2-(4-((4-(Hydroxymethyl)-2-methoxy-5-nitrophenoxy)methyl)-1*H*-1,2,3-triazol-1-yl)ethoxy)ethoxy)ethoxy)ethoxy)ethoxy)ethyl *tert*-butylcarbamate



Procedure:

Compound **23** (237 mg, 1.00 mmol), compound **16** (407 mg, 1.00 mmol), copper powder (50.0 mg, 0.787 mmol), and 200. μL of an aqueous 1M $\text{CuSO}_4 \cdot 5\text{H}_2\text{O}$ solution (40 mol%) were mixed together in 14 mL $t\text{BuOH}/\text{H}_2\text{O}$ (1:1) mixture in a scintillation vial. The reaction mixture was stirred for 24 h at room temperature then purified by flash chromatography eluting with 1:3 MeOH/acetone to give **24** as a yellow oil (186 mg, 29%); ^1H NMR (CDCl_3 , 300 MHz): δ (ppm) 1.34 (s, 9H), 3.20 (t, $J = 5.4$ Hz, 2H), 3.44 (t, $J = 3.8$ Hz, 2H), 3.49-3.57 (m, 18H), 3.80 (t, $J = 4.8$ Hz, 2H), 3.85 (s, 2H), 4.48 (t, $J = 5.1$ Hz, 2H), 4.91 (s, 2H), 5.16 (s, 3H), 7.29 (s, 1H), 7.73 (s, 1H), 7.87 (s, 1H); ^{13}C NMR (CDCl_3 , 75 MHz): δ (ppm) 28.07, 40.01, 50.05, 56.00, 61.37, 62.61, 68.96, 69.84, 70.04, 70.11, 70.15, 109.89, 109.97, 124.47, 134.37, 138.36, 142.21, 145.58, 154.12, 155.81; MS (ESI, m/z) 666.3 $[\text{M}+\text{Na}]^+$.

 ^1H NMR ^{13}C NMR



MS

VITA

Name: Sang Q. Lam

Permanent Address: 15255 Gray Ridge Dr. #734
Houston, TX 77082

Education

2002-2005	M.S., Chemistry, Texas A&M University College Station, TX
1996-2000	B.S., Chemistry, The University of Texas at Dallas Richardson, TX

Experience

2000-2002	Lab Technician I, Analytical Chemistry Coast to Coast Analytical Specialists, Inc., Dallas, TX
-----------	--